

---

# Physics-informed machine learning for combustion: A review

---

Jiahao Wu<sup>1</sup>, Xutun Wang<sup>2</sup>, Yuxin Wu<sup>\*1</sup>, Guihua Zhang<sup>1</sup>, Jiayue Liu<sup>1</sup>, Xin Li<sup>1</sup>

<sup>1</sup>*Department of Energy and Power Engineering, Key Laboratory for Thermal Science and Power Engineering of Ministry of Education, Tsinghua University, Beijing 100084, China*

<sup>2</sup>*School of Aerospace Engineering, Key Laboratory of Advanced Power and Propulsion of Ministry of Education, Tsinghua University, Beijing 100084, China*

## ABSTRACT

Physics-informed machine learning (PIML) represents an emerging paradigm that integrates various forms of physical knowledge into machine learning (ML) components, thereby enhancing the physical consistency of ML models compared to purely data-driven paradigms. The field of combustion, characterized by a rich foundation of physical laws and abundant data, is undergoing a transformation due to PIML. This paper aims to provide a comprehensive overview of PIML for combustion, systematically outlining fundamental principles, significant contributions, key advancements, and available resources. The application of PIML in combustion is categorized into three domains: combustion chemical kinetics, combustion reacting flows, and other combustion-related problems. Additionally, current challenges, potential solutions, and practical guidelines for researchers and engineers will be discussed. A primary focus of this review is to demonstrate how combustion laws can be integrated into ML, either through soft or hard constraints, via loss functions or representation models, and within coordinate-to-variable or field-to-field paradigms. This paper shows that PIML offers a unified framework linking physics, model, and data in combustion—integrating physical knowledge in model-to-data simulation and reconstruction tasks, as well as data-to-model modeling tasks—resulting in enhanced data, improved physical models, and more reliable ML models. PIML for combustion presents significant opportunities for both the combustion and ML communities, encouraging greater collaboration and cross-disciplinary engagement.

**Keywords** physics-informed machine learning (PIML) · combustion · chemical kinetics · reacting flow

## Contents

<b>1</b>	<b>Introduction</b>	<b>3</b>
<b>2</b>	<b>Physics-informed machine learning</b>	<b>5</b>
2.1	Fundamentals . . . . .	5
2.2	Reviews and scoping . . . . .	6
2.3	Developments . . . . .	8
2.3.1	Representation model . . . . .	9
2.3.2	Optimization process . . . . .	10
2.3.3	PDE system . . . . .	11
2.3.4	Other important topics . . . . .	11
2.4	Related applications . . . . .	12
<b>3</b>	<b>Physical laws in combustion</b>	<b>12</b>

---

\*Corresponding author: wuyx09@tsinghua.edu.cn

3.1	Multicomponent system	12
3.2	Thermodynamics	13
3.3	Diffusion "kinetics"	14
3.4	Chemical kinetics	15
3.5	Fluid dynamics	16
<b>4</b>	<b>PIML for combustion chemical kinetics (0D combustion)</b>	<b>16</b>
4.1	Solving ODEs of chemical kinetics	16
4.2	Surrogate models of chemical kinetics	20
4.3	Neural ODEs: surrogate models and kinetics discovery	23
4.3.1	Continuous surrogate models	24
4.3.2	Kinetics discovery	26
<b>5</b>	<b>PIML for combustion reacting flows</b>	<b>27</b>
5.1	(Advection-) Diffusion-reaction problems	27
5.2	Laminar combustion	29
5.3	Turbulent combustion and experimental data	31
5.4	Supersonic combustion	35
5.5	Combustion super-resolution via discrete PINNs	37
<b>6</b>	<b>PIML for other combustion problems</b>	<b>38</b>
6.1	Fire safety	38
6.2	Thermoacoustics	39
6.3	Combustion diagnostics	39
6.4	Others	39
<b>7</b>	<b>Public resources</b>	<b>40</b>
7.1	Datasets and benchmarks	40
7.2	Simulation tools (data generators)	41
7.3	PIML tools	42
<b>8</b>	<b>Discussions and outlooks</b>	<b>43</b>
8.1	Challenges and solutions	44
8.1.1	Limitations reinforced by combustion	44
8.1.2	Discrepancies between physics, (physical) model, and data	44
8.1.3	Reproducibility	45
8.2	Discussions on implementation choices	45
8.3	Opportunities for combustion and AI	46
<b>9</b>	<b>Conclusions</b>	<b>47</b>
	<b>Acknowledgments</b>	<b>48</b>
<b>A</b>	<b>A code demo of PIML for combustion</b>	<b>48</b>
	<b>Reference</b>	<b>50</b>

# 1 Introduction

Combustion, the core process of energy conversion, plays a pivotal role in modern industrial systems, underpinning key sectors such as power generation, transportation, chemical manufacturing, and space exploration. The objective of combustion science is twofold: to harness the benefits of combustion while mitigating its hazards<sup>1-3</sup>, such as environmental pollution and fires. Achieving this goal requires a deep understanding of combustion, which is inherently complex. By definition, combustion is a high-temperature exothermic redox chemical reaction between a fuel and an oxidant. Therefore, it encompasses multiple coupled physical processes, including chemical reactions, heat transfer, mass transfer, and fluid flow, spanning various temporal and spatial scales<sup>4-8</sup>. Consequently, combustion research poses substantial scientific and engineering challenges.

As shown in Figure 1(a), combustion research and applications involve three core elements: physics, model, and data. Physics represents the real world; models aim to represent physics either through theoretical/physical formulations or data-driven approaches; and data are recorded values that typically contain physics. Transformations among these elements constitute the forward and inverse problems in research. Forward problems include physics-to-data and model-to-data problems, which involve realizing combustion processes in the real and virtual world, respectively, to generate data. The former primarily refers to experimental research, such as designing methods for controllable combustion<sup>9</sup>, while the latter primarily refers to numerical simulations, including application to various combustion devices<sup>10-13</sup> and the development of numerical algorithms<sup>14,15</sup>. In contrast, inverse problems include physics-to-model and data-to-model problems, which develop models or theories based on first principles<sup>4-8</sup> and data patterns, respectively. Model development can involve constructing models from scratch or determining parameters for existing models, which may take either interpretable or purely fitted forms. Forward problems and inverse problems are inherently interdependent. For example, the model-to-data forward problems require the complete form and parameters of the model to be known in advance, while data-to-model inverse problems often depend on physics-to-data experiments<sup>16-19</sup>. Consequently, theoretical, experimental, and numerical methods are often adopted simultaneously<sup>20</sup>. However, these three types of methods differ substantially in implementation, resource requirements, cost, output form, and transferability, hindering their integration and slowing the research cycle. This highlights the need for a paradigm that can overcome these barriers, establish a unified framework linking physics, models, and data, and more effectively address a wide range of forward and inverse problems in combustion.

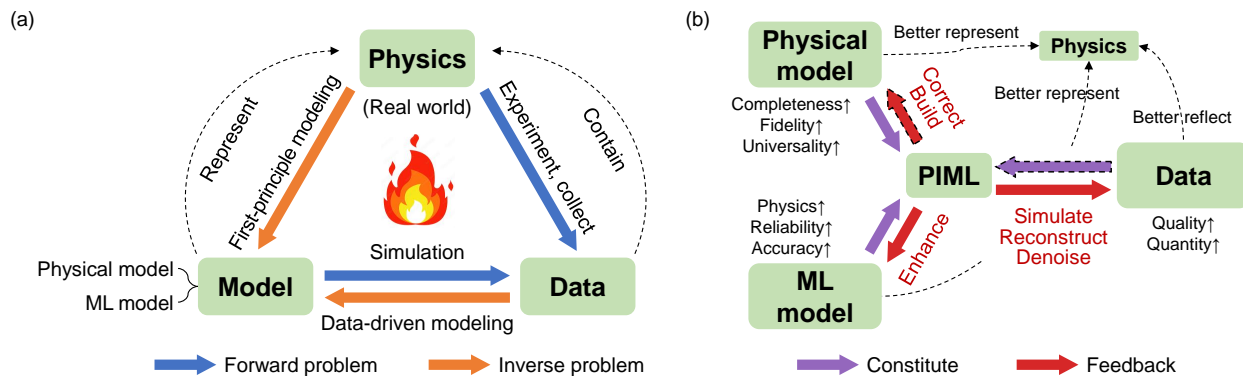


Figure 1: (a) Physics, model, and data are three elements in combustion. Physics represents the real world, physical models and ML models try to represent physics, while data are value records and usually contain physics. Their transformations constitute the forward and inverse problems, which are defined as generating data and modeling, respectively. (b) PIML can act as a unified bridge connecting physics, model, and data. PIML is constituted by physical model, ML model, and possible data, then each of them can be enhanced by the other two. The dashed colored arrows represent optional implementations.

Artificial intelligence (AI), machine learning (ML)<sup>21</sup>, and deep learning (DL)<sup>22</sup> have made remarkable achievements in recent years, transforming fields such as computer vision (CV)<sup>23</sup>, natural language processing (NLP)<sup>24</sup>, gaming<sup>25</sup>, and weather forecasting<sup>26-28</sup>. AI for science (AI4Sci) and scientific machine learning (SciML)<sup>29</sup> have emerged as key areas of interest for both the AI and scientific communities. These approaches leverage AI/ML to analyze scientific data, uncover patterns<sup>30</sup>, and solve scientific problems, and are recognized as the fourth paradigm of science<sup>31-33</sup>. They have produced transformative results, such as the AlphaFold in life sciences<sup>34,35</sup>. SciML has also made significant advances in fluid mechanics<sup>36-38</sup>, including both experimental fluid mechanics<sup>39</sup> and computational fluid dynamics (CFD)<sup>40-42</sup>. The combustion community has likewise embraced ML<sup>43,44</sup>, motivated not only by the power and versatility of ML methods, but also by the data-rich nature of combustion and the limitations of traditional approaches. ML

has been applied to combustion model optimization<sup>45–49</sup>, combustion chemistry<sup>50–54</sup>, combustion tabulation<sup>55–59</sup>, and surrogate modeling of combustion systems<sup>60–64</sup>. The applied ML techniques include supervised, unsupervised, and semi-supervised learning, which respectively focus on learning mappings from labeled data, identifying patterns in unlabeled data, and combining both approaches. These methods are built on diverse ML models, including neural networks (NNs), support vector machines (SVMs), and random forests (RFs). For more applications of ML for combustion, please refer to these reviews<sup>43,44</sup>. Data-driven ML has greatly advanced the data-to-model paradigm, enabling the exploitation of big data in combustion and the resolution of many longstanding challenges in the field.

Although data-driven ML has many successful applications in combustion, it has inherent limitations, including high data dependency, lack of physical consistency, and limited interpretability—and therefore reduced reliability. Consequently, purely data-driven ML is difficult to apply in scenarios with scarce or low-quality data, making it unsuitable for establishing a unified framework connecting physics, models, and data. To address this issue, the paradigm of physics-informed machine learning (PIML, /ˈpɪməl/ or /ˈpaɪməl/) has been proposed<sup>65</sup>, in which ML is integrated with various forms of physical priors, such as symmetries, conservation laws, and governing equations. Physics can be incorporated through data, models, and optimization, which are the three components of ML. PIML has become an important branch of SciML because it is naturally suited to scenarios where both some physical models and some data are available, which is the most common scenario in practice<sup>65</sup>, as illustrated in Figure 2. A representative work of PIML is the physics-informed NNs (PINNs)<sup>66</sup>, which employ neural networks as models and integrate differential equations (DEs) as physical constraints within the loss function. Before its former publication<sup>66</sup>, PINNs were first published as two preprints, solving the forward problems<sup>67</sup> and inverse problems<sup>68</sup> of DEs, respectively. Here, forward and inverse problems differ slightly from the earlier definitions in Figure 1: forward problems refer to well-posed DEs without observational data, whereas inverse problems refer to ill-posed DEs with possible observational data. PINNs map the space-time coordinates to solutions and use automatic differentiation (AD)<sup>69</sup> to compute the derivatives in DEs. In fact, the use of NNs to solve DEs dates back to the 1990s<sup>70–72</sup>, but their resurgence was enabled by modern DL, which provides efficient AD techniques. Compared to traditional numerical methods such as the finite difference method (FDM), finite volume method (FVM), and finite element method (FEM), PINNs are mesh-free and differentiable, exhibit no discretization errors, and more naturally suited to leveraging data for solving inverse problems, including field reconstruction and parameter inference. Therefore, PINNs serve as an important complement to traditional numerical methods for solving DEs. In short, PINN is an excellent example of integrating physics into ML, and PIML, as its broader framework, offers a unified approach for incorporating physics, building models, and utilizing data.

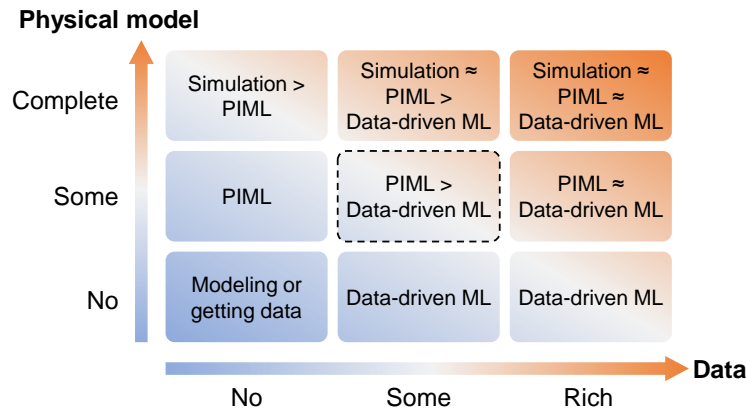


Figure 2: Scenarios under different conditions of physical models and data. PIML is naturally suitable for scenarios where both some physical models and some data are available, which is the most common scenario in practice (indicated by the dashed part). The "≈" sign means that which of the two is superior depends on the specific situation. Here only correct physical models and high-fidelity data are considered.

Due to the prevalence of ordinary DEs (ODEs), partial DEs (PDEs), and other physical laws across diverse phenomena in many disciplines, PINNs and PIML have garnered significant attention and have developed rapidly in recent years. Combustion, as a field inherently rich in physical laws, has experienced an exponential increase in PIML applications over the same period. While numerous reviews have addressed PIML in general and its applications across various domains (see Section 2.2), a comprehensive survey focusing specifically on combustion is still lacking. This paper seeks to fill that gap by providing an extensive review of PIML for combustion—introducing fundamental principles, summarizing major works, highlighting key advancements, proposing a taxonomy of applications and methods, and offering practical suggestions and guidelines for researchers and engineers. In reviewing the existing

literature, a central focus of this paper is to present how combustion laws and machine learning can be integrated, either through soft or hard constraints, via loss functions or representation models, and within coordinate-to-variable or field-to-field paradigms. More importantly, as illustrated in Figure 1(b), this paper aims to provide evidence that PIML can act as a unified bridge connecting physics, model, and data in combustion, thereby inspiring greater engagement from both combustion and AI research communities.

The structure of this paper is shown in Figure 3. Section 2 outlines the fundamental principles, existing reviews, key developments, and related applications of PIML, and also defines the scope and taxonomy adopted in this paper. Section 3 presents the fundamental laws of combustion commonly used in the literature. Sections 4 to 6 provide detailed discussions on PIML applications for combustion chemical kinetics, combustion reacting flows, and other combustion-related problems, respectively. Section 7 compiles publicly available resources, including datasets and benchmarks, simulation tools, and PIML tools. Section 8 offers discussions and future outlooks, while Section 9 concludes the paper.

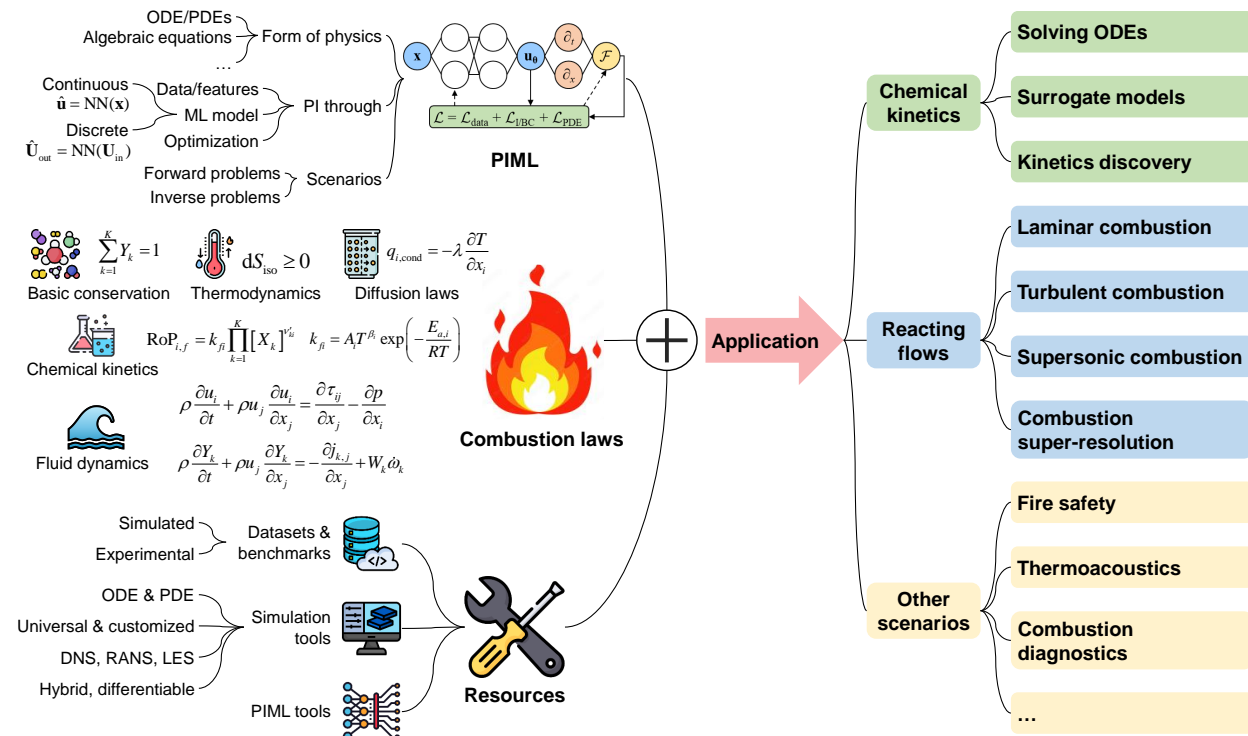


Figure 3: Overview of PIML for combustion. Section 2, Section 3, and Section 7 introduce PIML, combustion laws, and resources, respectively. Sections 4 to 6 introduce the PIML for combustion chemical kinetics, combustion reacting flows, and other combustion problems, respectively. (Some icons are from Flaticon)

## 2 Physics-informed machine learning

This section will give a detailed introduction to PIML. We first present the fundamentals of PIML, and then provide a review of reviews on PIML, from which the scope of this paper can be drawn. The developments and related applications of PIML are then presented.

### 2.1 Fundamentals

This subsection will present the fundamentals of PINNs for solving ODE/PDEs, which is the most basic part of PIML. Figure 4 gives a schematic of PINNs for solving forward and inverse problems of PDEs. As mentioned in Section 1, forward and inverse problems refer to well-posed PDE problems without observation data and ill-posed PDE problems with possible observation data, respectively. The ill-posed problems include incomplete equations, unknown

coefficients, and unknown initial and boundary conditions (IC/BCs). A general form of a PDE problem is given by:

$$\mathcal{F}_i[\mathbf{u}(\mathbf{z}); \boldsymbol{\lambda}] = 0, \quad \mathbf{z} \in \Omega, \quad i = 1, \dots, N_{\text{DE}} \quad (2.1)$$

$$\mathcal{B}_i[\mathbf{u}(\mathbf{z}); \boldsymbol{\lambda}] = 0, \quad \mathbf{z} \in \partial\Omega, \quad i = 1, \dots, N_{\text{IB}} \quad (2.2)$$

where  $\mathbf{u}$  is the solution,  $\mathbf{z} = (t, \mathbf{x}) = (t, x_1, \dots, x_d)$  is the space-time coordinate vector defined on domain  $\Omega$ ,  $\mathcal{F}_i[\cdot]$  is the operator for the  $i$ -th PDE, and  $\mathcal{B}_i[\cdot]$  is the operator for the  $i$ -th IC/BC. For time-independent PDEs,  $\mathbf{z} = \mathbf{x}$ . For ODEs,  $\mathbf{z} \in \mathbb{R}$ , i.e.,  $\mathbf{z} = t$  or  $x$ . The operators are parameterized by  $\boldsymbol{\lambda}$ , such as equation coefficients and boundary values. Note that the initial state is also considered as a part of  $\partial\Omega$ . For inverse problems, there may be observation conditions (OC):

$$\mathcal{O}_i[\mathbf{u}(\mathbf{z}); \boldsymbol{\lambda}] = 0, \quad \mathbf{z} \in \Omega, \quad i = 1, \dots, N_{\text{OC}} \quad (2.3)$$

In PINNs, an NN is used to approximate the solution, denoted by

$$\mathbf{u}_{\boldsymbol{\theta}}(\mathbf{z}) = \hat{\mathbf{u}}(\mathbf{z}) = \text{NN}(\mathbf{z}; \boldsymbol{\theta}) \quad (2.4)$$

where  $\boldsymbol{\theta}$  is the parameters of the NN. Using AD, the derivatives of  $\mathbf{u}_{\boldsymbol{\theta}}$  to  $\mathbf{z}$  can be computed conveniently and then substituted into the operators to get corresponding residuals. The mean squares of the residuals form the loss terms:

$$\mathcal{L}_{\text{DE},i}(\boldsymbol{\theta}, \boldsymbol{\lambda}) = \frac{1}{|\mathcal{S}_{\text{DE},i}|} \sum_{\mathbf{z} \in \mathcal{S}_{\text{DE},i}} |\mathcal{F}[\mathbf{u}_{\boldsymbol{\theta}}(\mathbf{z}); \boldsymbol{\lambda}]|^2, \quad \mathcal{S}_{\text{DE},i} \subset \Omega \quad (2.5)$$

$$\mathcal{L}_{\text{IB},i}(\boldsymbol{\theta}, \boldsymbol{\lambda}) = \frac{1}{|\mathcal{S}_{\text{IB},i}|} \sum_{\mathbf{z} \in \mathcal{S}_{\text{IB},i}} |\mathcal{B}[\mathbf{u}_{\boldsymbol{\theta}}(\mathbf{z}); \boldsymbol{\lambda}]|^2, \quad \mathcal{S}_{\text{IB},i} \subset \partial\Omega \quad (2.6)$$

$$\mathcal{L}_{\text{OC},i}(\boldsymbol{\theta}, \boldsymbol{\lambda}) = \frac{1}{|\mathcal{S}_{\text{OC},i}|} \sum_{\mathbf{z} \in \mathcal{S}_{\text{OC},i}} |\mathcal{O}[\mathbf{u}_{\boldsymbol{\theta}}(\mathbf{z}); \boldsymbol{\lambda}]|^2, \quad \mathcal{S}_{\text{OC},i} \subset \Omega \quad (2.7)$$

where  $\mathcal{S}_{\text{DE}}$  and  $\mathcal{S}_{\text{IB}}$  are the coordinate point sets sampled on the domain and its boundaries, respectively, and  $\mathcal{S}_{\text{OC}}$  is the coordinate point set for observed data. The total loss function is the weighted sum of all loss terms:

$$\mathcal{L}(\boldsymbol{\theta}, \boldsymbol{\lambda}) = \sum_{i=1}^{N_{\text{DE}}+N_{\text{IB}}+N_{\text{OC}}} w_i \mathcal{L}_i(\boldsymbol{\theta}, \boldsymbol{\lambda}) \quad (2.8)$$

where  $w_i$  is the weight for the  $i$ -th loss term. The NN parameters are updated by gradient-based optimization algorithms:

$$\boldsymbol{\theta}_{k+1} = \boldsymbol{\theta}_k - \eta_k f(\nabla_{\boldsymbol{\theta}} \mathcal{L}_k) \quad (2.9)$$

where  $\eta_k$  is the learning rate at the  $k$ -th iteration and  $f$  is a function related to the optimizer. For inverse problems where  $\boldsymbol{\lambda}$  is unknown, it can also be learned by:

$$\boldsymbol{\lambda}_{k+1} = \boldsymbol{\lambda}_k - \eta_k f(\nabla_{\boldsymbol{\lambda}} \mathcal{L}_k) \quad (2.10)$$

The training will stop after predefined iterations/epochs or when the convergence condition is met.

## 2.2 Reviews and scoping

This subsection will provide a brief review of reviews on PIML and PIML for some related fields. We point out two motivations for this subsection. First, these reviews can provide some important facts and perspectives that support some of the views, scoping, and taxonomy of this paper. Second, the reviews listed in this subsection provide a recommended list for readers interested in PIML itself. Readers who wish to learn more about the progress of PIML can refer to these reviews. We can save space on reviewing PIML itself and focus on PIML for combustion.

We first introduce the reviews on PIML in a chronological sequence. Karniadakis *et al.*<sup>65</sup> first provided a comprehensive review of PIML. They pointed out three ways to embed physics into machine learning: observational biases, inductive biases, and learning biases, which correspond to preprocessing the data, designing the model architecture, and modifying the training algorithm, respectively. The classical PINNs belong to the third category, which impose the physical constraints in the loss function, which is a soft manner. Inductive biases is another popular way, with CNNs being the most celebrated example, which respect the invariance in images. Other examples include encoding symmetries, PDEs<sup>73,74</sup>, and chemical laws<sup>75</sup> in model architectures. Shukla *et al.*<sup>76</sup> reviewed not only the classical PINNs but also how physics-informed learning can be accomplished with graph NNs (GNNs). Cuomo *et al.*<sup>77</sup> provided a comprehensive review of PINNs and their variants, covering the NN architectures, learning approaches, theories, applications, and software. Hao *et al.*<sup>78</sup> presented a survey on PIML from the perspective of machine learning researchers.

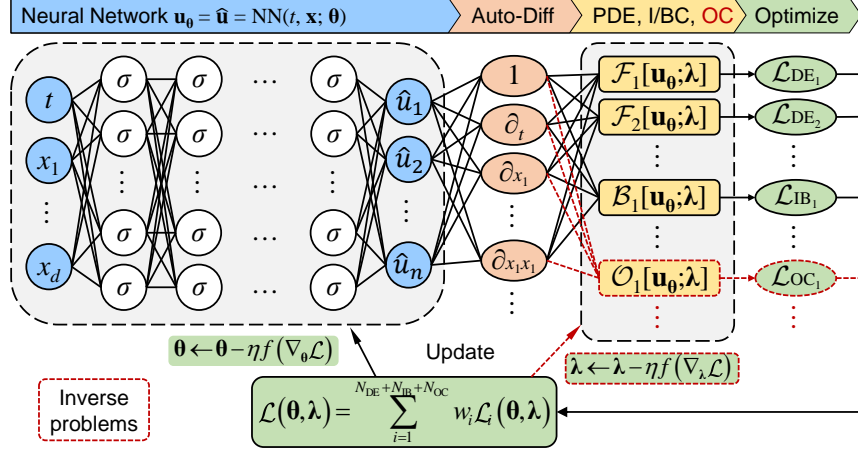


Figure 4: Schematic of PINNs for solving forward and inverse problems of PDEs. The red dashed parts only exist in inverse problems. The blue, green, yellow, and orange parts represent the representation model, optimization process, PDE system, and derivative computation, respectively.

The physics priors were categorized into three types: differential equations, symmetry constraints, and intuitive physics. Various approaches to incorporating physical prior into ML were identified: data, model, objective, optimizer, and inference. They categorized the PIML tasks into two classes: using PIML to solve scientific problems and to solve ML problems. For solving scientific problems, the neural simulation and inverse problems were introduced, where the neural simulation were classified into the neural solvers (i.e., PINNs) and neural operators (NOs). For solving ML problems, the PIML for computer vision and reinforcement learning was summarized. Wang *et al.*<sup>79</sup> provided an expert’s guide to training PINNs, presenting a series of best practices to improve the efficiency and accuracy of PINNs, such as non-dimensionalization, NN architectures, respecting temporal causality, loss balancing, and hard constraints. Faroughi *et al.*<sup>80</sup> presented a review of four NN frameworks: physics-guided NNs, physics-informed NNs, physics-encoded NNs<sup>73</sup>, and NOs. The former three frameworks correspond to the observational, learning, and inductive biases in Reference<sup>65</sup>, respectively. Kim *et al.*<sup>81</sup> reviewed the PINNs on both forward and inverse problems and gave special attention to the multiscale analysis using PINNs. Farea *et al.*<sup>82</sup> reviewed the techniques, applications, trends, and challenges of PINNs. The three ways of integrating prior knowledge into PINNs were pointed out: feature engineering, model construction, and regularization, which is consistent with the taxonomy in References<sup>65,80</sup>. Zhang *et al.*<sup>83</sup> summarized the limitations of PINNs and identified three root causes for their failure: poor multiscale approximation ability and ill-conditioning, weak mathematical rigor, and inadequate integration of physical information. Corresponding future directions and prospects were also provided. More recently, Toscano *et al.*<sup>84</sup> reviewed the recent advances in PIML. They identified three key components of the PIML framework: representation model, governing equation, and optimization process, which correspond to the blue, yellow, and green part of Figure 4, respectively, and is consistent with the taxonomy in Reference<sup>85</sup>. They also reviewed the applications, uncertainty quantification (UQ), theoretical advances, and computational frameworks of PIML, and provided a chronological overview of key advancements in PIML. Meng *et al.*<sup>86</sup> surveyed a wide variety of recent works in PIML. They presented four categories of physics knowledge in PIML: (1) classical mechanics and energy conservation laws, (2) symmetry, invariant and equivariant functions, (3) numerical methods for PDEs, and (4) Koopman theory. Consistent with References<sup>65,80,82</sup>, they also identified three ways to integrate physics knowledge into ML: data enhancement, NN architecture design, and optimization.

Some reviews focus on the PIML for fluid mechanics<sup>87–89</sup>, which can provide some insights for PIML for combustion flows. Note that the classification of PIML in Reference<sup>88</sup> is again consistent with the References<sup>65,80,82,86</sup>, including the physics-informed features and labels, architectures, and loss functions. However, these reviews rarely include combustion or reacting flows. Recently, Sophiya *et al.*<sup>90</sup> reviewed the PINNs in industrial gas turbines (IGTs) research, highlighting their diverse applications in aerodynamics and aeromechanics. However, there are few combustion applications introduced. A more combustion-related review is Reference<sup>91</sup>, which focuses on the PIML in multiphysics modeling in chemical engineering. The applications of PIML in momentum transfer/fluid flow, heat transfer, mass transfer, and chemical reaction were first reviewed separately, then the PIML for multiphysics coupling, surrogate model construction, and design optimization were presented. PIML for chemical engineering has also been briefly reviewed in Reference<sup>84</sup>. However, it should be noted that combustion and chemical engineering do not contain each other, but intersect with each other. They both involve chemical reactions but the range of combustion is more narrower:

a high-temperature exothermic redox chemical reaction by definition. On the other hand, combustion is not limited to chemical engineering, but also involves power generation, transportation, fire safety, and others.

In a broader context, the classical PIML belongs to the category of AI for PDEs (AI4PDEs), which also includes the operator learning. Some researchers have reviewed the AI4PDEs, including DL for PINN and related parameter identification problems<sup>92</sup>, promising directions of AI4PDEs<sup>93</sup>, and AI4PDEs in computational mechanics<sup>94</sup>. Function learning approximates the mapping between finite-dimensional tensor spaces, while operator learning approximates the mapping between infinite-dimensional function spaces. A representative operator is the solution operator of PDEs, which maps the IC/BCs or parameters (e.g., operating, geometrical, physical) to the solution functions. Function learning can only learn a single PDE solution per training, so the model needs to be retrained once conditions or parameters change. As a progress, operator learning can learn parametric PDE solutions at once, providing a method for rapid PDE-based predictions in practice. When the model of operator learning is an NN, it is referred to as neural operator (NO). Two common NOs are the deep operator network (DeepONet)<sup>95</sup> and the Fourier neural operator (FNO)<sup>96</sup>. However, they are both purely data-driven, so their physics-informed versions have also been proposed, i.e., the PI-DeepONet<sup>97</sup> and PI-FNO<sup>98</sup>.

Based on these reviews, some conclusions can be drawn. (1) The scope of PIML has been expanded from the classical PINNs to a broader sense. Table 1 compares the PIML in a narrow and in a broad sense from four aspects: model architecture, ways to inform physics, form of physics, and differentiation. In this paper, both types of PIML will be introduced. Unless otherwise specified, PIML in this paper refers to PIML in a broad sense, while PINNs refer to PIML using NNs as the representation model. Besides, some related terms, such as "physics-guided", "physics-embedded", "physics-encoded", "physics-enforced", "physics-constrained", and "physics-preserved", will all be viewed as "physics-informed" in a broad sense in this paper. (2) Many reviews have consensus on three ways to inform physics<sup>65,80,82,86,88</sup>: through data, (ML) model, and optimization, as summarized in Table 2. Although the data is obtained by scientific means, ML based solely on physics-informed data is still purely data-driven, so it is a weak mechanism for informing physics, as stated in Reference<sup>65</sup>. Therefore, this paper mainly introduces the latter two methods, and the first way will be introduced only if it has a strong embedding. (3) There is a lack of systematic reviews of PIML for combustion, which is the aim of this paper. (4) Many reviews introduce PIML and NOs together. However, most NOs are purely data-driven. This paper will only introduce PIML and physics-informed NOs (PINOs) in detail. By our definition, the latter can also be regarded as a kind of PIML.

Table 1: Comparisons between PIML in a narrow and broad sense.

Aspect	In a narrow sense	In a broad sense
Model architecture	MLP	All models: CNN <sup>99,100</sup> , Transformer <sup>101</sup> , DeepONet <sup>97,102-108</sup> , KAN <sup>109,110</sup> ...
How to inform physics	Loss function	All ways: Model architecture <sup>73-75</sup> , input transformation, output correction <sup>51,52,111-113</sup> , numerical solver <sup>113-116</sup> ...
Form of physics	PDEs	All forms: algebraic equation, inequality, known coefficients <sup>117-120</sup> ...
Differentiation	AD	All methods, such as ND: convolution kernels for space <sup>99,100</sup> , classical schemes for time <sup>73,121</sup> ...

Table 2: Three ways to inform physics into ML.

Aspect	Sub-aspect	Physics
Data	Generation (simulation or experiment), feature selection, cleansing...	Usually weak
Model	Architecture, input/output transformation, embedded numerical solver...	Usually hard constrained
Optimization	Loss addition, loss weights, multi-stage design...	Usually soft constrained

### 2.3 Developments

This subsection will briefly introduce the developments of PIML, focusing mainly on PINNs that use ODE/PDEs as physical constraints, as this is the main and classical part of PIML. Most introductions are brief; for detailed introduction, please refer to the reviews in Section 2.2. Consistent with the taxonomy of References<sup>84,85</sup>, this paper divides PIML into three components: representation model, optimization process, and PDE system, which will be introduced separately in this subsection. Then some miscellaneous important topics will be introduced.

### 2.3.1 Representation model

Representation model is used to represent the solution/field, and corresponds to Equation (2.4) and the blue part of Figure 4. Modifying the representation model can be achieved by designing input/output transformations, activation functions, and the whole architecture.

**Input transformation.** Input transformation, also known as feature embedding, can be denoted by  $\mathbf{u}_\theta(\mathbf{z}) = \text{NN}(f_{\text{input}}(\mathbf{z}); \theta)$ , where  $f_{\text{input}}$  is an input function. It is proven that NNs are more difficult to learn high-frequency features than low-frequency, known as spectral bias or frequency principle<sup>122–124</sup>, so multiscale embedding has been proposed to mitigate this issue. In this case,  $f_{\text{input}}$  can be linear functions<sup>125</sup> or Fourier functions<sup>126–128</sup>. Fourier embeddings can also be used to impose hard constraints on periodic BCs<sup>129,130</sup>.

**Output transformation.** Output transformation can be denoted by  $\mathbf{u}_\theta(\mathbf{z}) = f_{\text{output}}(\text{NN}(\mathbf{z}; \theta))$ , where  $f_{\text{output}}$  is an output function and can also be viewed as the activation function of the output layer.  $f_{\text{output}}$  can be used to constrain the range of  $\mathbf{u}_\theta$ . For example,  $f_{\text{output}}$  can be a positive function for temperature and the Sigmoid function for species mass fractions, which should be in the range of  $[0, 1]$ . Another important use of output transformation is to impose hard constraints on BCs<sup>129,131</sup>, which was adopted as early as the 1990s<sup>72</sup>. As a simple example, to ensure  $u_\theta(x_0) = u_0$ , one can let  $u_\theta = (x - x_0)\text{NN}(x; \theta) + u_0$ . The theory of functional connections (TFC) can systematically achieve the hard constraints of BCs through output transformation. The model is referred to as Deep-TFC<sup>132</sup> and X-TFC<sup>133</sup> when the free function is a deep NN and an extreme learning machine (ELM), respectively.

**Activation function.** Activation functions ( $\sigma$  in Figure 4) introduce nonlinearity to an NN. In order to implement AD to solve PDEs, the activation functions of PINNs need to have good differentiability. The  $\tanh()$  and  $\sin()$  are two common choices. Some adaptive activation functions have been proposed to accelerate the PINNs<sup>134,135</sup>.

**Architecture.** Based on the representation way of the NN, PINNs can be divided into two categories: continuous and discrete PINNs, which are compared in Table 3. Continuous PINNs follow the coordinate-to-variable (query-to-value) mapping way, i.e.,  $\hat{\mathbf{u}} = \text{NN}(\mathbf{z})$ , while discrete PINNs follow the field-to-field mapping way, i.e.,  $\hat{\mathbf{U}}_{\text{out}} = \text{NN}(\mathbf{U}_{\text{in}})$ , where  $\mathbf{U}_{\text{in}}$  and  $\hat{\mathbf{U}}_{\text{out}}$  are the input and output fields of the NN, respectively. Continuous PINNs provide continuous representations because they can directly predict the field values at any given query coordinates without interpolation, while discrete PINNs provide discrete representations because  $\mathbf{U}_{\text{in}}$  and  $\hat{\mathbf{U}}_{\text{out}}$  are always discrete fields on meshes. When  $\mathbf{U}_{\text{in}}$  and  $\hat{\mathbf{U}}_{\text{out}}$  are the fields defined on coarse and fine grids, respectively, the task is called super-resolution (SR) and has been applied to combustion (see Section 5.5). When  $\mathbf{U}_{\text{in}}$  and  $\hat{\mathbf{U}}_{\text{out}}$  are fields at time  $t$  and  $t + \Delta t$ , respectively, the task is usually referred to as autoregressive (AR) learning<sup>136,137</sup>. In this case, the NN can be called a time stepper, next-step predictor, forward propagator<sup>138</sup>, or emulator<sup>137,138</sup>. On the contrary, the classical continuous PINNs belong to the paradigm of non-autoregressive (NAR) learning<sup>136</sup>. The AR paradigm has been widely used in surrogate modeling of chemical kinetics. See Section 4.2 for details. Note that the AR and NAR learning can also be combined to form a hybrid paradigm<sup>136,139,140</sup>. Instead of using AD in continuous PINNs, discrete PINNs employ numerical differentiation (ND) to compute derivatives. In other words, the PDE residual is  $\mathcal{F}[\hat{\mathbf{U}}_{\text{out}}(\mathbf{U}_{\text{in}})]$  computed on  $\mathbf{U}$  using ND, instead of  $\mathcal{F}[\hat{\mathbf{u}}(\mathbf{z})]$  in Equation (2.5) computed on  $\hat{\mathbf{u}}$  and  $\mathbf{z}$  using AD. For spatial derivatives, ND can be achieved using differential convolution kernels (similar to the gradient operators in computer vision<sup>141</sup>), so convolutional NNs (CNNs) are usually adopted. For temporal derivatives, ND can be achieved via classical numerical schemes, such as the Euler scheme. In this case, recurrent NNs (RNN) can be used for modeling the temporal evolution. The choice between continuous and discrete PINNs will be discussed in Section 8.2.

- **Continuous PINNs.** The architectures of continuous PINNs mainly include the MLP, ELM<sup>142</sup>, radial basis network (RBN)<sup>143</sup>, PointNet<sup>144</sup>, DeepONet<sup>95</sup>, and Kolmogorov-Arnold network (KAN)<sup>145,146</sup>. Their physics-informed versions have been proposed: PI-ELM<sup>147</sup>, PI-RBN<sup>148</sup>, PI-PointNet<sup>149</sup>, PI-DeepONet<sup>97</sup>, and PI-KAN<sup>109,110</sup>. Moreover, the basic MLP has been modified in PINNs, including the multiple MLPs<sup>150</sup>, modified MLP<sup>79</sup>, and the physics-informed residual adaptive networks (PirateNets)<sup>151</sup>, which tackles the issue that PINNs have difficulty using very deep NNs. Some generative models, such as the generative adversarial network (GAN)<sup>152</sup> and variational autoencoder (VAE)<sup>153</sup>, can also use MLPs as the building blocks and be extended to the PI-GAN<sup>154</sup> and PI-VAE<sup>155</sup>.
- **Discrete PINNs.** Basic architectures of discrete PINNs include the RNN (represented by the long short-term memory (LSTM) network<sup>156</sup>), CNN<sup>23,157</sup>, recurrent CNN (RCNN), GNN<sup>158</sup>, and Transformer<sup>159</sup>. Some generative models usually use them as the backbone, such as the VAE, GAN, and diffusion model (DM)<sup>160–162</sup>. The basic architectures can also serve as the building blocks of NOs, such as the Fourier neural operator (FNO)<sup>96</sup>. Most of these NNs have their physics-informed extensions, including the PI-LSTM<sup>163</sup>, PI-CNN<sup>99,100</sup>, PI-RCNN (or PhyCRNet)<sup>121</sup>, PI-GNN<sup>164</sup>, PI-Transformer<sup>101,165</sup>, PI-DM<sup>166</sup>, and PI-FNO<sup>98</sup>. Note that the architectures mentioned in continuous PINNs can also be used in discrete PINNs as long as the mapping is a

field-to-field way. The same goes for the generative models, which are architecture-independent. See examples in Section 4.2 and Section 5.5. In fact, the discrete time models proposed in the original paper of PINN can be viewed as a discrete PINN on the temporal dimension<sup>66</sup>, which adopted the MLP and Runge-Kutta scheme. However, the architectures just mentioned (such as the CNNs) are rarely applied to continuous PINNs because they typically do not take coordinates as network inputs.

Table 3: Comparisons between continuous and discrete PINNs. HR and LR represent high-resolution and low-resolution, respectively.

	Continuous PINNs	Discrete PINNs
Definition	$\hat{\mathbf{u}} = \text{NN}(\mathbf{z})$ (coordinate-to-variable)	$\hat{\mathbf{U}}_{\text{out}} = \text{NN}(\mathbf{U}_{\text{in}})$ (field-to-field)
Representation	Continuous (direct query at any points)	Discrete (interpolation at non-grid points)
Differentiation	AD (zero differentiation error, but slower)	ND (faster, but has error)
Learning difficulty	More difficult	Easier
Impose hard constraints	More difficult, especially for PDEs	Easier
Handle large/infinite gradients	Less suitable	More suitable
Handle non-grid data	More suitable	Less suitable
Common architectures	MLP, DeepONet...	CNN, RNN, MLP, DeepONet... (1) AR learning: $\hat{\mathbf{U}}_{t+\Delta t} = \text{NN}(\mathbf{U}_t)$ , such as solving PDE problems and surrogate modeling of chemical kinetics; (2) SR: $\hat{\mathbf{U}}_{\text{HR}} = \text{NN}(\mathbf{U}_{\text{LR}})$
Application	NAR learning, such as solving PDE problems (forward and inverse)	

### 2.3.2 Optimization process

Optimization process corresponds to Equations (2.5) to (2.10) and the green part of Figure 4, during which the loss function will be evaluated and minimized. Therefore, ways to improve the optimization process mainly include modifying the loss definition, loss evaluation, and loss minimization.

**Sampling.** Sampling corresponds to the modification of  $\mathcal{S}$  in Equations (2.5) and (2.6). Basic sampling methods include the uniform, random, and Latin hypercube sampling. To account for the real-time information on the distribution of residuals, thus enhancing the convergence, some adaptive sampling algorithms have been proposed<sup>167-169</sup>.

**Loss weights.** Since PINNs belong to the multi-task learning, the imbalance/conflict among different loss terms is a common failure mode in PINNs<sup>170</sup>. Therefore, the modification of the loss weights, i.e.,  $w$  in Equation (2.8), is important. Some examples include designing learning rate annealing<sup>170</sup>, utilizing the neural tangent kernel (NTK) theory<sup>171</sup>, the self-adaptive loss balanced PINNs (lbPINNs)<sup>172</sup>, and the self-adaptive PINNs (SA-PINNs)<sup>173</sup>. For time-dependent problems, it is important to respect the temporal causality, which can be achieved by assigning different weights to the residual points at different time<sup>174,175</sup>.

**Loss definition.** Some algorithms add loss terms to Equation (2.8) to enhance regularization. Examples are the gradient-enhanced PINNs (gPINNs)<sup>176</sup> and region optimized PINNs (RoPINNs)<sup>177</sup>. Some algorithms replace the  $L^2$  loss in Equations (2.5) to (2.7) with  $L^\infty$  loss<sup>178</sup> and  $L^p$  loss<sup>128</sup>.

**Derivative calculation.** Although AD has no differentiation errors, it is time-consuming, especially for high-order derivatives. In contrast, ND is more efficient. ND can not only be used in discrete PINNs (see Section 2.3.1), but also in continuous PINNs<sup>179</sup>. Furthermore, AD and ND can be used together to form a coupled-automatic-numerical differentiation (can-PINNs)<sup>180</sup>. Although the modifications of derivative calculation directly correspond to the orange part of Figure 4, it will influence the green part (optimization process) through the changes of  $\mathcal{F}(\mathbf{u}_\theta)$  and  $\mathcal{B}(\mathbf{u}_\theta)$  in Equations (2.5) and (2.6).

**Domain decomposition.** Domain decomposition is important when the solution exhibits distinct behaviours in different domains. For time-dependent problems, the time-marching strategy that decomposes the temporal domain can improve the long-time prediction accuracy. In most cases, separate NNs are assigned to different subdomains and the interface conditions between adjacent subdomains need to be considered. Examples of PINNs using domain decomposition include distributed PINNs (DPINNs)<sup>181</sup>, conservative PINNs (cPINNs)<sup>182</sup>, extended PINNs (XPINNs)<sup>183</sup>, parareal PINNs (PPINNs)<sup>184</sup>, parallel PINNs<sup>185</sup>, spatiotemporal parallel PINNs (STPINNs)<sup>186</sup>, augmented PINNs (APINNs)<sup>187</sup>, finite basis PINNs (FBPINNs)<sup>188,189</sup>, and dtPINNs<sup>175</sup>.

**Optimizer.** The most used optimizers in Equations (2.9) and (2.10) are Adam<sup>190</sup> and L-BFGS<sup>191</sup>. Some improved optimizers for PINNs include the MultiAdam<sup>192</sup> and the NNCG<sup>193</sup>.

### 2.3.3 PDE system

An ODE/PDE system consists of ODE/PDEs and IC/BC/OCs, which corresponds Equations (2.1) to (2.3) and the yellow part of Figure 4. The development of this part includes the formal transformations and scope extensions of the PDE system.

**Normalization.** Normalization is essential for both numerical simulation and ML, which can mitigate the magnitude difference between different variables, thus stabilizing the convergence. The normalization of PINNs include the normalization of data, PDEs, IC/BC/OCs, and network inputs and outputs, so it contains the topic of input/output transformation in Section 2.3.1. Normalization is usually a linear transformation, including the non-dimensionalization<sup>79</sup>, standardization<sup>194</sup>, thin-layer normalization<sup>85</sup>, variable scaling<sup>195</sup>, and general linear transformation<sup>85</sup>. The unknown physical parameters (i.e.,  $\lambda$ ) should also be normalized in inverse problems<sup>85</sup>.

**Variational form.** The variational form of PDEs is essential for traditional FEM solvers and has been applied to PINNs<sup>196,197</sup>. Similar to the variational form, the energy form of PDEs is important in solid mechanics<sup>94</sup> and has also been adopted in PINNs<sup>198–201</sup>. An advantage of variational form is the reduction of derivative order compared to the original PDEs, thus accelerating the computation.

**Other formal transformations.** For example, the stream function can be used in 2D incompressible flow problems<sup>170,202</sup>. In this way, the continuity/incompressibility equation can be exactly satisfied but higher-order derivatives are introduced. Besides, the common velocity-pressure form of incompressible NS equations can be transformed to the vorticity-velocity form<sup>203</sup>. For inverse problems with sparse and noisy data, the filtered PDEs can serve as an effective substitute for the original PDEs<sup>204</sup>.

**Other DE types.** PINNs have also been applied to non-traditional types of DEs, such as fractional DEs<sup>205</sup> and stochastic DEs<sup>154,155</sup>.

### 2.3.4 Other important topics

There are some other important topics that either do not fall under any of the above topics or may involve more than one of them.

**Hard constraint.** The classical PINNs impose the physical constraints in a soft manner, so there is still a possibility that physical constraints will be violated if the corresponding residuals do not converge. In contrast, hard constraints can ensure the physical laws are exactly satisfied, thus reducing the number of loss terms in most cases. Hard constraints are also referred to as physics "-embedded", "-encoded", "-enforced", "-preserved" in many papers. For IC/BCs, they can be enforced by input and output transformations as mentioned in Section 2.3.1. BCs can also be strictly encoded in discrete PINNs via padding operations<sup>99,121</sup>. For PDEs, one example is to enforce the continuity equation using the stream function as mentioned in Section 2.3.3. PDEs can also be constrained by linear projection<sup>111</sup>. For discrete PINNs, PDEs can be encoded using convolutional kernels, such as the physics-encoded RCNN (PeRCNN)<sup>73</sup> and the PDE-preserved NN (PPNN)<sup>74</sup>, and can be constrained using traditional numerical methods/solvers<sup>113–116</sup>. In a broad sense, any explicitly written physical laws that are always satisfied can be regarded as hard constraints. For combustion, the species and element conservations can also be enforced. See Section 4.2 and Equation (5.2) for details. The laws of chemical kinetics can also be embedded, which will be introduced in Section 4.3. The choice between soft and hard constraints will be discussed in Section 8.2.

**Parametric/surrogate modeling.** Parametric/surrogate modeling aims to overcome the limitation of PINNs that can only solve a single PDE at a time. The simplest and most common way is to directly add the parameters to the network inputs, i.e., Equation (2.4) becomes  $\mathbf{u}_\theta(\mathbf{z}, \lambda) = \text{NN}(\mathbf{z}, \lambda; \theta)$ . See some examples in Section 2.4. Other algorithms include utilizing the metalearning<sup>206</sup>, generative pretrained PINNs (GPT-PINNs)<sup>207</sup>, and the P<sup>2</sup>INN<sup>208</sup>. Furthermore, the PINOs mentioned in Section 2.2 are specifically designed for parametric/surrogate modeling, so they can be regarded as a type of parametric PINNs as well.

**Ill-conditioning and preconditioning.** Similar to traditional numerical methods, ill-conditioning is also present in PINNs and may also be referred to as pathology<sup>170</sup> or failure mode<sup>209</sup> in some cases. In a narrow sense, ill-conditioning in PINNs has been attributed to the PDE system/problem or differential operator (i.e.,  $\mathcal{F}$ ) itself. Examples in combustion include the stiffness in ODEs of chemical kinetics (see Section 4.1), the chaoticity of turbulence, and any other intrinsic complexities. Ill-conditioning in PINNs has been analyzed from different perspectives: a derived operator<sup>210</sup>, loss landscape<sup>193</sup>, error-residual ratio<sup>211</sup>, and control system<sup>212</sup>, in which different definitions of the condition number have also been proposed to evaluate the ill-conditioning. Corresponding preconditioning strategies include scaling the model parameters (i.e.,  $\theta$ )<sup>210</sup>, using second-order optimizers<sup>193</sup>, discretizing the PDE system<sup>211</sup>, and leveraging the pseudo time-stepping method<sup>212</sup>. The normalization strategies mentioned in Section 2.3.3 can also be viewed as a kind of preconditioning for the PDE system. In a broad sense, ill-conditioning in PINNs can also originates from the

representation model and optimization process, such as the aforementioned spectral bias of NNs (Section 2.3.1) and the issue of loss imbalance/conflict (Section 2.3.2).

**Uncertainty quantification (UQ).** UQ is important for reliable modeling of practical systems due to the intrinsic incompleteness of data and model as well as the discrepancies between them<sup>213</sup>. UQ has been applied in PINNs for quantifying both data uncertainty<sup>214–216</sup> and model uncertainty<sup>217</sup>.

**Theory.** The total error of PINNs can be decomposed into three parts<sup>218</sup>: approximation error, estimation error, and optimization error. Many studies have estimated the errors of PINNs, such as for forward problems<sup>219</sup>, inverse problems<sup>220</sup>, Kolmogorov PDEs<sup>221</sup>, and NS equations<sup>222</sup>. The aforementioned NTK theory for PINNs<sup>171</sup> and ill-conditioning in PINNs are also theoretical advances in PIML.

## 2.4 Related applications

PIML has been widely applied to fluid mechanics, ranging from incompressible flows<sup>202,203</sup> to supersonic flows<sup>223–225</sup>, from laminar flows<sup>202</sup> to turbulent flows<sup>226–230</sup> and transitional flows<sup>231</sup>, from single-phase flows to two-phase flows<sup>232–234</sup>, from internal flows to external flows such as boundary layer flows<sup>85,235–237</sup>, and from analytical and computational fluid mechanics<sup>203</sup> to experimental fluid mechanics<sup>204,238–243</sup>. Compared to forward problems, solving inverse problems using PINNs serves as a new paradigm in fluid mechanics which compensates for the shortcomings of traditional algorithms. One representative method is the hidden fluid mechanics (HFM)<sup>244</sup>, which can reconstruct the velocity and pressure fields based on the observations of concentration. Flow field reconstruction is quite important for experimental fluid mechanics because the data are always sparse, noisy, and partial. For that, PINNs have been widely applied to enhance the experimental data obtained from particle image velocimetry (PIV)<sup>239,240</sup>, particle tracking velocimetry (PTV)<sup>239,243</sup>, and other measurements<sup>204,238,241,242</sup>. Inverse problems are also important for turbulence modeling based on Reynolds-averaged Navier-Stokes (RANS) equations and large eddy simulations (LES), where PINNs have been applied to both the task of field reconstruction<sup>226–228</sup> and parameter inference<sup>229,230</sup>. The parametric/surrogate modeling mentioned in Section 2.3.4 has also been applied to fluid mechanics, including the cardiovascular flows<sup>245</sup>, Euler equations<sup>225</sup>, and flows around airfoils<sup>246–248</sup>. For more details of PINNs for fluid mechanics, readers can refer to these reviews<sup>87–89</sup>. In addition to pure fluid flows, PINNs have also been applied to heat transfer<sup>249–251</sup>, mass transfer, and multi-species flows<sup>252</sup>. These are all subprocesses of combustion reacting flows. For a detailed introduction, please refer to this review<sup>91</sup>.

## 3 Physical laws in combustion

Combustion is a typical convection-diffusion-reaction (CDR) process, where reaction is the main feature that distinguishes it from other types of flow. Therefore, many physical laws exist in combustion and can be integrated into PIML, either in a soft or hard manner. This section will present the basic physical laws in combustion, which are summarized from References<sup>4–8</sup> and are categorized into the laws of multicomponent system, thermodynamics, diffusion "kinetics", chemical kinetics, and fluid dynamics. Although this section is common knowledge for combustion-side researchers, we believe it can serve as an important reference for AI-side researchers.

### 3.1 Multicomponent system

Consider a gaseous multicomponent system consisting of  $K$  species. The molecular weight, mass fraction, mole fraction, and molar concentration of species  $k$  are denoted as  $W_k$ ,  $Y_k$ ,  $X_k$ , and  $[X_k]$ , respectively. Species conservation is expressed by:

$$\sum_{k=1}^K Y_k = 1, \quad \sum_{k=1}^K X_k = 1 \quad (3.1)$$

Element conservation demands the total mass or amount of each element  $i$  keep constant in a closed system:

$$m_{e,i} = m \sum_{k=1}^K \frac{\alpha_{ik} W_{e,i}}{W_k} Y_k = \text{const}, \quad i = 1, \dots, N_e \quad (3.2)$$

$$n_{e,i} = n \sum_{k=1}^K \alpha_{ik} X_k = \text{const}, \quad i = 1, \dots, N_e \quad (3.3)$$

where  $m$  denotes the mass,  $n$  denotes the amount of substance, the subscript  $e$  represents element, and  $\alpha_{ik}$  is the number of element  $i$  in the chemical formula of species  $k$ . The mean molecular weight of the mixture is calculated by:

$$W = \sum_{k=1}^K X_k W_k = \left( \sum_{k=1}^K Y_k / W_k \right)^{-1} \quad (3.4)$$

and the mean density is given by:

$$\rho = \sum_{k=1}^K [X_k] W_k = W \sum_{k=1}^K [X_k] \quad (3.5)$$

Note that  $Y_k$ ,  $X_k$ , and  $[X_k]$  are dependent:

$$X_k = \frac{W}{W_k} Y_k \quad (3.6)$$

$$[X_k] = \frac{\rho}{W_k} Y_k \quad (3.7)$$

### 3.2 Thermodynamics

The basic thermodynamic properties include the pressure  $p$ , temperature  $T$ , volume  $V$ , entropy  $S$ , and four energy functions: internal energy  $U$ , enthalpy  $H = U + pV$ , Helmholtz free energy  $A = U - TS$ , and Gibbs free energy  $G = H - TS$ . The species and their mixture must satisfy a state equation. Take the simplest ideal gas equation for example:

$$pV = nRT \quad \text{or} \quad pW = \rho RT \quad (3.8)$$

where  $n$  is the amount of substance and  $R = 8.314 \text{ J}/(\text{mol} \cdot \text{K})$  is the universal gas constant.

The first law of thermodynamics for a closed system, which is equivalent to the energy conservation, is given by:

$$dU = \delta Q - \delta W \quad (3.9)$$

where  $\delta Q$  is the heat supplied to the system from its surroundings and  $\delta W$  is the work done by the system. The second law of thermodynamics states that the entropy of an isolated system will not decrease:

$$dS_{\text{iso}} \geq 0 \quad (3.10)$$

where "=" holds only for reversible processes and equilibrium states. For closed systems, many inequalities can be derived:  $(dS)_{U,V} \geq 0$ ,  $(dS)_{H,p} \geq 0$ ,  $(dU)_{S,V} \geq 0$ ,  $(dH)_{S,p} \geq 0$ ,  $(dA)_{T,V} \geq 0$ ,  $(dG)_{T,p} \geq 0$ , where the last one is always used for chemical equilibrium. Based on the first and second laws, the basic differential relations of thermodynamics can be derived:  $dU = TdS - pdV$ ,  $dH = TdS + Vdp$ ,  $dA = -SdT - pdV$ , and  $dG = -SdT + Vdp$ , which hold for systems with constant compositions.

In combustion simulations, the temperature-dependent relations of thermodynamic properties are needed, which are often provided for the heat capacity  $C_p$ ,  $H$ , and  $S$  at standard pressure  $p^\circ$ :  $C_{p,k}^\circ(T)$ ,  $H_k^\circ(T)$ , and  $S_k^\circ(T)$ , where the superscript  $\circ$  denotes standard pressure. The relations must satisfy the definition of  $C_p$  and the aforementioned differential relation of  $H$ :

$$C_{p,k}^\circ = \frac{dH_k^\circ}{dT} = T \frac{dS_k^\circ}{dT} \quad (3.11)$$

The relations are often in the form of polynomials of  $T$ , such as the NASA 7-coefficient polynomials. At pressure  $p$ , the corresponding properties are:  $C_{p,k} = C_{p,k}^\circ$ ,  $H_k = H_k^\circ$ , and  $S_k = S_k^\circ - R \ln(p/p^\circ)$ . Compared to mole-based properties, mass-based properties are more commonly used:  $c_{p,k} = C_{p,k}/W_k$ ,  $h_k = H_k/W_k$ ,  $s_k = S_k/W_k$ . The mean thermodynamic properties can be calculated by<sup>7</sup>:

$$C_p = \sum_{k=1}^K C_{p,k} X_k, \quad c_p = \frac{C_p}{W} = \sum_{k=1}^K c_{p,k} Y_k \quad (3.12)$$

$$H = \sum_{k=1}^K H_k X_k, \quad h = \frac{H}{W} = \sum_{k=1}^K h_k Y_k \quad (3.13)$$

$$S = \sum_{k=1}^K (S_k - R \ln X_k) X_k, \quad s = \frac{S}{W} \quad (3.14)$$

Other properties such as  $U$ ,  $A$ , and  $G$  can be obtained by their definitions.

### 3.3 Diffusion "kinetics"

Combustion involves the basic transport phenomena, including the diffusion of momentum, heat, and mass. The corresponding transport properties are the viscosity  $\mu_k$ , thermal conductivity  $\lambda_k$ , and binary diffusion coefficients  $D_{kj}$  between species  $k$  and  $j$ . These properties can be calculated either by theories such as the molecular theory or by temperature-dependent relations<sup>4,7,8</sup>. Diffusion laws describe the relationship between momentum flux (i.e., viscous tensor)  $\boldsymbol{\tau}$ , energy flux  $\mathbf{q}$ , and species mass flux  $\mathbf{j}_k$  with respect to their driving forces. The momentum flux is given by the definition of Newtonian fluid:

$$\tau_{ij} = \mu \left( \frac{\partial u_i}{\partial x_j} + \frac{\partial u_j}{\partial x_i} - \frac{2}{3} \frac{\partial u_k}{\partial x_k} \delta_{ij} \right) \quad (3.15)$$

where  $u$  is the velocity and the subscripts  $i, j$  denote the spatial dimensions. The energy flux is given by:

$$q_i = -\lambda \frac{\partial T}{\partial x_i} + \sum_{k=1}^K j_{k,i} h_k - \sum_{k=1}^K \frac{RT}{W_k X_k} D_k^T d_{k,i} \quad (3.16)$$

where the three terms represent the contributions of temperature gradient (Fourier's law), species diffusion, and Dufour effect, respectively.  $d_{k,i}$  is the diffusion driving force, and  $D_k^T$  is the thermal diffusion coefficient.  $d_{k,i}$  and  $j_{k,i}$  are given by:

$$d_{k,i} = \frac{\partial X_k}{\partial x_i} + (X_k - Y_k) \frac{1}{p} \frac{\partial p}{\partial x_i} \quad (3.17)$$

$$j_{k,i} = \rho Y_k V_{k,i} \quad (3.18)$$

$$V_{k,i} = \frac{1}{X_k W} \sum_{j=1}^K W_j D_{kj} d_{j,i} - \frac{D_k^T}{\rho Y_k T} \frac{\partial T}{\partial x_i} \quad (3.19)$$

where  $V_{k,i}$  is the diffusion velocity of species  $k$  on dimension  $i$  and its second term represents the Soret effect.

The mean properties can be calculated either by the multicomponent method or by mixture-averaged approximations. In the latter case, for example, the mixture-averaged properties are calculated by:

$$\mu = \sum_{k=1}^K \frac{\mu_k X_k}{\sum_{j=1}^K \Phi_{kj} X_j} \quad (3.20)$$

$$\Phi_{kj} = \frac{1}{\sqrt{8}} \left( 1 + \frac{W_k}{W_j} \right)^{-\frac{1}{2}} \left[ 1 + \left( \frac{\mu_k}{\mu_j} \right)^{\frac{1}{2}} \left( \frac{W_j}{W_k} \right)^{\frac{1}{4}} \right]^2 \quad (3.21)$$

$$\lambda = \frac{1}{2} \left( \sum_{k=1}^K X_k \lambda_k + \frac{1}{\sum_{k=1}^K X_k / \lambda_k} \right) \quad (3.22)$$

$$D_{km} = \frac{1 - Y_k}{\sum_{j \neq k}^K X_j / D_{jk}} \quad (3.23)$$

where  $D_{km}$  is the mean diffusion coefficient of species  $k$  to other species. In an isobaric process, the diffusion velocity can be simplified to:

$$V_{k,i} = -\frac{1}{X_k} D_{km} \frac{\partial X_k}{\partial x_i} - \frac{D_k^T}{\rho Y_k T} \frac{\partial T}{\partial x_i} \quad (3.24)$$

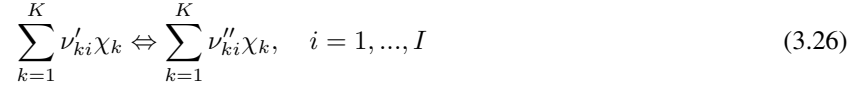
where the first term represents the Fick's law. Note that the mixture-averaged approximations violate the mass flux conservation:

$$\sum_{k=1}^K \mathbf{j}_k = \rho \sum_{k=1}^K Y_k \mathbf{V}_k = 0 \quad (3.25)$$

A common trick to address this is to further correct  $\mathbf{j}_k$  by  $\mathbf{j}_k \leftarrow \mathbf{j}_k - Y_k \sum_{k=1}^K \mathbf{j}_k$ .

### 3.4 Chemical kinetics

Here only gas-phase chemical reactions are considered. Practical reactions consist of multiple elementary reactions. A reaction system involving  $K$  species and  $I$  reactions can be represented as:



where  $\chi_k$  is the symbol of species  $k$ ,  $\nu'$  and  $\nu''$  indicate forward and reverse stoichiometric coefficients, respectively. The net stoichiometric coefficient is defined as:

$$\nu_{ki} = \nu''_{ki} - \nu'_{ki} \quad (3.27)$$

The rate-of-progress variable of reaction  $i$  (unit: mol/(m<sup>3</sup>·s)) can be computed by the law of mass action:

$$\text{RoP}_i = k_{fi} \prod_{k=1}^K [X_k]^{\nu'_{ki}} - k_{ri} \prod_{k=1}^K [X_k]^{\nu''_{ki}} \quad (3.28)$$

where  $k_{fi}$  and  $k_{ri}$  are forward and reverse rate constants of reaction  $i$ . Then the production rate of species  $k$  is:

$$\dot{\omega}_k = \sum_{i=1}^I \nu_{ki} \text{RoP}_i \quad (3.29)$$

The mass conservation of chemical reactions is written as:

$$\sum_{k=1}^K \nu_{ki} W_k = 0, \quad i = 1, \dots, I \quad (3.30)$$

so that

$$\sum_{k=1}^K W_k \dot{\omega}_k = \sum_{i=1}^I \left( \text{RoP}_i \sum_{k=1}^K \nu_{ki} W_k \right) = 0 \quad (3.31)$$

The forward rate constants are usually computed by the Arrhenius law:

$$k_{fi} = A_i T^{\beta_i} \exp\left(-\frac{E_{a,i}}{RT}\right) \quad (3.32)$$

where  $A$ ,  $\beta$ , and  $E_a$  are the pre-exponential factor, temperature exponent, and activation energy, respectively. The reverse rate constants are computed by chemical equilibrium:

$$k_{ri} = k_{fi} / K_{c,i} \quad (3.33)$$

$$K_{c,i} = K_{p,i} \left(\frac{p^\circ}{RT}\right)^{\sum_{k=1}^K \nu_{ki}} \quad (3.34)$$

$$K_{p,i} = \exp\left(-\frac{\Delta G_i^\circ}{RT}\right) = \exp\left(\frac{\Delta S_i^\circ}{T} - \frac{\Delta H_i^\circ}{RT}\right) \quad (3.35)$$

$$\Delta S_i^\circ = \sum_{k=1}^K \nu_{ki} S_k^\circ \quad (3.36)$$

$$\Delta H_i^\circ = \sum_{k=1}^K \nu_{ki} H_k^\circ \quad (3.37)$$

where  $K_c$  and  $K_p$  are concentration-based and pressure-based equilibrium constants, respectively.

The above discussions are the most basic models. In practical reaction mechanisms, some exceptions exist, such as specified reaction order, three-body reactions, pressure-dependent reactions, and irreversible reactions<sup>4,7,8</sup>. In these cases, Equations (3.28) and (3.32) may be modified. For irreversible reactions (i.e., " $\Leftrightarrow$ " become " $\Rightarrow$ "),  $k_{ri} = 0$  instead of Equation (3.33).

### 3.5 Fluid dynamics

The governing equations for reacting flows include the conservations of mass, momentum, energy, and species<sup>5,6</sup>:

$$\frac{\partial \rho}{\partial t} + \frac{\partial \rho u_i}{\partial x_i} = 0 \quad (3.38)$$

$$\rho \frac{\partial u_i}{\partial t} + \rho u_j \frac{\partial u_i}{\partial x_j} = \frac{\partial \tau_{ij}}{\partial x_j} - \frac{\partial p}{\partial x_i} \quad (3.39)$$

$$\rho \frac{\partial e}{\partial t} + \rho u_j \frac{\partial e}{\partial x_j} = -\frac{\partial q_j}{\partial x_j} - (\tau_{ij} - p\delta_{ij}) \frac{\partial u_i}{\partial x_j} \quad (3.40)$$

$$\rho \frac{\partial Y_k}{\partial t} + \rho u_j \frac{\partial Y_k}{\partial x_j} = -\frac{\partial j_{k,j}}{\partial x_j} + W_k \dot{\omega}_k, \quad k = 1, \dots, K \quad (3.41)$$

where the Einstein summation convention is adopted and  $e$  is the energy, containing both sensible and chemical energy. Note that the external forces and heat sources are not considered. The energy equation is usually rewritten as the equation of  $T$ <sup>5</sup>:

$$\begin{aligned} \rho c_p \frac{\partial T}{\partial t} + \rho c_p u_j \frac{\partial T}{\partial x_j} = & \frac{\partial}{\partial x_j} \left( \lambda \frac{\partial T}{\partial x_j} \right) - \left( \sum_{k=1}^K j_{k,j} c_{p,k} \right) \frac{\partial T}{\partial x_j} \\ & - \sum_{k=1}^K h_k W_k \dot{\omega}_k + \left( \frac{\partial p}{\partial t} + u_j \frac{\partial p}{\partial x_j} \right) + \tau_{ij} \frac{\partial u_i}{\partial x_j} \end{aligned} \quad (3.42)$$

where the five terms of the RHS represent the contributions of thermal conduction, species diffusion, reaction heat release, pressure change, and viscous heating, respectively.

Equations (3.38) to (3.42) are the unsimplified governing equations for reacting flows and are used for direct numerical simulation (DNS). To save computational resources, simplified models are used in many cases. For example, the concepts of reaction progress variable ( $c$ ) and mixture fraction ( $Z$ ) can be derived in the contexts of premixed and non-premixed combustion, respectively<sup>5</sup>. Under certain assumptions, their governing equations can also be derived, which are fewer than the original equations. For turbulent combustion, the governing equations for Reynolds-averaged Navier-Stokes simulation (RANS) and large eddy simulation (LES) are also different from Equations (3.38) to (3.42). For two types of turbulent combustion models, namely the transport probability density function (TPDF) method<sup>253</sup> and the flamelet-like method<sup>13,254</sup>, including the flamelet generated manifolds (FGM)<sup>15,255</sup> and flamelet/progress variable (FPV) method<sup>256,257</sup>, the corresponding governing equations are also different from Equations (3.38) to (3.42). For the sake of brevity, these simplified methods are not described in detail here. For details, readers can refer to the corresponding references.

## 4 PIML for combustion chemical kinetics (0D combustion)

Combustion chemical kinetics can be regarded as a kind of 0D combustion, because it mainly involves combustion state variables and their time derivatives and does not involve spatial processes such as flow and diffusion. Chemical reactions are probably the most central feature of combustion, so there is a lot of research on PIML for the chemical kinetics of combustion, which will be presented in this section. Based on the research status, the introduction in this section is not limited to PIML in the narrow sense and chemical kinetics in combustion. On the one hand, these studies not only inform physics through loss functions, but also in other ways, such as network structures. As mentioned in Section 2.3, these physics-guided, physics-embedded, and physics-constrained ML can be regarded as PIML in a broad sense, so the related work will also be introduced in this section. On the other hand, chemical kinetics is not only present in combustion but also in other chemical processes. The studies of PIML for general chemical kinetics is instructive and can even be directly applied to combustion chemical kinetics, so some of the related work is also introduced in this section. Some representative studies on PIML for combustion chemical kinetics are listed in Table 4, which can be divided into three categories: solving ODEs of chemical kinetics, surrogate modeling of chemical kinetics, and applications of neural ODEs to surrogate modeling and kinetics discovery, which are detailed in the next three subsections, respectively.

### 4.1 Solving ODEs of chemical kinetics

As shown in Equations (3.38) to (3.42), the governing PDEs become ODEs of chemical kinetics when the spatial gradients are all zero, and the reaction source terms become the only driving force for the combustion system. The

Table 4: Recent studies on PIML for combustion and combustion-like chemical kinetics.  $C_{\text{ele}}$ ,  $C_{\text{spe}}$ , and  $C_{\text{ene}}$  represent the conservations of elements (atoms), species (total mass), and energy, respectively. PVG and MA mean progress variable generation and manifold approximation, respectively.

Study	Method abbreviation	Aim	How to inform/embed physics	Codes
Ji <sup>258</sup> , 2021.8	stiff-PINN	Solve stiff ODEs	Loss of ODEs	<a href="#">URL</a>
De Florio <sup>259</sup> , 2022.6	–	Solve stiff ODEs	Loss of ODEs	–
Wang <sup>260</sup> , 2022.7	–	Solve stiff ODEs	Loss of ODEs	–
Galaris <sup>261,262</sup> , 2021.8	PI-RPNN	Solve stiff ODEs	Loss of ODEs	<a href="#">URL</a>
Li <sup>263</sup> , 2021.10	–	Solve ODEs	Loss of ODEs	–
Weng <sup>264</sup> , 2022.11	M-PINN	Solve stiff ODEs (inverse)	Loss of ODEs	–
Gusmao <sup>265</sup> , 2022.4	KINN	Solve ODEs (forward and inverse)	Loss of ODEs, $C_{\text{spe}}$ by trigonometric transformation	<a href="#">URL</a>
Bibeau <sup>266</sup> , 2023.12	–	Solve inverse ODEs (parameter inference)	Loss of ODEs	<a href="#">URL</a>
Almeldein <sup>267</sup> , 2023.7	–	Surrogate model	Loss of $C_{\text{ele}}$	–
Zhang <sup>268</sup> , 2024.8	CRK-PINN	Surrogate model	Losses of ODEs, $C_{\text{ele}}$ , $C_{\text{spe}}$ , and $C_{\text{ene}}$	–
Wan <sup>51</sup> , 2020.7	–	Surrogate model of reduced chemistry	$C_{\text{ele}}$ by correction	–
Wang <sup>113</sup> , 2025.3	ANN-hard	Surrogate model	$C_{\text{ele}}$ by correction, $C_{\text{ene}}$ by using equations	<a href="#">Dataset</a>
Kumar <sup>102,103</sup> , 2023.12	–	Surrogate model	Losses of $C_{\text{ele}}$ and $C_{\text{spe}}$	–
Zanardi <sup>104</sup> , 2021.12	–	Surrogate model	Loss of ODEs	–
Zanardi <sup>105</sup> , 2023.9	CG-DeepONet	Surrogate model	Loss of ODEs, Boltzmann layer, hierarchical architecture	–
Weng <sup>269</sup> , 2024.11	EFNO	Surrogate model	Losses of $C_{\text{ele}}$ and $C_{\text{spe}}$	–
Readshaw or Ding <sup>270-272</sup> , 2021.3	HFRD-MMP	Surrogate model	$C_{\text{spe}}$ by normalization	–
Readshaw <sup>273</sup> , 2023.4	–	Surrogate model	$C_{\text{ele}}$ by recalculating residual species	–
Salunkhe <sup>274,275</sup> , 2022.6	ChemTab	Surrogate model (PVG and MA)	Constraints on the projection matrix and progress variables	–
Vijayarangan <sup>276</sup> , 2023.11	–	Surrogate model by NODE	Dynamics-informed discovery of latent space	–
Kumar <sup>277,278</sup> , 2023.11	PC-NODE	Surrogate model by NODE	Loss of $C_{\text{ele}}$	–
Kumar <sup>279</sup> , 2024.12	Phy-ChemNODE	Surrogate model by NODE	Dynamics-informed discovery of latent space, loss of $C_{\text{ele}}$	–
Koenig <sup>280</sup> , 2025.7	ChemKAN	Surrogate model by NODE	Architecture that mimics the chemical kinetics, loss of $C_{\text{ele}}$	–
Sorourifar <sup>117</sup> , 2023.9	r-NODE, k-NODE	Surrogate model by NODE	Embedded stoichiometric and rate information	–
Fedorov <sup>118</sup> , 2023.10	KC-NODE	Surrogate model by NODE	Embedded stoichiometry and rate expression	<a href="#">URL</a>
Kircher <sup>119,120</sup> , 2024.2	GRNN	Surrogate model by NODE	Embedded stoichiometry and thermodynamics	–
Ji <sup>75</sup> , 2021.1	CRNN	Discover kinetics	Embedded rate expression	<a href="#">URL</a>
Su <sup>281</sup> , 2023.3	–	Learn kinetics parameters	Embedded rate expression	–
Doeppel <sup>282</sup> , 2024.7	AC-CRNN	Discover kinetics	Embedded rate expression, $C_{\text{ele}}$ by a NN layer	–

ODEs are given by:

$$\frac{dT}{dt} = -\frac{1}{\rho c_p} \sum_{k=1}^K h_k W_k \dot{\omega}_k \quad (4.1)$$

$$\frac{dY_k}{dt} = \frac{1}{\rho} W_k \dot{\omega}_k, \quad k = 1, \dots, K \quad (4.2)$$

An general ODE system can be written as:

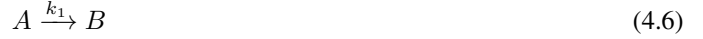
$$\frac{d\mathbf{y}}{dt} = \mathbf{f}(\mathbf{y}, t), \quad t \in [0, T] \quad (4.3)$$

$$\mathbf{y}(t=0) = \mathbf{y}_0 \quad (4.4)$$

which is an initial value problem (IVP) and  $\mathbf{y} = [y_1, \dots, y_N]^T$  is the vector of dependent variables. One of the most challenging aspects of solving ODEs is the stiffness, where an ODE system is characterized by dynamics with widely separated time scales, which is also common in combustion chemical kinetic problems. A commonly used indicator to quantify the stiffness is the stiffness ratio. Consider a linearized ODE system:  $d\mathbf{y}/dt = \mathbf{J}\mathbf{y}$ , where  $\mathbf{J}$  is the Jacobian matrix, then the stiffness ratio is defined as:

$$S = \frac{\max_j \{|\Re(\lambda_j)|\}}{\min_j \{|\Re(\lambda_j)|\}} = \frac{\tau_{\text{slowest}}}{\tau_{\text{fastest}}} \quad (4.5)$$

where  $\lambda_j \in \mathbb{C}$  are the eigenvalues of  $\mathbf{J}$ . The reciprocals of the eigenvalues can represent the time scales,  $\tau$ , of the system<sup>276</sup>. To validate the algorithms (traditional and PINNs) for solving stiff ODEs, some classical problems are widely tested, including the ROBER and POLLU problems, which consist of 3 species and 3 reactions, and 20 species and 25 reactions, respectively. As an example, the ROBER problem describes the following reaction:



So the evolution of the species concentrations are described by the following ODEs:

$$\frac{dy_1}{dt} = -k_1 y_1 + k_3 y_2 y_3 \quad (4.9)$$

$$\frac{dy_2}{dt} = k_1 y_1 - k_2 y_2^2 - k_3 y_2 y_3 \quad (4.10)$$

$$\frac{dy_3}{dt} = k_2 y_2^2 \quad (4.11)$$

where  $y_1$ ,  $y_2$ , and  $y_3$  are the concentrations of  $A$ ,  $B$ , and  $C$ , respectively. The default IC is  $\mathbf{y}(0) = [1, 0, 0]^T$ . The reaction rate constants are  $k_1 = 0.04$ ,  $k_2 = 3 \times 10^7$ , and  $k_3 = 10^4$ , which vary in a range of nine orders of magnitude, thus resulting in the strong stiffness of the system.

Ji *et al.*<sup>258</sup> first proposed the stiff-PINNs (shown in Figure 5), using PINNs to solve stiff chemical kinetic ODEs, where the quasi-steady-state assumption (QSSA) was employed to reduce the stiffness of the system. In QSSA, QSS species are identified by assuming that their net production rates are negligible compared to their consumption and production rates, then the ODEs of QSS species become differential-algebraic equations (DAEs). For example,  $B$  can be chosen as the QSS species in the ROBER problem, so its algebraic equation can be obtained by assuming  $dy_2/dt = 0$ . Because QSS species are usually radicals and unstable intermediates with short time scales, the elimination of their ODEs can greatly reduce the stiffness. The stiff-PINNs were used to solve the ROBER and POLLU problems with one and ten QSS species, respectively, and yielded satisfactory results. De Florio *et al.*<sup>259</sup> used X-TFC<sup>133</sup> (see Section 2.3.2) to solve stiff chemical kinetic ODEs, where the TFC can guarantee the ICs are exactly satisfied, as illustrated in Figure 6. The temporal domain was decomposed into several intervals to deal with the long-time issue. The X-TFC showed great performance for 4 tested problems, and even outperformed the traditional numerical methods in some cases. Wang *et al.*<sup>260</sup> used PINNs to solve the ROBER problem. Hard constraints on ICs via logarithmic functions were employed, yielding accurate results. Galaris *et al.*<sup>261</sup> proposed the physics-informed random projection NNs (PI-RPNNs) to solve stiff ODEs, where the single-layer NN had fixed weights between the input and hidden layer so only the parameters from the hidden to the output layer needed to be optimized. The loss functions were minimized by the Gauss-Newton method and the hard constraints on ICs were designed. Four stiff ODE problems were tested and

PI-RPNN yielded good accuracy and can outperform the traditional solvers in the cases with steep gradients. Later, Fabiani *et al.*<sup>262</sup> extended the PI-RPNNs to other stiff ODEs and three index-1 DAEs. For more practical applications, Li *et al.*<sup>263</sup> applied PINNs to solve the coal gasification chemical kinetic problems. The unreacted-core shrinking model was adopted for the gas-solid reactions, the temperature was simplified to be constant, and the ICs were hardcoded. Results showed that PINNs could accurately predict the production rates of the gaseous species.

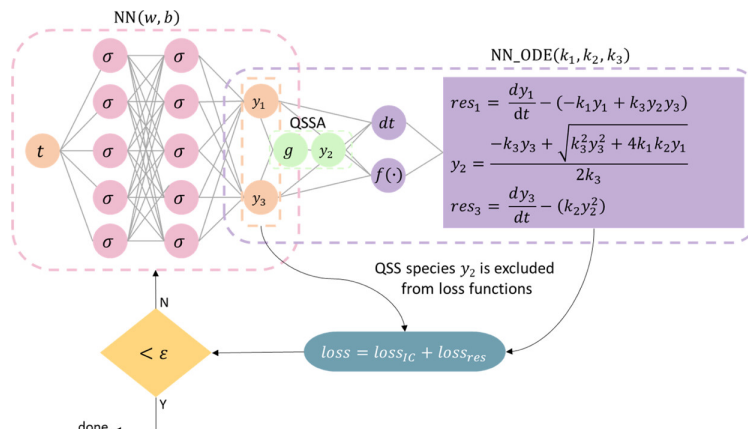


Figure 5: Schematic of the stiff-PINN for the ROBER problem. Reprinted from Reference<sup>258</sup>, with permission.

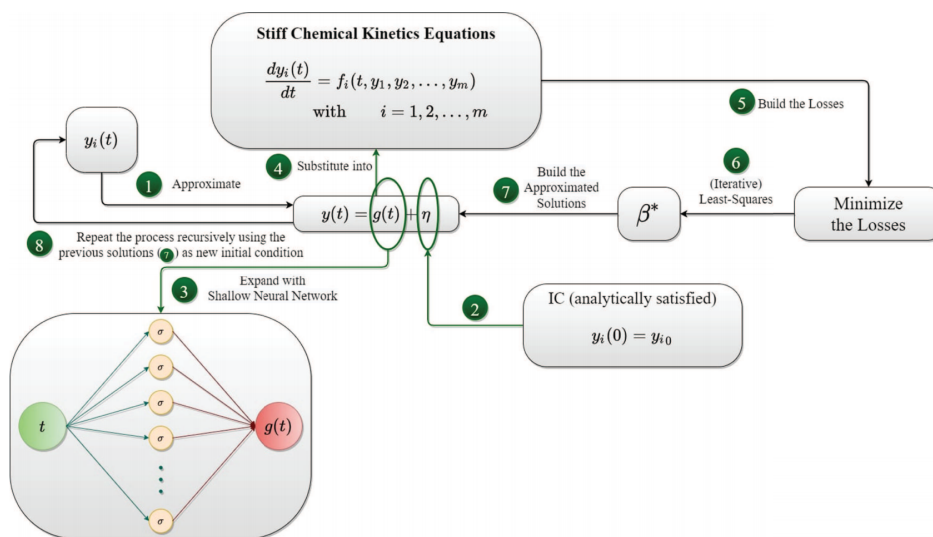


Figure 6: Schematic of the X-TFC algorithm to solve stiff chemical kinetics equations. Reprinted from Reference<sup>259</sup>, with permission.

Although the above studied focus on solving the chemical kinetic ODEs in a forward way without data supervision, inverse problems can also be solved when the available data are utilized. Weng *et al.*<sup>264</sup> developed the multiscale PINNs for stiff chemical kinetic problems, where the species with different time scales were classified and trained by multiple NNs. By introducing ground truth data points, the proposed method showed superior ability on solving three stiff chemical kinetic problems. Gusmao *et al.*<sup>265</sup> proposed the kinetics-informed NNs (KINNs) to solve forward and inverse problems of chemical kinetics, as shown in Figure 7. Practical species and reaction types were considered, including three types of species (gas, adsorbed molecules, and surface radicals) and five types of reactions (denoted by  $g$ ,  $a$ ,  $d$ ,  $c$ , and  $s$ ). ICs were enforced by an IC operator coupled with a shallow NN and species conservation was enforced by trigonometric transformations. In forward problems, no data were provided, while in inverse problems, synthetic data were available and three scenarios were designed based on the information about chemical intermediates and adsorbed molecules, and the presence of noise. The unknown kinetic parameters were optimized together with the NN parameters in inverse problems. The results showed that KINNs can accurately solve the ODEs in forward problems and estimate the kinetic parameters in inverse problems. Later, KINNs were applied to model the data from temporal analysis of

products<sup>283</sup> and extended to a robust version by incorporating the maximum likelihood approach<sup>284</sup>. Bibeau *et al.*<sup>266</sup> used PINNs to predict the kinetics of biodiesel production in microwave reactors. The system contained five species and three reactions. The Arrhenius equation was linearized and the temperature evolution was simplified to a first-order ODE, resulting in 15 unknown parameters related to the reaction kinetics and energy balance, which were estimated by PINNs from experimental data. Results showed that the reaction kinetics of the biodiesel process could be identified successfully by PINNs with satisfactory extrapolation ability.

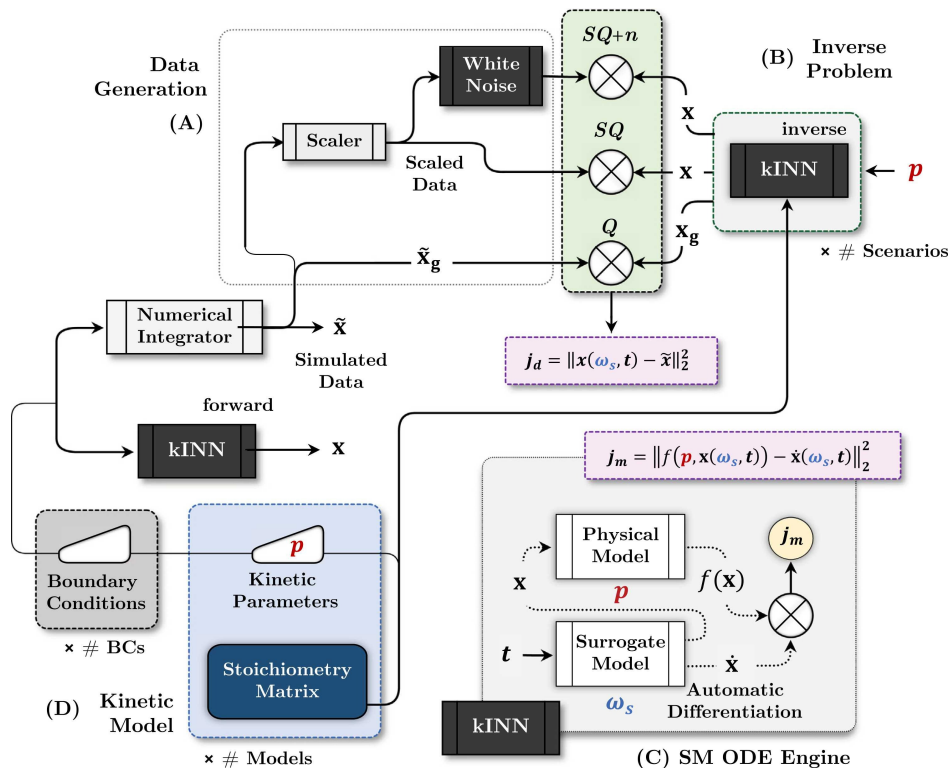


Figure 7: Kinetics-informed neural networks. Reprinted from Reference<sup>265</sup>, with permission.

## 4.2 Surrogate models of chemical kinetics

In combustion simulations, the direct integration of the chemical reaction source terms is computationally expensive and is the main bottleneck for fast simulations of industrial combustion. Therefore, many methods have been proposed to accelerate the computation<sup>43,44,113,269</sup>, such as tabulation methods, reduced chemistry, and manifold methods. ML methods have also been adopted for computation acceleration, usually by constructing NN surrogate models of the chemical kinetics<sup>43</sup>. The NNs are usually first trained using kinetic data, and then used to replace the integration of reaction source terms, so the overall computation efficiency can be improved. Based on the type of NN outputs, the NN surrogate models can be classified into two paradigms: discrete and continuous models. Specifically, the discrete models learn the mapping between the state variables at the current time and next time (i.e., following the AR paradigm), or the corresponding changes:

$$\mathbf{y}(t + \Delta t) = \text{NN}(\mathbf{y}(t)) \quad (4.12)$$

$$\text{or } \Delta \mathbf{y}(t) = \mathbf{y}(t + \Delta t) - \mathbf{y}(t) = \text{NN}(\mathbf{y}(t)) \quad (4.13)$$

For continuous models, the continuous dynamics can be learned by predicting the derivatives or source terms of the state variables:

$$\frac{d\mathbf{y}(t)}{dt} = \text{NN}(\mathbf{y}(t)) \quad (4.14)$$

$$\text{or } \dot{\omega}_{\mathbf{y}}(t) = \text{NN}(\mathbf{y}(t)) \quad (4.15)$$

where  $\dot{\omega}_{\mathbf{y}}$  is the source terms of  $\mathbf{y}$ . If only the data of  $\mathbf{y}$  are available, then Equation (4.14) needs to be integrated to approximate  $\mathbf{y}$ . This is the paradigm of neural ODEs, which will be discussed in Section 4.3.1.

To enhance the robustness and physical consistency of the surrogate models, many studies consider the constraints of physical conservations to train the models in a physics-informed way. As an example, the total mass, mass of each element, mass of non-reacting species, and energy at time  $t + \Delta t$  should be equal to the corresponding values at time  $t$ , so corresponding loss terms can be easily added when using Equation (4.12) or (4.13) as surrogate models. Theoretically, the total mass conservation will be automatically satisfied if the conservation of each element is satisfied. The species conservation is given by Equation (3.1), which is a more strict constraint on total mass conservation than the aforementioned one ( $\sum Y(t + \Delta t) = \sum Y(t)$ ). Note that this kind of physics-informed surrogate NNs are different from the PINNs in the narrow sense in that they take  $\mathbf{y}(t)$  as inputs instead of  $t$ .

Almeldein *et al.*<sup>267</sup> developed the physics-informed surrogate NNs for accelerating chemical kinetics calculations following Equation (4.12), where the conservation of four elements was added in the loss function. The mixture-of-experts architecture was adopted to allow multiple subnetworks to specialize in different regimes, such as pre-ignition low-temperature chemistry, high-temperature reactions, and post-combustion equilibriums. The 0D CH<sub>4</sub>-air combustion was tested, demonstrating the effectiveness of element conservation and the acceleration ability of the surrogate models on both CPUs and GPUs. Zhang *et al.*<sup>268,285</sup> proposed the parametric physics-informed surrogate NNs for combustion reaction kinetics (CRK-PINNs) based on the paradigm of Equation (4.12). As illustrated in Figure 8, the kinetic ODEs and the conservations of elements, species, and energy were considered in the loss function to improve the physical completeness and low data dependence. A logarithmic normalization strategy was adopted to mitigate the multiscale of species and stiffness of the system. Based on the H<sub>2</sub>-air mechanism with 10 species and 21 reactions, the CRK-PINN was validated in three scenarios: solving forward and inverse problems, surrogate chemical kinetics, and accelerating simulations of combustion reacting flows. In the first scenario, CRK-PINN can solve the ignition process without data, reconstruct the process with sparse data, and infer intermediate species and temperature with the data of major species. In the second scenario, CRK-PINN can surrogate chemical kinetics in wide operating conditions and exhibited higher accuracy and lower data dependence than data-driven NNs for both time-continuous and time-advanced predictions. In the last scenario, CRK-PINN can replace the direct integration solver to predict the reaction source terms in the DNS of a 2D laminar Bunsen flame and a 3D turbulent jet flame, showing superior accuracy than data-driven NNs and great acceleration compared to the direct integration method.

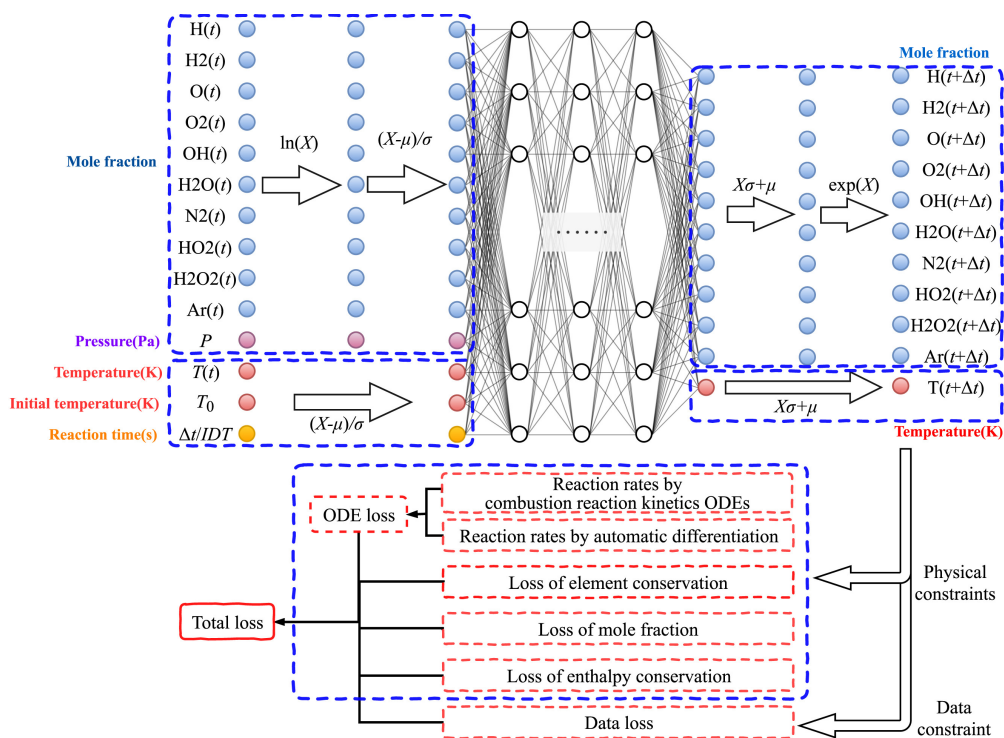


Figure 8: CRK-PINN architecture. Reprinted from Reference<sup>268</sup>, with permission.

In addition to the soft constraints in the form of loss functions, there are also studies that impose hard constraints on physical conservations. Zhang *et al.*<sup>114</sup> proposed a multiscale sampling method to enhance the accuracy and robustness of NNs to surrogate chemical kinetics, showing superior ability than the manifold, Monte Carlo, and GAN sampling.

The Box-Cox transformation (BCT) was adopted to preprocess the data of species mass fractions:

$$f(x) = \begin{cases} \frac{x^\lambda - 1}{\lambda} & \lambda \neq 0 \\ \ln x & \lambda = 0 \end{cases} \quad (4.16)$$

which is a good alternative to the logarithmic normalization<sup>268</sup>. Although the paradigm of Equation (4.13) was adopted, only the species were directly predicted by the NNs, while the temperature and pressure were updated by transport fluxes, thus ensuring the mass and energy conservation. The algorithm has been validated on various CFD cases of combustion and been applied to DeepFlame<sup>115</sup>, a deep learning empowered open-source platform for reacting flow simulations. Wang *et al.*<sup>113</sup> extended the method by imposing constraints on element conservations in both soft and hard ways. As illustrated in Figure 9, the ANN-soft penalized the element conservations by adding a loss term, while ANN-hard enforced the element conservations by adding a correction term,  $\Delta Y_c$ , to the NN-predicted mass fractions. The correction term can be easily derived by the element conservations and the changes of species mass fractions, and was first computed in the Box-Cox transformed space to avoid the multiscale issue. One advantage of ANN-hard over ANN-soft is that there is no cumbersome adjustment of the loss weights. In terms of prediction accuracy and error of element conservations, ANN-hard exhibited superior performance than ANN-soft and they all outperformed the regular ANN on various flame cases. The computational overhead caused by the correction term was negligible, demonstrating the efficiency of ANN-hard. In fact, the correction method to ensure element conservations has been adopted in earlier studies<sup>51,52</sup>, where the NNs were trained to surrogate the kinetics of reduced chemistry, following the paradigm of Equation (4.15).s

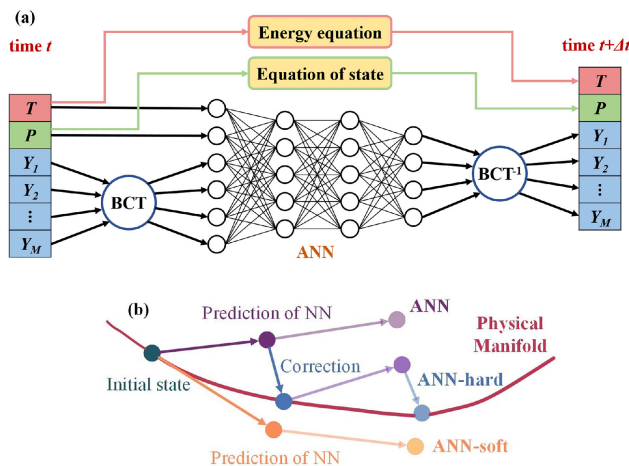


Figure 9: ANN-hard: schematic and comparisons with other approaches. Reprinted from Reference<sup>113</sup>, with permission.

In addition to the paradigm of function learning, some studies follow the paradigm of operator learning to learn combustion chemical kinetics, using neural operators such as the DeepONet<sup>95</sup> and FNO<sup>96</sup>. Some data-driven DeepONets have been used to surrogate chemical kinetics<sup>139,140,286</sup>, where the input of branch nets and the final output are similar to Equation (4.12), while the input of truck nets is related to the temporal coordinates or increments, enabling the models to learn kinetics with variable  $\Delta t$ , which is often fixed in classical surrogate models. To some extent, they can be viewed as a hybrid paradigm of AR and NAR learning. One insight that these works can provide is that learning kinetics in the latent space with reduced dimension can improve computational efficiency, which can be achieved by integrating a self-supervised autoencoder (AE)<sup>139,140</sup>, as shown in Figure 10. Kumar *et al.*<sup>140</sup> also accelerated the computation by selecting representative species for kinetics learning. The other scalars can be reconstructed by a pre-trained correlation NN. This strategy was also adopted in Reference<sup>102,103</sup>, where the species and element conservations were integrated into the loss functions of both correlation NN and DeepONet, thus constituting a physics-informed learning. The framework was tested for  $\text{CH}_4$  oxidation, demonstrating that the physical constraints can reduce the conservation errors without loss of prediction accuracy. Zanardi *et al.*<sup>104</sup> used the PI-DeepONets to learn the solution operator of non-equilibrium chemistry in hypersonic flows, where the coarse-grained (CG) kinetic ODEs were considered. The input of the branch and truck nets were the ICs and temporal coordinates, respectively. The framework was tested on the  $\text{O}_2$ - $\text{O}$  mixture, exhibiting two orders of magnitude in speedup compared to numerical integrators. Later, Zanardi *et al.*<sup>105</sup> extended the framework to be more physics-informed by many strategies, including a Boltzmann transformation layer to enforce local equilibrium distributions between states in the same group, the hierarchical architecture and transfer learning between different temporal scales, and the adaptive online pruning technique. Weng *et al.*<sup>269</sup> applied

FNO to learn stiff chemical kinetics, following the paradigm of Equation (4.12). The loss of element and species conservations were considered and the BCT (Equation (4.16)) was also adopted. Based on the focal loss<sup>287</sup>, a balanced loss function was proposed to address the unbalanced sampling issue in complex reacting flow problems. The results on four test cases (ROBER, POLLU, H<sub>2</sub> autoignition, and H<sub>2</sub>-NH<sub>3</sub> turbulent jet flame) demonstrated the effectiveness of physical constraints, BCT, and the balanced loss function.

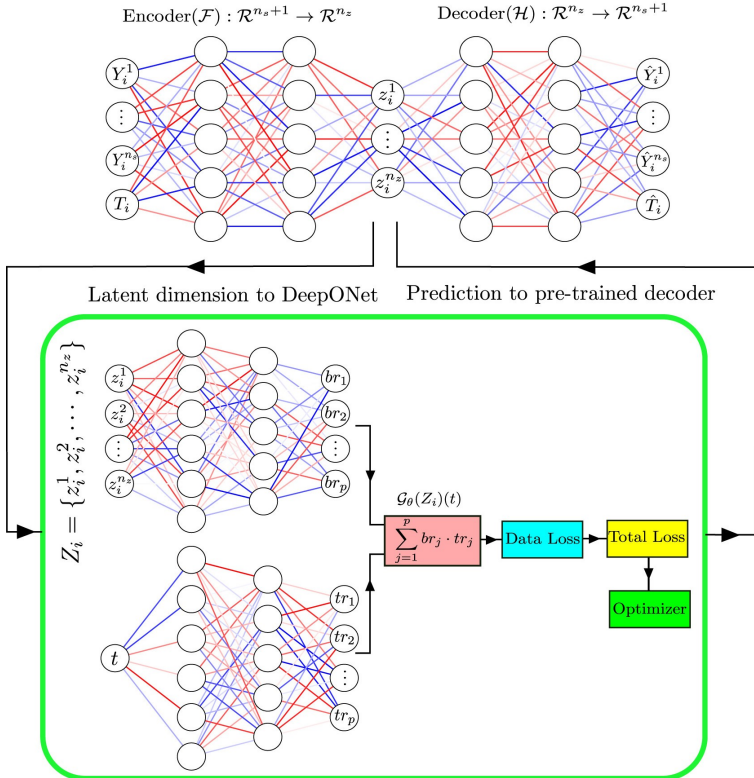


Figure 10: AE integrated DeepONet for stiff chemical kinetics. Reprinted from Reference<sup>139</sup>, with permission.

Some studies used NNs to learn chemical tabulations, which can be viewed as surrogate modeling of chemical kinetics as well. In References<sup>270-272</sup>, NNs were used to learn the tabulation of thermochemistry following the paradigm of Equation (4.13). The hybrid flamelet/random data were generated for training and multiple NNs were used to predict each species with different magnitudes of concentration changes. The species conservation (Equation (3.1)) was enforced by normalizing the predicted species concentrations. Readshaw *et al.*<sup>273</sup> extended this framework by imposing constraints on element conservation, which was achieved by recalculating the mass fractions of selected residual species after the initial prediction. The results demonstrated that this conserved NN exhibited higher accuracy and physical consistency than the non-conserved NNs. Salunkhe *et al.*<sup>274</sup> developed the framework of ChemTab to jointly learn the progress variable generation (PVG) and manifold approximation (MA). For the PVG, the high dimensional species mass fractions are linearly embedded to the progress variables:  $\mathbf{C}_{\text{pv}} = \mathbf{Y}\mathbf{W}$ , while MA means the mapping between  $\mathbf{C}_{\text{pv}} \oplus Z$  and the source terms is learned by a NN, where  $Z$  is the mixture fraction. Therefore, the overall framework is similar to Equation (4.15). Inspired by the principal component analysis (PCA), some constraints were added in the loss function, including the orthogonality of  $\mathbf{W}$  and  $\mathbf{C}_{\text{pv}} \oplus Z$ , and the unit-norm constraint on  $\mathbf{W}$ . It was demonstrated that removing any of these constraints will make the results worse. Salunkhe *et al.*<sup>275</sup> extended the ChemTab by adding another NN to learn the relationship between  $\mathbf{C}_{\text{pv}} \oplus Z$  and lower dimensional source terms, which was computed using the same projection method and the same  $\mathbf{W}$ , as illustrated in Figure 11. The unit-norm constraint on  $\mathbf{W}$  was replaced with the non-negativity constraint, which was achieved in a hard manner by truncating the negative values.

### 4.3 Neural ODEs: surrogate models and kinetics discovery

Neural ODE (NODE) was first proposed by Chen *et al.*<sup>288</sup> to develop a new family of NNs that parameterize the derivative of the hidden state using NNs, which is different from the traditional approach that defines discrete sequence of hidden layers, such as the ResNet and RNNs. Equation (4.14) is the basic expression of NODEs, while state variables

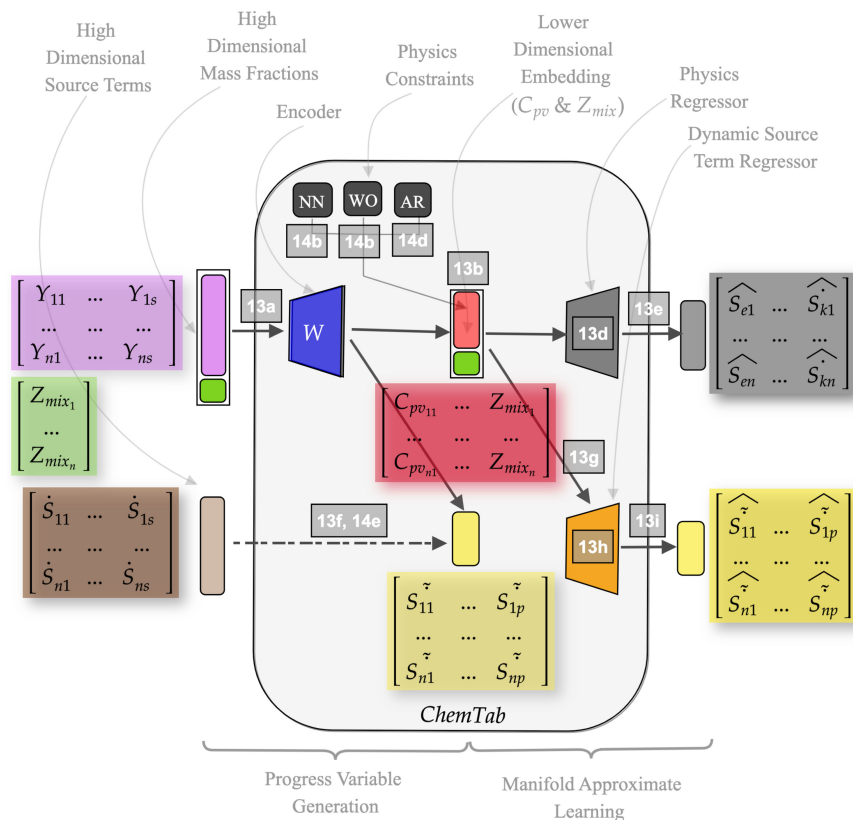


Figure 11: ChemTab extended architecture and training procedure. Reprinted from Reference<sup>275</sup>, with permission.

are computed by integrating the Equation (4.14):

$$\mathbf{y}(t_1) = \mathbf{y}(t_0) + \int_{t_0}^{t_1} \text{NN}(\mathbf{y}(t)) dt = \text{ODESolve}(\mathbf{y}(t_0), t_0, t_1, \text{NN}) \quad (4.17)$$

Compared to discrete approaches, NODEs can better learn the continuous dynamics of a system, thus showing better reconstruction and extrapolation performance<sup>288</sup>. Since NODE is proposed for learning the first-order dynamics of sequential systems, it is natural to apply it to chemical kinetic systems. Extensive studies have applied NODEs to the modeling of chemical kinetics for both building surrogate models and discovering kinetics, where many of them have informed/embedded physics to the NODEs.

### 4.3.1 Continuous surrogate models

As mentioned in Section 4.2, NODEs can be viewed as continuous surrogate models of chemical kinetics following the paradigm of Equation (4.14). Owoyele *et al.*<sup>54</sup> first applied NODEs to model chemical kinetics, termed as ChemNODE and shown in Figure 12. To improve the training stability, a progressive training strategy was employed, where the species were trained sequentially. For a homogeneous hydrogen-air reactor, ChemNODE showed accurate results across various operating conditions and yielded a speedup of 2.3x over the full chemical mechanism method. Kim *et al.*<sup>289</sup> used NODEs to learn stiff ODEs. The tests on the ROBER and POLLU problems demonstrated that the scaling of equations and loss functions was essential for NODEs to learn stiff ODEs.

Although the name contains the "ODE", the vanilla NODE is indeed a data-driven method because no information of the ODEs is utilized. Recall that PINNs predict  $\mathbf{y}$  by  $\mathbf{y} = \text{NN}(t)$  and differentiate it to get  $\dot{\mathbf{y}}$ , while NODEs, in contrast, predict  $\dot{\mathbf{y}}$  by  $\dot{\mathbf{y}} = \text{NN}(\mathbf{y}(t))$  and integrate it to get  $\mathbf{y}$ . Therefore, if the ODEs can be explicitly added to the loss functions of NODEs, they can be viewed as PINNs in a broad sense, or an integral version of PINNs. Some studies have made the NODEs physics-informed in different ways. Sholokhov *et al.*<sup>290</sup> developed the physics-informed NODE (PI-NODE) to build reduced-order models (ROMs) for dynamical systems, where an AE was employed to perform model reduction and the NODE was used to learn the nonlinear dynamics in the latent space. Based on the ODEs in the physical space, the latent-space dynamics was derived and constitute a physics-informed loss, which was evaluated on a

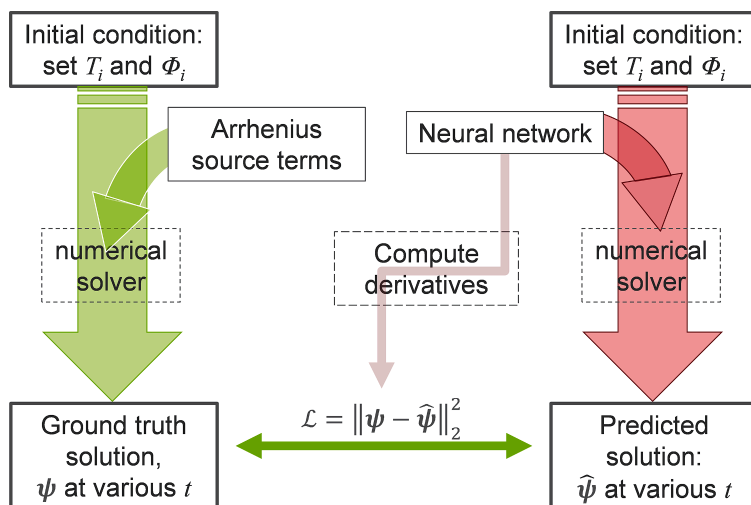


Figure 12: The ChemNODE approach.  $\psi$  indicates the thermochemical scalars. Reprinted from Reference<sup>54</sup>, with permission.

set of collocation points. The addition of the physics-informed loss improved the long-term performance, the robustness to data scarcity and noise, and the compressibility of the ROMs. Vijayarangan *et al.*<sup>276</sup> developed an AE-based ROM for stiff chemical kinetics using dynamics-informed training, where the NODE was used to learn the latent-space dynamics. The "dynamics-informed" means that the discovery of the latent space is informed by the latent dynamical evolution rule during the training procedure, which is different from the definition of "physics-informed" in a narrow sense. Two additional losses were added to ensure the mapping of the encoder and decoder was bijective. Results demonstrated that the proposed ROM could serve as an effective stiffness-removal framework. Kumar *et al.*<sup>277,278</sup> developed the physics-constrained NODE (PC-NODE) to learn stiff chemical kinetics, where the conservations of each element were constrained by including corresponding loss terms. Here the element conservation was constrained between the predicted and true values, instead of the values at time  $t$  and  $t + \Delta t$  in the paradigm of discrete surrogate models. Compared to the purely data-driven NODE, results demonstrated that the PC-NODE framework improved not only the physical consistency but also the training efficiency. Later, Kumar *et al.*<sup>279</sup> combined the NODE with AE to develop the Phy-ChemNODE. The four loss terms can be considered as a combination of the bijective constraints of the dynamics-informed NODE<sup>276</sup> and the element conservation constraints of the PC-NODE<sup>277,278</sup>. Phy-ChemNODE was tested on a  $\text{CH}_4\text{-O}_2$  combustion kinetics, where the 33 physical variables were reduced to 4 latent variables. The element conservation constraints were shown to help the model to obey the mass conservation better.

Although the vanilla NODEs are purely data-driven, their interpretability can be enhanced by using the KANs as the network architecture. Koenig *et al.*<sup>291</sup> proposed the KAN-ODEs, combining the advantage of NODEs that do not require prior knowledge and the advantages of KANs that have increased interpretability and faster neural scaling laws compared to MLPs. The KAN-ODE was validated on learning Lotka-Volterra ODEs, modeling source terms of the Fisher-KPP PDE, and learning 1D PDEs. The scaling performance was shown superior to MLPs and the model performance could be further enhanced by sparsification and using symbolic regression. Subsequently, based on the KAN-ODEs and LeanKAN<sup>292</sup>, Koenig *et al.*<sup>280</sup> proposed the ChemKAN for modeling and acceleration of combustion chemical kinetics. The physics was informed in two ways. First, the architecture strongly mimicked the chemical kinetics, as illustrated in Figure 13. A KAN was first used to represent the species production rates (core structure), then they were linearly combined to represent the temperature rate (thermodynamic superstructure) with another KAN to reflect the thermophysical parameter variation. This serial architecture offers the flexibility that one can only learn the species when temperature is not a variable. Second, an optional loss function for element conservation was introduced, which is similar to the PC-NODE and Phy-ChemNODE. The first test case was a biodiesel production modeling, where the thermodynamic superstructure and physical loss were "turned off". Compared with DeepONet, ChemKAN exhibited stronger scaling behaviour on test sets, less tendency toward overfitting, and stronger robustness to noise. In the second case of  $\text{H}_2\text{-air}$  combustion, the ability of ChemKAN for computation acceleration was validated. Compared to MLP-based ChemNODE, ChemKAN showed similar speed-up ratios, but solved more species.

In addition to inform physics in the form of loss functions, some studies embed the information of stoichiometry and/or rate expressions into the NODEs to enhance the physical consistency. According to Equation (3.29), the rates of species and reactions are linearly related by the stoichiometric matrix. Thus, if the stoichiometric matrix is known, one

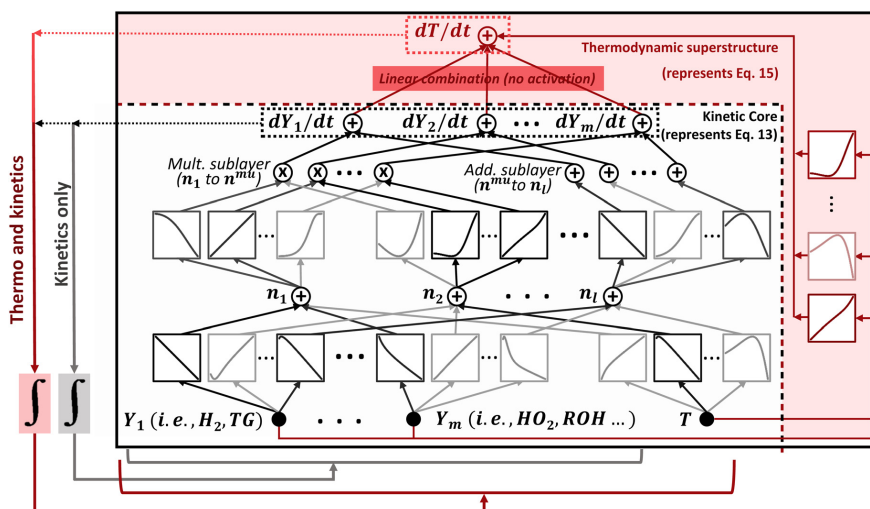


Figure 13: The structure of ChemKAN. Reprinted from Reference<sup>280</sup>, with permission.

can use NODEs to directly predict  $\mathbf{RoP}$  and then transform it to  $\dot{\omega}$ , or vice versa. Based on the known information, Sorourifar *et al.*<sup>117</sup> developed two versions of physics-enhanced NODEs for chemical reaction systems: r-NODE and k-NODE. The r-NODE approximates  $\mathbf{RoP}$  when only the stoichiometry is known and embedded, while the k-NODE approximates the kinetic constants when the mass-action parts of  $\mathbf{RoP}$  are further known and embedded. Results suggest that a ground truth model that accurately reflects the data can be learned only when the embedded information accurately reflects the underlying mechanics. Fedorov *et al.*<sup>118</sup> developed the kinetics-constrained NODEs (KC-NODEs) for kinetic modeling, where the kinetic and thermodynamic knowledge were embedded into the NN architecture, including the stoichiometric matrix, the law of mass action, and the Arrhenius dependency of the rates on temperature. The KC-NODE was successfully applied to the kinetic modeling of the hydrogenation of  $\text{CO}_2$  to methane using numerical data and to higher hydrocarbons using real experimental data. Kircher *et al.*<sup>119,120</sup> proposed the global reaction neural network (GRNN) to learn kinetics from reactor data, where the stoichiometry and thermodynamics were explicitly embedded as the network layers, as shown in Figure 14. The GRNN can be trained directly when source data are provided and trained in a NODE way when only reactor data are available, which is a 1D plug flow reactor model in the study. It was demonstrated that the embedded knowledge enhanced the model robustness to significant noise in the data.

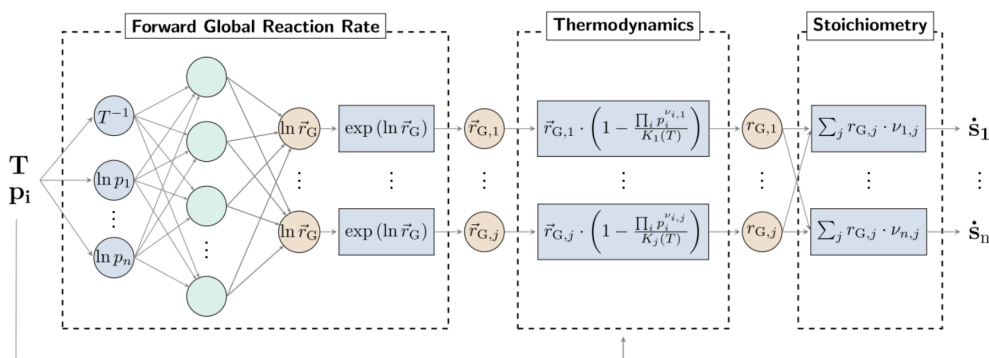


Figure 14: GRNN architecture with embedded stoichiometry and thermodynamics. Reprinted from Reference<sup>119</sup>.

### 4.3.2 Kinetics discovery

In terms of embedding the knowledge of chemical kinetics into NNs, the chemical reaction neural network (CRNN), proposed by Ji *et al.*<sup>75</sup> for kinetics discovery, is an earlier work than References<sup>117–119</sup> and is also trained in a NODE-way. As shown in Figure 15, a neuron of CRNN represents a single-step reaction, where the law of mass action (Equation (3.28)) and Arrhenius law (Equation (3.32)) are embedded as the nodes and weights. For the input layer, the weights represent the reaction orders and the bias represents the rate constant in the logarithmic scale. The weights

of the output layer correspond to the stoichiometric coefficients. A multi-step reaction system can be represented by stacking the neurons to formulate a CRNN with one hidden layer, where the number of hidden neurons is equal to the number of reactions. Due to the physical interpretability, once the CRNN has been trained, the kinetic parameters can be easily recovered by checking the weights and biases, then the reaction pathways can be fully revealed. The number of hidden nodes/reactions, which is a hyperparameter, can be determined by grid searching and a threshold pruning strategy is suggested to clip the NN weights below a certain threshold<sup>75</sup>. The CRNN was first tested on three cases with increasing complexity: an elementary reaction network without temperature dependence, biodiesel production with temperature dependence, and an enzyme reaction network in which some species are present in both reactants and products. Results demonstrated that CRNN could accurately learn the reaction pathways and kinetic parameters from noisy data and even from incomplete data with missing species.

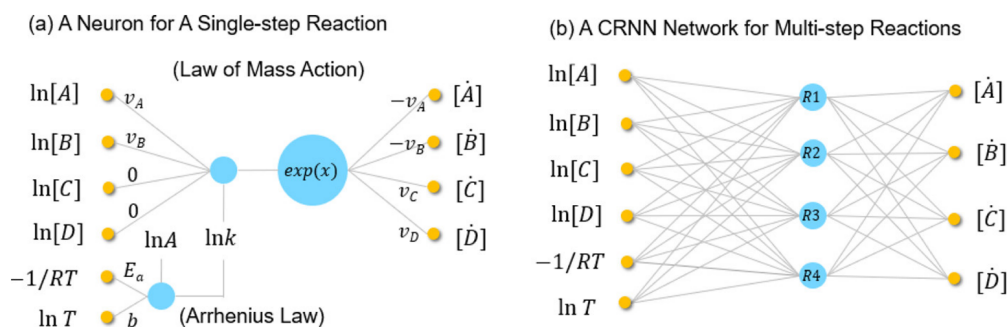


Figure 15: Schematic of the CRNN illustrated for a reaction system with four species and four reaction steps. Reprinted from Reference<sup>75</sup>, with permission.

Later, CRNN has been applied to many reaction systems, such as the biomass pyrolysis<sup>293</sup> and the decomposition of energetic materials<sup>294–297</sup>. Li *et al.*<sup>298</sup> developed the Bayesian CRNN to simultaneously infer the reaction pathways and perform uncertainty quantification on the identified reaction pathways, kinetic parameters, and concentration predictions with unseen initial conditions. Su *et al.*<sup>281</sup> used NODEs for kinetic parameter optimization of hydrocarbon fuels, where the framework can be viewed as CRNN with only kinetic parameters unknown, all pathways fixed and all other unnecessary connections trimmed. Considering that CRNN does not ensure mass and element/atom conservations, Doeppel *et al.*<sup>282</sup> developed the atom conserving CRNN (AC-CRNN), where the atom conservation was enforced by adding a NN layer that multiplied the key species coefficients with a conservation matrix. The standard cases in Reference<sup>75</sup> was tested. Compared to CRNN, the AC-CRNN exhibited improved stability and robustness against noisy and missing data, and was more efficient due to the reduced number of trainable parameters.

## 5 PIML for combustion reacting flows

The previous section focuses on reaction problems, but most of the practical combustion is a convection-diffusion-reaction (CDR) process, where the laws in Section 3.5 need to be considered to describe the spatial processes such as flow and diffusion. This section will present the studies on PINNs for combustion reacting flows, with representative studies listed in Table 5, which provides the dimension, problem type, adopted physical losses, treatment of reaction, and other information. Based on the combustion problem type, the studies in Table 5 are classified into four parts: laminar combustion, turbulent combustion, supersonic combustion, and combustion SR via discrete PINNs, which will be introduced in four subsections respectively. Before that, some studies on PINNs for diffusion-reaction (DR) and advection-diffusion-reaction (ADR) problems are first introduced.

### 5.1 (Advection-) Diffusion-reaction problems

Conceptually, DR and ADR problems are more complex than pure reaction problems due to the increase of problem dimension and existence of diffusion and advection, but are simpler than CDR problems due to the lack of nonlinear convection terms. Nevertheless, they share the feature of spatial processes and reactions in CDR problems, so we first briefly review the PINNs for DR and ADR problems before moving to CDR problems, which may shed light on the studies on PINNs for practical combustion reacting flows.

For DR problems, many DR systems are not encountered in the area of combustion, such as the well-known Allen-Cahn equation:

$$u_t - 0.0001u_{xx} + 5u(u^2 - 1) = 0 \quad (5.1)$$

Table 5: Recent studies on PINNs for combustion reacting flows. The four parts in this table represent the laminar combustion, turbulent combustion, supersonic combustion, and combustion SR via discrete PINNs, respectively.  $\mathbf{U}$  is the velocity vector. FRC means finite-rate-chemistry. "Sim." and "exp." represent "simulation" and "experiment", respectively. The tilde (" $\sim$ ") indicates (Favre) averaged values in turbulent conditions.

Study	Dimension	Problem type	Physical loss (equation of)	Turbulence	Reaction in physical loss	Ref. data	NN architecture	Codes
Choi <sup>299</sup> , 2022.1	3D+t	Inverse	Mass, $\mathbf{U}$ , $T$ , $Y_{1-3}$	No	Van de Vusse	Sim.	MLP	–
Wang <sup>260</sup> , 2022.7	2D	Forward	$Z$	No	Absent (fast chemistry)	Sim.	MLP	–
Sitte <sup>300</sup> , 2022.8	2D+t	Inverse	Mass, $\mathbf{U}$	No	Absent	Sim.	MLP	–
Liu <sup>301</sup> , 2023.9	1D, 2D, 2D+5	Forward	Mass, $\mathbf{U}$ , $T$ , $Y_{1-5}$	No	1-step CH <sub>4</sub>	Sim.	MLP	–
Song <sup>302</sup> , 2024.10	2D	Both	Mass, $\mathbf{U}$ , $Z$ , $c$	No	Detailed CH <sub>4</sub> (FPV table)	Sim.	MLP	–
Cao <sup>303</sup> , 2024.11	2D	Forward	Mass, $\mathbf{U}$ , $T$ , $Y_{1-5}$	No	1-step CH <sub>4</sub>	Sim.	MLP	–
Wu <sup>112</sup> , 2025.1	1D	(1) Both (2) Forward (3) Inverse	(1) $T$ (2) $T$ , $Y_{1-5}$ (3) Mass, $V$ , $T$ , $Y_{1-5}$	No	(1) Simplified FRC (2)(3) 1-step CH <sub>4</sub>	Sim.	(1) MLP (2)(3) MMLP-RWF	<a href="#">URL</a>
von Saldern <sup>226</sup> , 2022.11	2D	Inverse	Mass	Filtered	Absent	Sim.	MLP	–
Liu <sup>304</sup> , 2023.12	3D+t	Inverse	Mass, $\mathbf{U}$ , $T$ , $Y_{1-6}$ , $\sum Y$	Direct	2-step CH <sub>4</sub>	Sim.	MLP	–
Peng <sup>305</sup> , 2024.4	2D+t	Inverse	Mass, $\tilde{\mathbf{U}}$ , $\tilde{T}$ , $k$ , $\varepsilon$	Mean	Absent	Sim.	MLP	–
Taassob <sup>306</sup> , 2023.10	2D+1	Inverse	Mass, $\tilde{\mathbf{U}}$ , $\tilde{P}C_{1-2}$ , $\tilde{Z}$ , $\mu_t$	Mean (learned)	Learned	Exp.	MLP	–
Taassob <sup>106</sup> , 2024.6	2D+2	Inverse	Mass, $\tilde{\mathbf{U}}$ , $\tilde{Y}_{1-6}$ , $\tilde{Z}$ , $\mu_t$	Mean (learned)	Learned	Exp.	DeepONet	–
Liu <sup>107</sup> , 2024.6	(1) 2D+t (2) 2D	Inverse	(1) $\mathbf{U}$ , $T$ (2) $Y_{soot}$	No	(1) Absent (2) Learned	Exp.	(1) MLP (2) AE-DeepONet	–
Yadav <sup>307</sup> , 2024.12	(1) 1D (2)(3) 2D	Inverse	Mass, (1) $c$ ( $\mathbf{U}$ ) (2) $c$ (3) $\tilde{c}$	(1)(2) No (3) Mean (learned)	(1)(2) Pre-learned (3) EBU model	(1)(2) Sim. (3) Exp.	MLP	–
Wang <sup>308</sup> , 2023.7	1D+t	Inverse	Mass, $u$ , $E$ , $c$	No	Simplified FRC	Sim.	MLP	–
Deng <sup>309</sup> , 2024.7	2D+t+2	Inverse	Mass, $\tilde{\mathbf{U}}$	Mean	Absent	Sim.	ResUNet	–
Bode <sup>310</sup> , 2021.1	3D	Inverse	Mass	Filtered to full	Absent	Sim.	ESR-GAN	<a href="#">URL</a>
Bode <sup>311</sup> , 2023.2	3D+t	Inverse	Mass, $\sum Y$	Filtered to full	Absent	Sim.	ESR-GAN	–
Wang <sup>312</sup> , 2023.11	2D	Inverse	Mass, $\mathbf{U}$	No	Absent	Sim.	GAN	–
Wang <sup>313</sup> , 2024.8	2D+t	Inverse	Mass	No	Absent	Sim.	R-GAN	<a href="#">URL</a>

which describes the process of phase separation in multi-component alloy systems, and has become a benchmark problem for validating PINN algorithms<sup>66,173–175</sup>. It can be seen that the reaction source term is quite different from the combustion ones (Section 3.4), and only one variable is considered. Other DR systems, such as  $\lambda$ - $\omega$ , FitzHugh-Nagumo, and Gray-Scott equations have been solved by PhyCRNet<sup>121</sup> and PeRCNN<sup>73</sup>. Although these problems involve more than one variable, the polynomial reaction kinetics still differ from the chemical kinetics of practical combustion. Nevertheless, these studies have validated the feasibility of PINNs to solve PDEs with both diffusion terms and highly nonlinear reaction source terms. Niaki *et al.*<sup>314</sup> used PINNs to solve the DR PDEs of the thermochemical curing process of composite-tool systems during manufacture, where the cure kinetics contained the Arrhenius law, further validating the applicability of PINNs to solve combustion-like DR problems.

For ADR problems, their difference from CDR problems is that the velocities are constants or functions instead of field variables, so the nonlinearity is mainly caused by reaction instead of convection. Ngo *et al.*<sup>315</sup> applied PINNs to the solution and parameter inference of a fixed-bed reactor model for catalytic CO<sub>2</sub> methanation. The momentum and energy equations were neglected due to the low pressure drop and isothermal conditions, respectively, so the governing equations were 1D advection-reaction equations of four species, which considered the law of mass action and Arrhenius law. Results showed that the forward PINN could solve the reactor model, whereas the inverse PINN could reveal an unknown effectiveness factor using the pre-trained forward PINN. Hou *et al.*<sup>316</sup> applied PINNs to forward and inverse one-dimensional one-component (1D1C) ADR problems, where both location-dependent and linear reaction terms were considered. The adopted first derivative constraint (FDC) method, which is similar to gPINN<sup>176</sup>, has been demonstrated to enhance the model stability and accuracy. To avoid the slow training speed caused by FDC, Sun *et al.*<sup>317</sup> proposed an NN connection structure named deep function family construction, which added residual connections to fully connected NNs. The modified PINN was applied to forward and inverse 1D3C ADR problems, where the reaction source terms were given by the law of mass action for a reaction system of three species and five reactions. Both steady and unsteady problems were solved and the modified PINN outperformed the vanilla PINN, especially for cases with steep fronts. The results of inverse problems indicated the capability of PINNs to learn missing physics (multiple unknown parameters) in ADR systems. This was further demonstrated by Hou *et al.*<sup>318</sup>, where the inverse problem of the 1D3C ADR system was also solved. Laghi *et al.*<sup>319</sup> compared four PINNs on six 1D steady-state ADR problems with analytical solutions. The four PINNs were vanilla PINNs, PI-ELM<sup>147</sup>, Deep-TFC<sup>132</sup>, and X-TFC<sup>133</sup>. Comparative analysis demonstrated that X-TFC was the best-performing framework in terms of both accuracy and computational time.

In summary, the above studies on DR and ADR problems have validated the applicability of PINNs to physical processes with diffusion, constant flow, and nonlinear reactions. However, they do not consider not only the velocity variable but also the temperature variable, and thus the reaction rate constants described by the Arrhenius law and the changes in physical properties due to heat release. For practical combustion reacting flows, some representative studies on PINNs for solving them are listed in Table 5 and will be reviewed in the following subsections.

## 5.2 Laminar combustion

This subsection will present a chronological overview of studies on PINNs for laminar subsonic combustion. Choi *et al.*<sup>299</sup> used PINNs to reconstruct the 3D transient fields of a continuous stirred tank reactor (CSTR) with van de Vusse reaction. The governing equations of two reference frames were considered to enable the reconstruction of the multi-reference frame system. The fields can be accurately reconstructed from the data of velocity, temperature, and species, and some proposed strategies, such as the similarity-based sampling, have been shown to improve the model performance. Wang *et al.*<sup>260</sup> used PINNs to forward solve the  $Z$ -equation for a jet diffusion flame and obtained accurate results. Because the assumptions of unity Lewis number and infinite fast chemistry are adopted, the  $Z$ -equation is free of reaction source terms and the temperature and species can be determined solely by  $Z$ . Sitte *et al.*<sup>300</sup> used PINNs to reconstruct the velocity fields in puffing pool fires based on the observations of density, pressure, and temperature, following the HFM framework<sup>244</sup>, as illustrated in Figure 16. The continuity and momentum equations are taken as the physical losses and a two-stage training strategy is adopted. The results show that PINNs can provide satisfactory velocity results and can act as a physics-based denoiser to smooth out the noise on the measured data.

Liu *et al.*<sup>301</sup> applied PINNs to solve forward problems of 1D and 2D premixed combustion with temperature-dependent properties and a one-step global mechanism of CH<sub>4</sub>. To the best of our knowledge, although some simplifications are adopted for the transport models and the reaction mechanism is simple, this is the first study on PINNs for combustion reacting flows with detailed physical models and chemical kinetics based on the laws of mass action and Arrhenius. More importantly, after validating the model accuracy on 1D and 2D problems, a surrogate model was constructed for the 2D combustion, where five parameters were added to the NN inputs so that the model can learn multi-condition solutions, as shown in Figure 17. The parameterized PINN surrogate model was shown to accurately predict the fields, be applicable to sensitive analysis, and be much more efficient for industrial designs than traditional numerical simulations. Song *et al.*<sup>302</sup> applied PINNs to 2D laminar premixed flames considering detailed chemistry

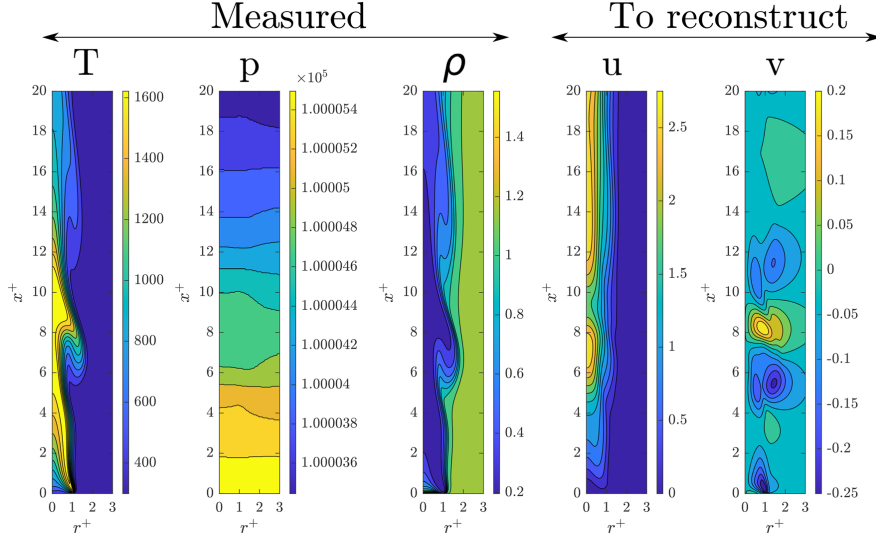


Figure 16: Applying the HFM framework to reconstruct puffing pool fires. Reprinted from Reference<sup>300</sup>.

of  $\text{CH}_4$ , which was accomplished by integrating the flamelet/progress variable (FPV) model. The equations of mass, momentum,  $Z$ , and  $c$  were solved by PINN, during which the thermophysical properties and source term of  $c$  were extracted from the pre-tabulated FPV library, as illustrated in Figure 18. The model can accurately solve the fields with and without observation data, demonstrating the feasibility of PINNs to integrate detailed reaction mechanisms using tabulation methods. Using pseudo-time stepping PINNs (PTS-PINNs)<sup>212</sup>, Cao *et al.*<sup>303</sup> solved the premixed and non-premixed flames with a one-step mechanism of  $\text{CH}_4$  and obtained satisfactory results. Vanilla PINNs failed to solve the premixed combustion with large gradients and tended to predict non-reacting solutions, but PTS-PINNs showed great convergence performance not only for the premixed combustion but also for non-premixed combustion where the thin reaction zones introduced a higher level of complexity.

The above studies only involve forward problems or inverse problems of field reconstruction without parameter inference, which is another important aspect of inverse problems. In computational 1D laminar flames, which are important for the study of flame limit, stretch, laminar flame speed ( $s_L$ ), and flamelet tabulation, unknown eigenvalues exist even in forward problems, such as  $s_L$  in freely-propagating premixed flames<sup>4,7,8</sup>. Wu *et al.*<sup>112</sup> established the FlamePINN-1D framework to solve both forward and inverse problems of 1D laminar flames in a unified manner, as illustrated in Figure 19. Three cases were solved: freely-propagating premixed flames with simplified and detailed physical models, and counterflow premixed flames with detailed physical models. The detailed physical models are the same as those in Section (3.1) to (3.5) with a one-step global mechanism of  $\text{CH}_4$  being considered, except that the governing equations are for 1D reacting stagnation flows. A warmup pretraining strategy and some hard physical constraints were proposed. For example, the predicted species mass fractions are transformed by the Softmax function:

$$Y_k = \text{Softmax}(Y_k^\#) = \frac{\exp(Y_k)}{\sum_{k=1}^K \exp(Y_k)} \quad (5.2)$$

where  $Y_k^\#$  is the output of NN. The transformation ensures that the range constraint ( $0 \leq Y_k \leq 1$ ) and species conservation ( $\sum_k Y_k = 1$ , Equation (3.1)) can be exactly satisfied, so it can be used for various combustion problems.  $Y^\#$  can be viewed as the logarithmic normalization of  $Y$ <sup>268</sup>, which can mitigate the multiscale of their magnitudes. The results show that for forward problems, FlamePINN-1D can accurately solve the flame fields and simultaneously infer the  $s_L$  of freely-propagating premixed flames. For inverse problems, FlamePINN-1D can accurately reconstruct the continuous fields and infer the transport properties and chemical kinetics parameters from noisy sparse observations, which indicates the possibility of optimizing chemical mechanisms from observations of laboratory 1D flames. In fact, in their inverse problems where the activation energy was unknown, the chemical kinetics part can be considered as a CRNN with other parameters are known. It is proven that the model tends to get unburned solutions without warmup pretraining, the similar situation to Reference<sup>303</sup>. Other adopted strategies, such as hard constraints, thin-layer normalization<sup>85</sup>, and modified MLP with random weight factorization (MMLP-RWF)<sup>79</sup>, have also been proven to be essential for the model performance.

In addition to the classical PINNs, the PINNs in a broad sense (Table 1) can also be applied to laminar combustion problems. For example, Corrochano *et al.*<sup>320</sup> developed a physics-aware ROM for an axisymmetric laminar  $\text{CH}_4\text{-O}_2$

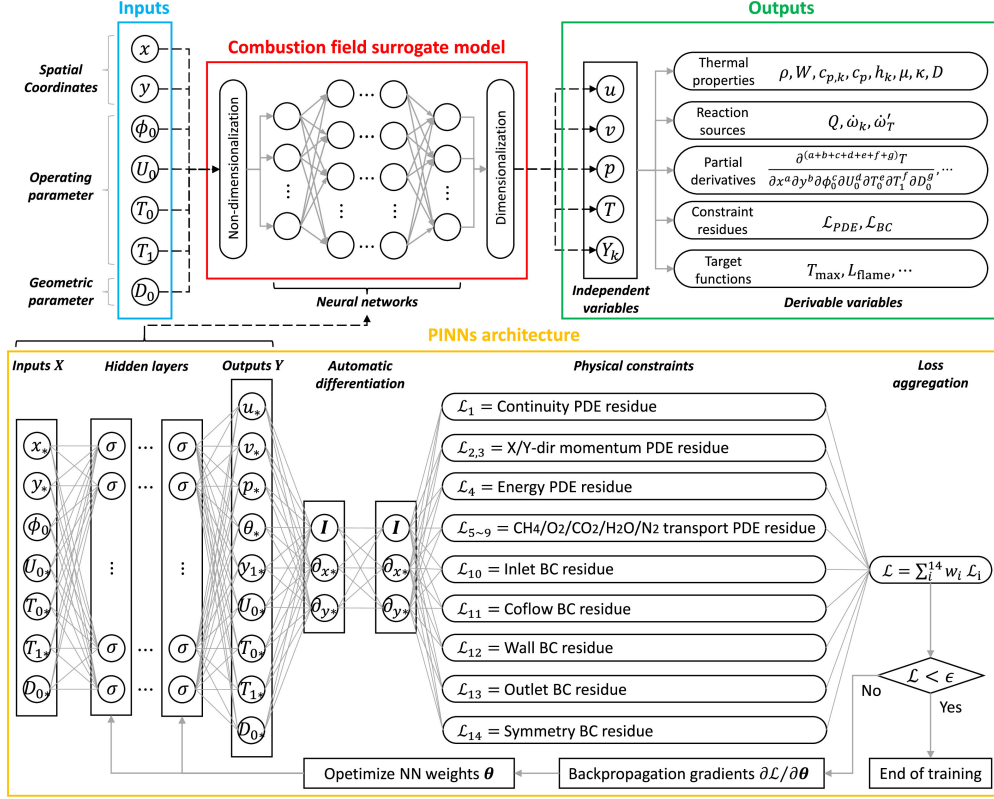


Figure 17: Schematic of the parameterized combustion field surrogate model based on PINNs. Reprinted from Reference<sup>301</sup>, with permission.

flame. The simulation data were preprocessed to obtain the proper orthogonal decomposition (POD) modes, then deep learning models were used as a time integrator to advance temporal modes in time, i.e., the models took the AR paradigm instead of the NAR paradigm adopted in classical PINNs (see Section 2.3.1). A physics-aware loss function was introduced which constrained the predicted species mass to be equal to the true ones in each time instant. This loss differed from the classical PINN losses in that it was still a data-driven loss without PDE information, so it was called "physics-aware" rather than "physics-informed", but can still be called "physics-informed" in a broad sense in our extended definition. Two models, including the LSTM and 1D CNN, were tested, demonstrating that the physics-aware loss could slightly improve the model performance.

### 5.3 Turbulent combustion and experimental data

Compared to laminar combustion and using simulation data for learning or validating, the problems are more complex for turbulent combustion and when only practical experimental data are available due to high uncertainty of these situations. As an early attempt, Nandi *et al.*<sup>321,322</sup> used PINNs to develop digital twins for 2D and 3D industry-scale boiler combustion without observation data (forward problems). The zero-equation model was used for the turbulent Reynolds stresses<sup>321</sup> and various reaction source terms were tested, including the linear form of two species<sup>321</sup> and one-step mechanism of CH<sub>4</sub><sup>322</sup>. Some strategies were proposed to handle the coupling between the source terms of  $T$  and  $Y$ . Von Saldern *et al.*<sup>226</sup> applied PINNs to the assimilation of turbulent mean flow data of axisymmetric jet flows. In their first example, the mean density fields of a turbulent jet flame were reconstructed based on the data of velocity fields, which were generated by LES. Although only the continuity equation was considered in the physical loss, the velocity and density fields were accurately reconstructed. Liu *et al.*<sup>304</sup> used PINNs to reconstruct the fields of 3D turbulent flames based on sparse, noisy data sampled from high-fidelity DNS data. Three cases were tested: freely-propagating planar premixed flames with low and high levels of turbulence, and slot-jet flames with a jet Reynolds number of 850. For the physical models, temperature-dependent properties, constant Prandtl number, and unity Lewis number were considered. A two-step mechanism of CH<sub>4</sub> was adopted, which consisted of six species and two reactions. Three PINN sub-models were employed to learn momentum, species, and temperature equations, respectively, and the species conservation was also considered in the losses (Equation (3.1)). Self-adaptive linear layers

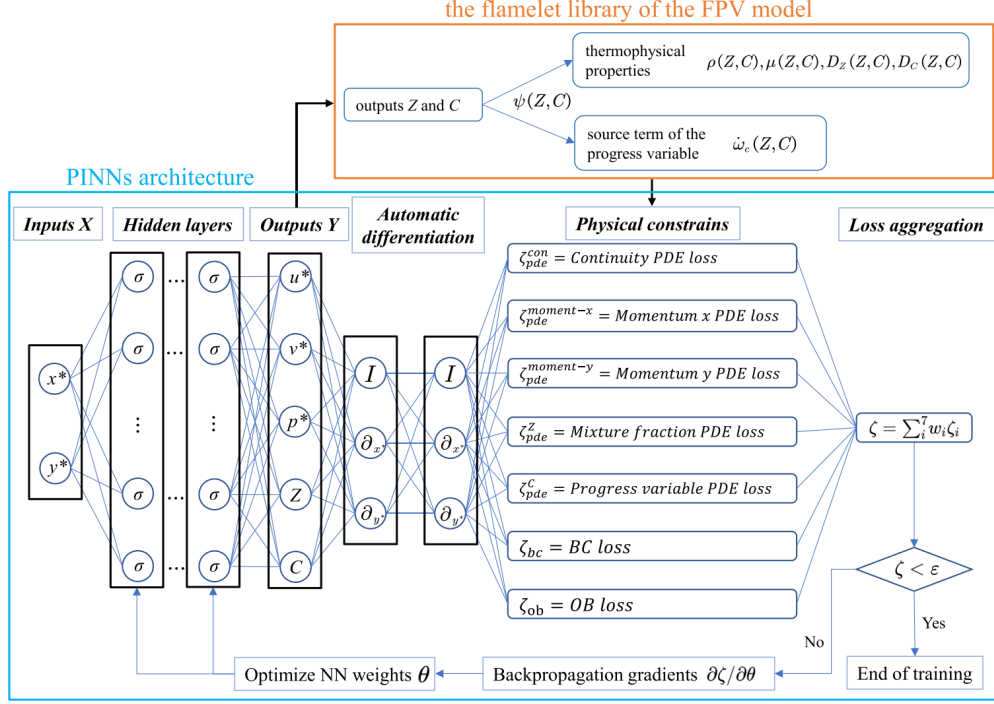


Figure 18: Schematic of the PINNs coupled with the FPV model. Reprinted from Reference<sup>302</sup>, with permission.

were utilized and a warmup pretraining was conducted to facilitate model convergence. It is shown that the model can accurately reconstruct the fields and get satisfactory results of flow modes, vortical structures, and PDFs of variables and flame curvature, and the results were more accurate than the linear interpolation method, as shown in Figure 20. Peng *et al.*<sup>305</sup> used PINNs to reconstruct the heat flow field of Sandia Flame D<sup>323</sup> based on the data of velocity and temperature, which were obtained by simulation with the partially premixed combustion model. The predicted variables and physical losses did not consider the species and chemical reactions, but considered the turbulence kinetic energy ( $k$ ), its dissipation rate ( $\varepsilon$ ), and their transport equations, which is a common turbulence model. The results showed that PINNs could accurately reconstruct the fields within both small and large time intervals. Compared to data-driven methods, PINNs was shown to yield more accurate results and require less data when accuracy requirements are the same.

For experimental combustion, there are discrepancies between the data and pre-specified physical models, especially for turbulence and reaction models. As shown in Table 5, two strategies are adopted in existing studies to deal with this issue: (1) Reduce or simplify the models; (2) Learn the models, i.e., closure terms. Taassob *et al.*<sup>306</sup> used PINNs to evaluate closure terms for turbulence and chemical source terms in the Sandia turbulent nonpremixed flames<sup>323</sup>. As illustrated in Figure 21, the NN took coordinates ( $x, r$ ) and Reynolds number as input for parametric learning, and output not only the mean flow fields, including  $\bar{p}$ ,  $\bar{\mathbf{U}}$ ,  $\bar{p}$ ,  $\bar{Z}$ , and two principal components ( $\bar{PC}$ ) of  $T$  and  $Y$ , but also the Reynolds stress ( $\overline{u'v'}$ ) and turbulent viscosity ( $\mu_t$ ) to learn the turbulence closure, which was achieved by adding the  $\mu_t$  relation to the physical losses:

$$-\bar{\rho}\overline{u'v'} = \mu_t \left( \frac{\partial \tilde{u}}{\partial r} + \frac{\partial \tilde{v}}{\partial x} \right) \quad (5.3)$$

To learn the reaction closure, a second NN was used to learn the mapping from  $\bar{PC}$  to their averaged reaction source terms. The PINNs were trained on Sandia flames D and F, and were validated on flames D, F, and E. The results showed that the reconstructed fields matched well with the experimental data and the learned closure terms were physically reasonable. Later, Taassob *et al.*<sup>106</sup> extended this method to Sydney flames. The extensions include: (1) Using DeepONet instead of MLP because more parameters are involved than Sandia flames. (2) Using six  $Y_k$  instead of  $\bar{PC}$  and learn the six reaction source terms, whose estimated observations were available. A two-stage training was conducted to learn the turbulence and reaction closures sequentially. The model was trained on three flames and validated on four flames and could predict satisfactory flow fields and species source terms.

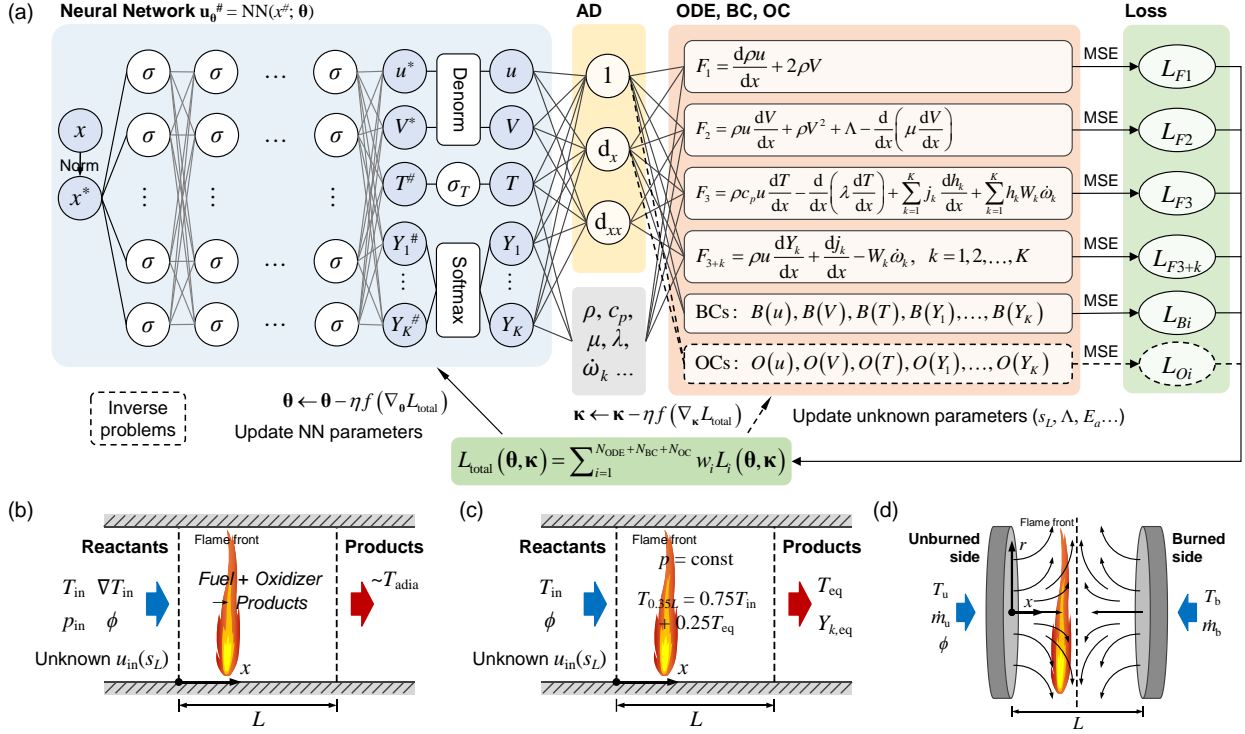


Figure 19: FlamePINN-1D for solving forward and inverse problems of 1D laminar flames. (a) Schematic of the FlamePINN-1D framework. (b) Case 1: freely-propagating premixed flames with simplified physical models. (c) Case 2: freely-propagating premixed flames with detailed physical models. (d) Case 3: counterflow premixed flames with detailed physical models. Reprinted from Reference <sup>112</sup>, with permission.

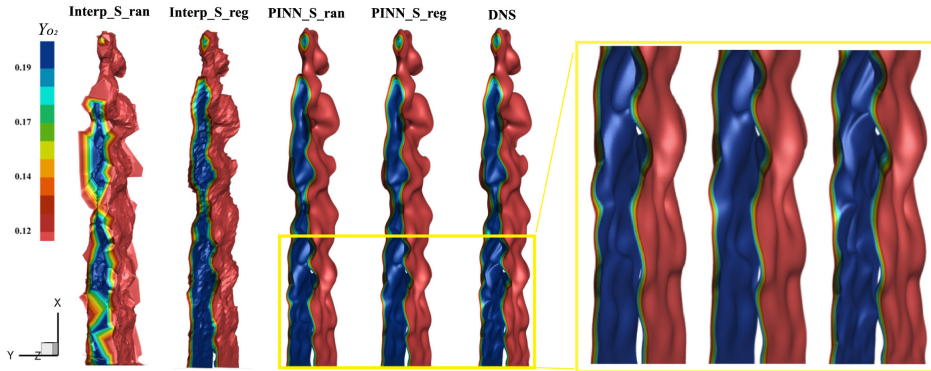


Figure 20: PINNs reconstruct turbulent flames: comparisons of the instantaneous 3D distributions of  $Y_{O_2}$  from linear interpolation, PINNs and DNS data. Reprinted from Reference <sup>304</sup>, with permission.

Liu *et al.* <sup>107</sup> used PINNs to reconstruct the soot fields in acoustically forced laminar sooting flames in two steps. In the first step, since the velocity data measured by particle image velocimetry (PIV) were missing in sooting regions, and the temperature data measured by non-linear excitation regime two-line atomic fluorescence (nTLAF) were missing in low-temperature regions, a PINN was used to reconstruct the velocity and temperature fields. The momentum and temperature equations were used as physical losses where the heat release and radiation were neglected due to low temperatures. Results showed that PINN could learn the available data well and reconstruct the missing fields. Next, a physics-informed AE-based DeepONet (PI-AE-DeepONet) with two AEs was used to reconstruct the soot fields, as shown in Figure 22. The simplified transport equation of soot mass fraction was taken as the physical loss where the unknown source term was learned by the second AE. The first AE was used to learn the latent features of OH images and PINN-reconstructed  $T$  images via supervised learning. The DeepONet took the latent features as the branch inputs and

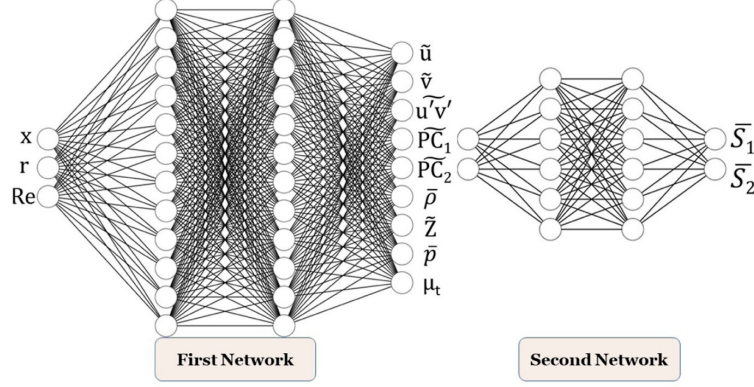


Figure 21: Schematic of the PINNs for turbulent combustion closure. Reprinted from Reference <sup>306</sup>, with permission.

output the soot volume fraction. It was shown that PI-AE-DeepONet yielded better predictions than various data-driven models, including U-Net, FNO, the first AE, and AE-DeepONet, and could learn the source terms accurately.

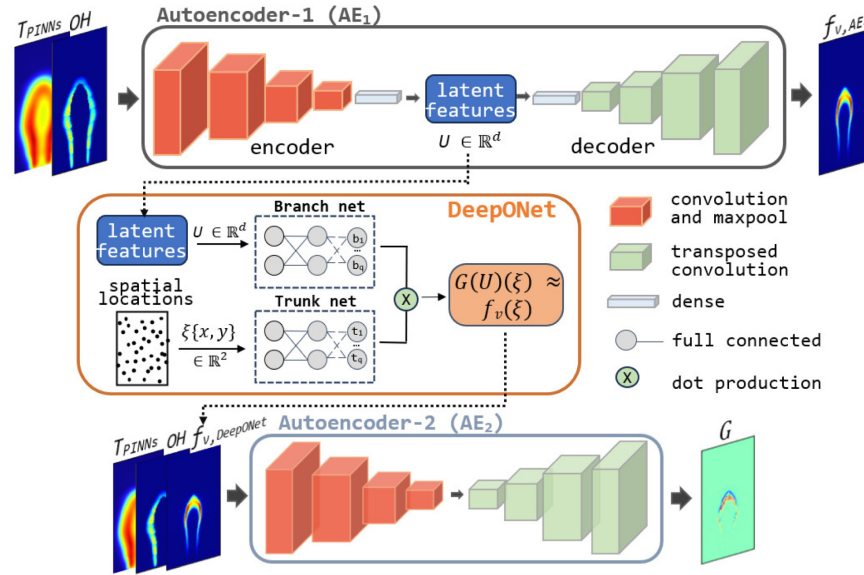


Figure 22: Schematic of the AE-based DeepONet framework to reconstruct the soot fields. Reprinted from Reference <sup>107</sup>, with permission.

Yadav *et al.* <sup>307</sup> developed the reactive flow PINNs (RF-PINNs) to reconstruct all flow quantities of interest solely based on sparse velocity or temperature data. The framework of RF-PINNs is given in Figure 23. Three cases were tested: 1D freely-propagating flames, 2D laminar slit flames, and 2D experimental turbulent flames. Based on some assumptions, the equations of  $T$  and  $Y_k$  were reduced to the equation of the progress variable  $c$ , which was denoted as  $\theta$  in the original paper. For laminar cases, the reaction source term of  $c$  was pre-learned by a data-driven NN:  $\dot{\omega}_c = \text{NN}(c)$ , while for turbulent cases, the source term was computed by the eddy break-up (EBU) model:

$$\bar{\omega}_c = C \frac{\varepsilon}{k} \bar{\rho} \tilde{c} (1 - \tilde{c}) \quad (5.4)$$

where  $C$  was a model constant. In the first case, by comparative analysis, it was shown that using only the mass and  $c$  equations was enough to get accurate results, so the momentum equation was not considered in the latter two cases to alleviate the computational burden. In the third case, two scalar turbulent flux terms were added to the NN output so that they can be learned by the NN instead of being explicitly modeled. The results showed that either from sparse velocity or temperature data, the missing fields could be well reconstructed.

PINNs in a broad sense have also been applied to turbulent combustion. Sharma *et al.* <sup>116</sup> applied the PIML approach to predict the dynamic behaviour of hydrogen jet flames in an AR manner (see Section 2.3.1). As illustrated in Figure

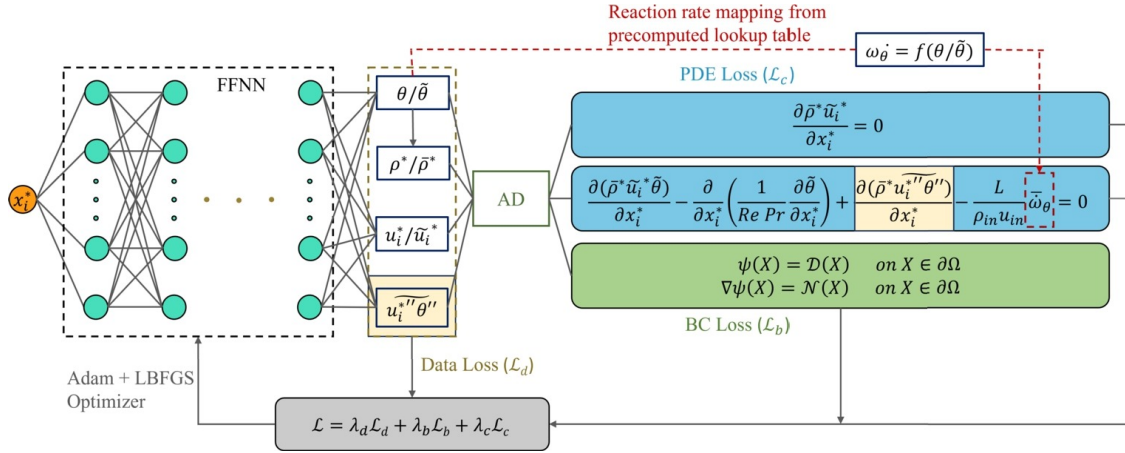


Figure 23: The framework of RF-PINNs. Reprinted from Reference<sup>307</sup>.

24, the physics-informed hybrid multiscale and partitioned network (PiMAPNet) was constructed that integrated low-resolution physics-based models (numerical solver) with trainable NNs, so it can be viewed as a hybrid solver. The coarse grid numerical solver served as the physics-informed component of the model, which was similar to the physics-informed way in References<sup>113–115</sup> that integrated a numerical solver. Three other methods were selected for comparison: a coarse grid numerical solver without ML component, a purely data-driven CNN without physics-informed component, and a PPNN variant. As mentioned in Section 2.3.4, the original PPNN preserves/embeds the PDEs by discretizing the PDE RHS using convolutions filters instead of a numerical solver. Compared to the PPNN variant, PiMAPNet decomposed the state vector into hydrodynamic/flow variables and thermochemical variables. The flow variables were learned by a single CNN while the thermochemical variables were learned by a mixture-of-experts (MoE) that partitioned the thermochemical state-space so that separate CNNs could be assigned to different regions of the manifold. Results showed that the data-driven CNN yielded unphysical values and the PPNN variant exhibited the hotspot issue. In contrast, PiMAPNet successfully mitigated the issues of bias accumulation and hotspots and showed superior extrapolation performance. It was showed that the MoE effectively partitioned the manifold in a physically meaningful way, distinctly isolating the fuel-rich, fuel-lean, and mixing regions, which was the core reason for its superior performance. Speed analysis also showed that PiMAPNet was faster than a numerical solver with comparable accuracies.

## 5.4 Supersonic combustion

For supersonic combustion, the core feature is the presence of shock waves and their interaction with combustion, which poses challenges for experimental implementation, numerical solutions, and PINNs. In the early work of Mao *et al.*<sup>324</sup>, they applied the DeepM&Mnet<sup>325</sup> for hypersonics to predict the coupled flow and finite-rate chemistry behind a normal shock. DeepM&Mnet was proposed as a data assimilation framework for fast simulating multiphysics and multiscale problems, where the pretrained DeepONets were used as building blocks to constrain the solutions<sup>325</sup>. In Reference<sup>324</sup>, the global mass conservation was constrained by adding a loss term, thus making the framework physics-informed. Comparative analysis demonstrated the effectiveness of this constraint on accuracy improvement. Guo *et al.*<sup>326</sup> developed the physics-informed residual CNNs to reconstruct the flow field at the inlet of scramjet with the Mach number  $Ma = 10$ , where the flow was non-viscous and non-reacting. After this study, Deng *et al.*<sup>309</sup> developed a physics-informed U-shaped residual NN (PI-ResUNet) to reconstruct the unsteady combustion flow field in a scramjet combustion chamber with  $Ma = 2$ . As shown in Figure 25, the 2D unsteady compressible NS equations without reaction source terms were taken as the physical constraints and the operating parameters (Mach number and effective viscosity coefficient) were taken as the inputs to form a parametric learning. Comparing the PI-ResUNet, ResNet, PI-ResNet, and PI-UNet, it was demonstrated that introducing the physical constraints and residual structures could effectively improve the model robustness. Note that although the hidden layers of PI-ResUNet are convolutional layers, the inputs and outputs are still linear layers. Therefore, it is still a continuous PINN that uses AD for differentiation instead of the convolutional differentiation adopted in discrete PINNs (Section 2.3.1).

Wang *et al.*<sup>308</sup> applied PINNs to reconstruct the combustion field in rotating detonation combustors (RDCs) based on partially observed data. As shown in Figure 26, a PINN was built to describe the 1D RDC numerical model and estimate the continuous physical fields, taking the space-time coordinates as inputs and physical fields as outputs. In this study, the observations included only ten sets of points with fixed spatial coordinates, representing measured data with

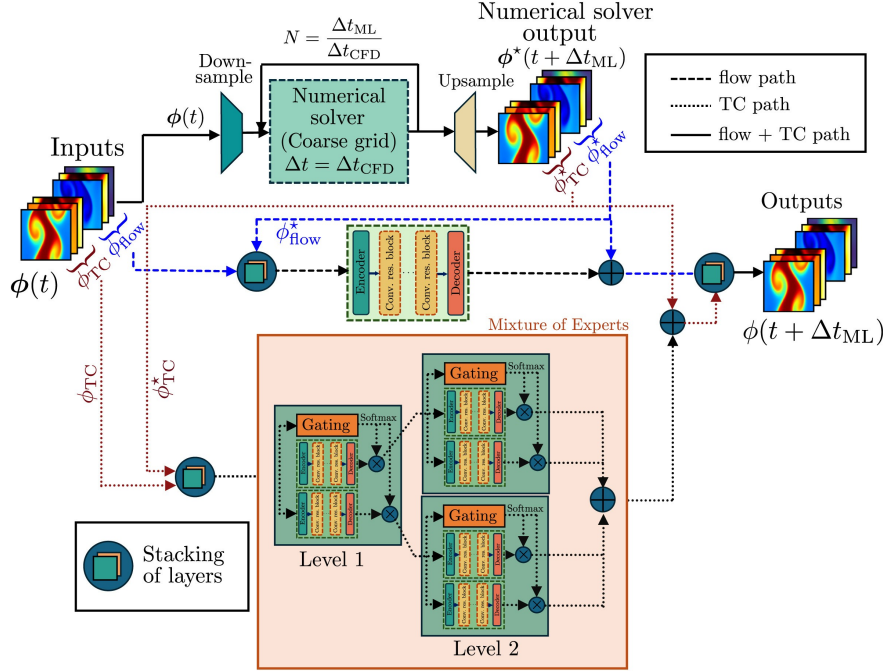


Figure 24: The architecture of PiMAPNet. Reprinted from Reference<sup>116</sup>, with permission.

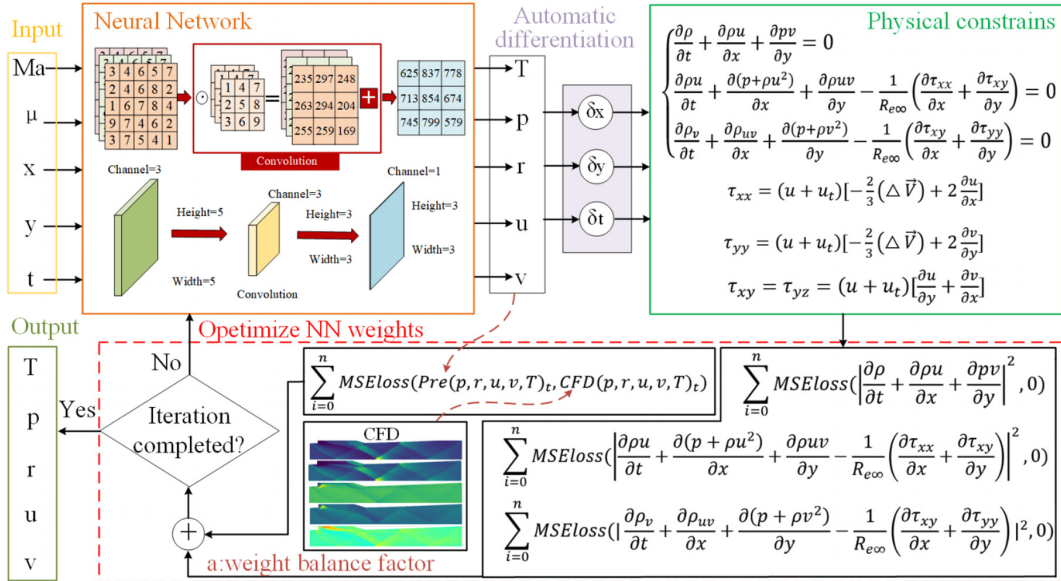


Figure 25: The framework of PI-ResUNet for reconstructing the combustion flow field in a scramjet combustor, where  $r$  indicates the density ( $\rho$ ) and  $\mu$  includes both the turbulent and laminar viscosity coefficients. Reprinted from Reference<sup>309</sup>, with permission.

fixed sensors. The studied problem was an inverse problem, where the equations and partial true results were known, but the overall solution of the equations was unknown. Results showed that compared to interpolation-based methods, PINN could better capture different distribution patterns for the flow characteristics before and after the detonation wave, which matched the ground truth satisfactorily. The proposed PINN can serve as a surrogate model of the RDC, which has promising engineering value in the design optimization and real-time monitoring of RDCs. After this study, Wang *et al.*<sup>312,313</sup> further used the discrete PINNs for SR in RDCs, which will be discussed in Section 5.5.

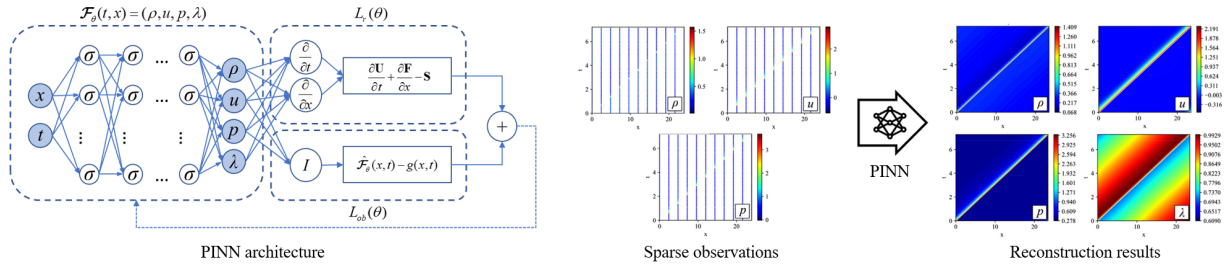


Figure 26: Illustration of the flow field reconstruction problem for RDCs. Reprinted from Reference<sup>308</sup>, with permission.

## 5.5 Combustion super-resolution via discrete PINNs

As mentioned in Section 2.3.1, discrete PINNs can be applied to SR reconstruction tasks. This field-to-field modeling paradigm is particularly suited for SR reconstruction tasks, offering advantages such as enhanced scalability for high-dimensional data, improved generalization to complex working conditions, and efficient handling of structured grid-based simulation results. Given the inherent complexity of combustion modeling, researchers have further augmented the regular discrete PINNs with generative modeling techniques, such as GANs. Compared to discriminative modeling approaches, generative modeling demonstrates superior capability in capturing small-scale turbulence dynamics<sup>310</sup> and refining predictions of discontinuous features<sup>312</sup>. Research on the application of discrete PINNs to combustion problems remains relatively limited. This subsection categorizes the discussion into two parts: subsonic combustion and supersonic combustion.

For subsonic combustion, Bode *et al.*<sup>310</sup> first used the physics-informed enhanced super-resolution generative adversarial network (PI-ESR-GAN) to model turbulent combustion. As shown in Figure 27, the PI-ESR-GAN framework combines unsupervised deep learning with physics-informed loss functions, employing a two-step training methodology to enhance network generalization, particularly for extrapolation tasks. In decaying turbulence tests involving turbulent mixing, the model demonstrated strong *a priori* and *a posteriori* performance, with the physics-informed continuity loss term proving essential. The PI-ESR-GAN methodology has been extended to diverse combustion configurations, demonstrating remarkable versatility. In spray combustion applications, the model was successfully implemented for different cases, with validation against experimental data revealing superior predictive capability compared to classical LES approaches<sup>327</sup>. For lean premixed combustion and gas turbine combustors, by developing a modified architecture for finite-rate chemistry flow, the enhanced model demonstrated superior accuracy in both *a priori* and *a posteriori* validations while maintaining computational efficiency<sup>328</sup>. For turbulent non-premixed flames, a multi-mesh strategy was developed to optimize prediction accuracy across different grid resolutions, enabling reliable extrapolation to untrained Reynolds numbers<sup>329</sup>. The approach was subsequently extended to premixed combustion<sup>311</sup>. For that, the physical information in the loss function were adjusted, the training process was smoothed, and especially the effects of density changes were considered. When applied to DNS data of turbulent premixed flame kernels, the enhanced model achieved remarkable accuracy in reproducing fine-scale dynamics on coarse computational meshes. This advancement enables more efficient statistical analysis, while significantly reducing computational costs compared to traditional approaches. Using high-fidelity DNS data, Chung *et al.*<sup>330</sup> benchmarked the scaling behaviour of five DL models on the 3D combustion SR task. One of the models incorporated a physics-based loss (i.e., physics-informed loss in a broad sense), which penalized the gradients of channel variables in a supervised manner. It was demonstrated that the benefits of this loss can persist with increasing model size.

For supersonic combustion, Wang *et al.*<sup>312</sup> developed the PI-GAN for flow field super-resolution reconstruction on RDCs. The model utilized a GAN architecture enhanced with additional physical loss terms to ensure the outputs adhere to fundamental physical principles. Compared to interpolation and other methods, PI-GAN greatly improved the resolution of the flow field while accurately capturing detailed flow structures. Subsequently, Wang *et al.*<sup>313</sup> proposed an advanced physics-informed recurrent GAN (PI-RGAN), as shown in Figure 28. This innovative framework incorporated temporal derivatives as intermediate variables during the data generation process within a recurrent architecture, while simultaneously employing spatial derivatives of the output to establish comprehensive physical constraints. Experimental analysis revealed some features of the proposed model. The PI-RGAN model could well capture the detailed flow field structures and temporal characteristics in RDCs. Moreover, the introduction of a recurrent structure in the PI-RGAN model enhanced the model robustness against noisy inputs.

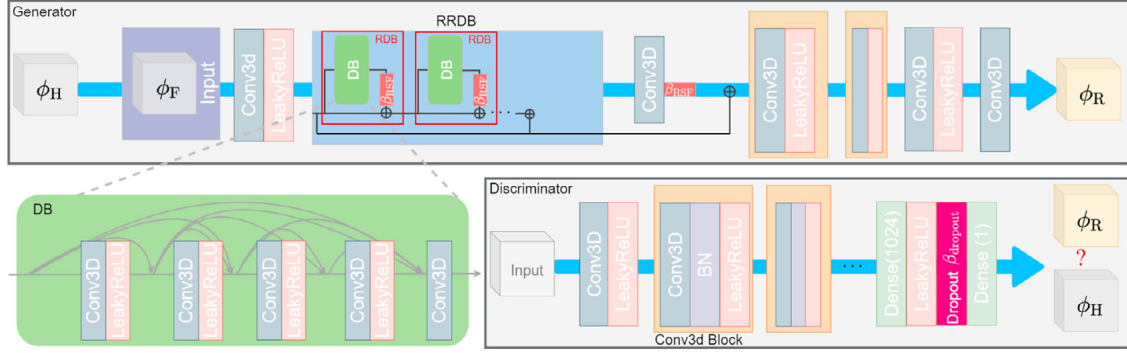


Figure 27: Diagram of the PI-ESR-GAN architecture. Reprinted from Reference<sup>310</sup>.

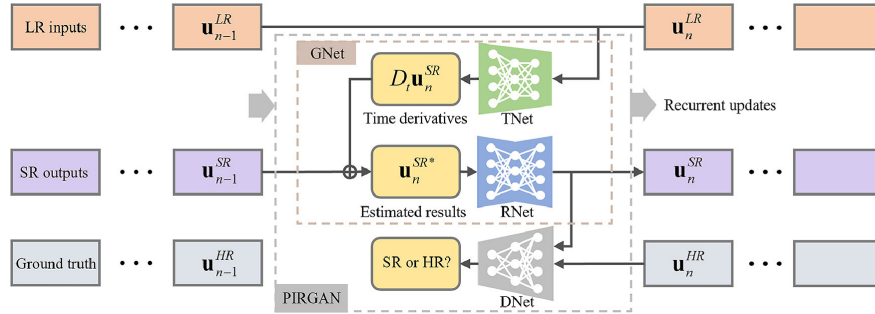


Figure 28: The PI-RGAN for the SR reconstruction of flow fields in RDCs. Reprinted from Reference<sup>313</sup>, with permission.

## 6 PIML for other combustion problems

Some studies on PIML for combustion cannot be classified to the previous two sections but are also important and enlightening. Therefore, they will be introduced in this section, which are categorized into four parts: fire safety, thermoacoustics, combustion diagnostics, and others.

### 6.1 Fire safety

Bottero *et al.*<sup>331</sup> replaced the PDE solver in the fire simulator to achieve real-time prediction of wildfire spread, where the level set equation was utilized. Tests on an ideal case and a real wildfire both demonstrated that the PINNs were able to capture the shape of the firelines. Dabrowski *et al.*<sup>332</sup> used PINNs to solve the level set equation for modeling the wildfire fire-front. A forecast likelihood was introduced to deal with the issue that PINNs failed to maintain temporal continuity when there are extreme changes in exogenous forcing variables. Moreover, the B-PINN was incorporated to provide UQ in fire-front predictions. The models were successfully applied to modeling two recorded grassland fires. Vogiatzoglou *et al.*<sup>333</sup> applied PINNs to infer the parameters in the wildfire spread model, consisting of energy and mass fraction equations. The parameters included the dispersion coefficient vector, mean gaseous velocity vector, and the overall heat transfer coefficient, so the number of parameters was three in 1D cases and five in 2D cases. Five cases were tested, including both clean and noisy data, and both synthetic and real-world data, demonstrating the accuracy of parameter inference and wildfire prediction. Some other wildfire-related applications do not focus on the spread prediction. For post-fire applications, Seydi *et al.*<sup>334</sup> used PIML to estimate the soil burn severity and reveal the intricate relationships between soil and vegetation burn severities. For firefighting, the AI Firefighter<sup>335</sup> was proposed to predict the optimal firefighting strategy given an arbitrary terrain and an arbitrary fire distribution, where the NN combined PIML with a decision-making process.

Other applications are not related to wildfire. Kim *et al.*<sup>336</sup> used PINNs to model and predict the lithium-ion battery thermal runaway, which is an important topic of fire safety. The PDEs of temperature and lithium concentration served as the governing equations, which was a DR system. The model applicability to semi-supervised learning, unsupervised learning, and surrogate modeling was investigated, showing that PINNs exhibited better performance than purely data-driven NNs. Lu *et al.*<sup>108</sup> used the PI-DeepONet for surrogate modeling of the radiative heat transfer, where the radiation transfer equation (RTE) and its BCs were considered as the physical losses. The model took the location and

propagation direction as trunk net inputs, the parameters (such as the absorption coefficients) as branch net inputs, so the solution operator of the RTE could be approximated. The surrogate model offers significant speedup over traditional methods, thus possessing the potential to replace the traditional RTE solvers in industry-scale fire simulations, where the solution of RTE is often a major performance bottleneck. Parsa *et al.*<sup>337</sup> applied PINNs to predict the transient burning rates of non-charring materials, where the energy equations in the temperature rise phase and burning phase were considered in the loss function. Results showed that PINNs could effectively capture the intricate dynamics of transient burning behavior and were more efficient than traditional numerical methods.

## 6.2 Thermoacoustics

Ozan *et al.*<sup>338</sup> used PINNs to learn the nonlinear limit cycles and adjoint limit cycles occurred in thermoacoustic oscillations. The physics was informed in two ways: (1) the governing equations that are derived from mass, momentum and energy conservation were integrated into the loss function, and (2) the periodicity was enforced using periodic activation functions in the NN. It was demonstrated that the PDE losses could promote the model performance in noisy-data and scarce-data situations, and only the NN with periodic activation functions could accurately extrapolate to the validation set. Mariappan *et al.*<sup>339</sup> used PINNs to learn thermoacoustic interactions in a bluff body anchored flame combustor, where three PDEs arising from the acoustic model and the van der Pol (VDP) oscillator model served as the physical losses. Based on the available data of the acoustic pressure fluctuations at three locations and the total flame heat release rate, the model aimed to identify four physical parameters and recover the entire fields of the acoustic pressure, velocity, and total heat release. Five cases were tested in the order of increasing complexity with the final case using the experimental data. The satisfactory results indicated the potential of PINNs to improve existing or design new thermoacoustically stable and structurally efficient combustors. Xie *et al.*<sup>340</sup> extended the VDP equation by introducing three parameters to enhance the model applicability, and then a PINN was applied to infer these parameters, where the data were generated for a horizontal Rijke tube with acoustically compact heat sources. The optimized PINN-EVDP model was shown to be capable of replicating the thermoacoustic system instability behaviour. Further investigations were conducted to compare the Hopf bifurcation and amplitude death characteristics of the coupled extended VDP system with the coupled theoretical Rijke tube systems, showing the physical significance of the extended VDP system in the field of thermoacoustics.

## 6.3 Combustion diagnostics

Wang *et al.*<sup>341</sup> used PINNs to reconstruct the 3D soot volume fraction in flames, where the NN took the 2D images of the accumulated projection value of the extinction coefficients as input, and output the local 3D extinction coefficients, as shown in Figure 29. The losses included the physical loss of the Lambert-Beer law, the boundary loss that constrained the positivity of the extinction coefficients, and the smoothness loss as a regularization term. Tested on two numerical cases and an experimental case, the model showed superior performance compared to conventional reconstruction methods. Later, Wang *et al.*<sup>342</sup> used PINNs to simultaneously reconstruct the soot temperature and volume fraction fields in experimental laminar ethylene flames. The inputs of the NN were the 2D matrix of the experimental soot radiation field and flame thickness in the line-of-sight (LoS), and the outputs were soot temperature, volume fraction fields, and an auxiliary variable. The physical loss was a first-order PDE for the auxiliary variable, which was derived from the LoS soot radiation integral equation. It was demonstrated that the physical constraint improved not only the predictive capability but also the adaptability and reliability across various combustion conditions.

## 6.4 Others

Chi *et al.*<sup>343</sup> applied PIML to discover the heat release rate (HRR) marker for premixed  $\text{NH}_3/\text{H}_2/\text{air}$  flames. Specifically, a physical loss term was added to infer the free parameters in the approximation equation for HRR. Several markers were identified and then tested on various operating conditions to find the most accurate combinations. Hosseini *et al.*<sup>344</sup> used the PINNs to solve the steady-state Bratu equation arising from solid biofuel combustion theory, which was a 1D nonlinear boundary value problem. Results showed that the trained PINNs were more accurate than the decomposition method and Laplace method. Yadov *et al.*<sup>345</sup> developed the PI-LSTM to predict the linear and nonlinear response of a premixed laminar flame to incoming velocity perturbations. The low-frequency limit for perfectly-premixed flames was incorporated as a physical loss term, which effectively improved the prediction accuracy of the flame transfer functions in the minimal data limit. Kim *et al.*<sup>346</sup> developed the PI-GNN to predict the cetane number (CN) with systematic data quality analysis. Based on the physical insights, the CN-related physical properties were embedded in the global state input, thus improving the model accuracy.

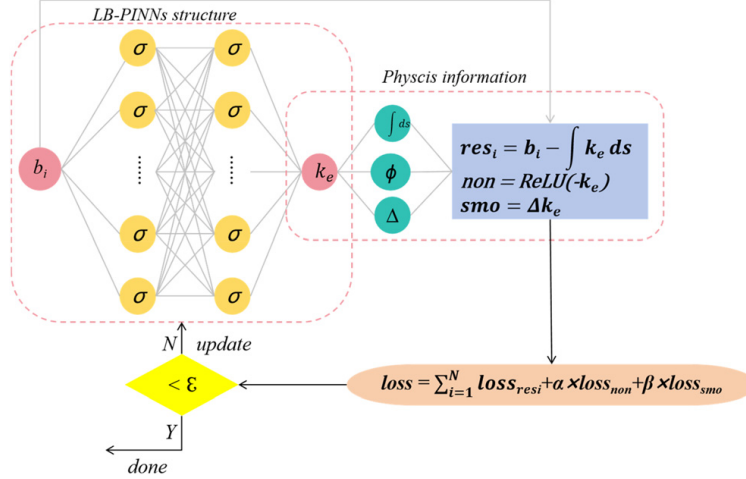


Figure 29: Schematic of the Lambert-Beer law PINN (LB-PINN) structure. Reprinted from Reference<sup>341</sup>, with permission.

## 7 Public resources

This section will introduce some public resources that can promote the development of PIML for combustion, including the dataset/benchmarks, simulation tools, and PIML tools. We list these resources as references not only for combustion researchers but also for AI researchers.

### 7.1 Datasets and benchmarks

It is known that data, algorithms, and computing power are the three driving forces behind AI development, reflecting the important role of data in AI. Specifically, data are the foundation for training models and their quality and quantity can directly influence the model performance. Therefore, it is important to establish public datasets and related benchmarks which can reduce redundant work, facilitate reproducibility, and standardize model evaluation and comparison. By definition, a benchmark is composed of the dataset(s) on which the benchmark is trained or evaluated, and a reference implementation in any language<sup>347</sup>. Note that although PIML for forward problems is purely physics-driven and data-free, ground-truth data is also necessary for model evaluation, especially in academia. A large number of datasets and benchmarks have been established for various AI tasks, with the most famous of which is the ImageNet<sup>348</sup> for CV. In contrast, the datasets and benchmarks for SciML and fluid, and combustion are fewer, but have been growing rapidly in recent years. Compared to traditional AI datasets, datasets for SciML, fluid, and combustion usually exhibit unique properties due to their physics-driven nature, such as high-dimensional, multiscale, costly-generated, and interdisciplinary, which pose challenges for the generation, storage, sharing, and use of the datasets.

Table 6 lists some representative public datasets and benchmarks for SciML, fluid, and combustion. Since fluid mechanics is an important topic of SciML, fluid datasets are included in many SciML dataset/benchmarks, such as those listed in Table 6. Takamoto *et al.*<sup>138</sup> developed the PDEBench, providing 35 datasets based on 11 well-known time-dependent and time-independent PDEs and evaluating popular SciML models, such as the FNO, U-Net, and PINNs, in an AR way (see Section 2.3.1). Luo *et al.*<sup>136</sup> constructed the CFDBench for evaluating the NOs on four CFD cases in both AR and NAR ways. Koehler *et al.*<sup>137</sup> established the APEBench not only for evaluating AR neural emulators, but also providing an integrated differentiable simulation framework. As a PINN-specific benchmark, PINNacle developed by Hao *et al.*<sup>349</sup> provides a diverse dataset covering over 20 distinct PDEs from various domains. PINNacle also serves as a user-friendly toolbox that incorporate more than ten PINN methods, some of which are introduced in Section 2.3. A detailed comparison of fluid-contained SciML dataset/benchmarks can be found in the paper of FlowBench<sup>350</sup>. Note that although some SciML benchmarks evaluate the models on AR tasks, their datasets can also be used for evaluating the classical NAR PIML models. In addition to the fluid data in SciML dataset/benchmarks, there are also some classical fluid datasets in the fluid community, such as the well-known Johns Hopkins turbulence database (JHTDB)<sup>351</sup> and the ERCOFTAC (European Research Community On Flow, Turbulence, And Combustion) classic collection database<sup>352</sup>. They were originally established for use in fluid tasks, such as turbulence modeling, but now they can also be used for SciML. A list of fluid databases and collections from the fluid community can be found in Reference<sup>353</sup>. In addition to datasets and benchmarks, knowledge bases also serve as important resources for both

academia and industry. An example is the ERCOFTAC knowledge base wiki<sup>354</sup>, which provides structured knowledge and advice for CFD, covering non-reacting and reacting flows.

Table 6: Some public datasets and benchmarks for SciML, fluid, and combustion.

Name	Description	Link
ScalarFlow <sup>355</sup>	A large-scale volumetric dataset of real-world scalar transport flows	<a href="#">URL</a>
PDEBench <sup>138</sup>	A benchmark suite for evaluating SciML methods on time-dependent PDE-based tasks	<a href="#">URL</a>
AirfRANS <sup>356</sup>	A dataset of solutions of 2D incompressible RANS equations over airfoils	<a href="#">URL</a>
PINNacle <sup>349</sup>	A comprehensive benchmark of PINNs for solving PDEs	<a href="#">URL</a>
CFDBench <sup>136</sup>	A benchmark for evaluating the generalization ability of NOs in CFD problems	<a href="#">URL</a>
FlowBench <sup>350</sup>	A large-scale benchmark for flow simulation over complex geometries	<a href="#">URL</a>
APEBench <sup>137</sup>	A benchmark suite for evaluating AR neural emulators for solving PDEs	<a href="#">URL</a>
The Well <sup>357</sup>	A large-scale simulation dataset of diverse spatiotemporal physical systems	<a href="#">URL</a>
JHTDB <sup>351</sup>	Johns Hopkins turbulence database	<a href="#">URL</a>
ERCOFTAC <sup>352</sup>	ERCOFTAC classic collection database	<a href="#">URL</a>
NASA TMR <sup>358</sup>	Turbulence modeling resource of NASA Langley Research Center	<a href="#">URL</a>
Towne <i>et al.</i> <sup>359</sup>	A database for reduced-complexity modeling of fluid flows	<a href="#">URL</a>
TNF library <sup>360</sup>	A library of well-documented flames established by the TNF workshop	<a href="#">URL</a>
BLASTNet <sup>330,361,362</sup>	A large-scale community-involved network-of-datasets of reacting and non-reacting flows obtained from DNS for benchmarking ML methods	<a href="#">URL</a>
GlobFire <sup>363</sup>	A global wildfire dataset for the analysis of fire regimes and fire behaviour	<a href="#">URL</a>
Sim2Real-Fire <sup>364</sup>	A multi-modal simulation dataset for forecast and backtracking of real-world forest fire	<a href="#">URL</a>
FireBench <sup>365</sup>	An ensemble of LES dataset of 3D wildfire spread	<a href="#">URL</a>

For combustion, the datasets and benchmarks are fewer than those for SciML and fluid. The TNF workshop is an international collaboration on turbulent combustion and established a library of well-documented flames that includes multiscalar and velocity data<sup>360</sup>. The flame types cover from simple jet flames to piloted jet flames, bluff body flames, and swirl flames. Some classic flames such as the Sandia flames<sup>323</sup> are also included and have already been studied using PIML<sup>305,306</sup> (see Section 5.3). Chung *et al.*<sup>361,362</sup> established the BLASTNet (Bearable Large Accessible Scientific Training Network-of-datasets), a network-of-datasets of reacting and non-reacting flows which combines community involvement, public data repositories, and lossy compression algorithms. Figure 30 gives an overview of the BLASTNet, which is still developing. Using the DNS data of a H<sub>2</sub>-air lifted flame, the authors showcased the usage of BLASTNet by benchmarking the CNNs on both the tasks of combustion regime classification and filtered reaction rate regression<sup>362</sup>. Later, the BLASTNet 2.0<sup>330</sup> was established with extended samples, configurations, and size, and has been used for benchmarking the scaling behaviour of five DL models on the 3D volumetric SR task. One of the five models adopted the physics-informed loss in a broad sense, as mentioned in Section 5.5. BLASTNet has also been used for other PIML tasks, such as the PiMAPNet<sup>116</sup> introduced in Section 5.3. Table 6 also provides some datasets of fire, including the GlobFire<sup>363</sup>, Sim2Real-Fire<sup>364</sup>, and FireBench<sup>365</sup>. The FireBench has also been uploaded to the BLASTNet. For a detailed comparison of datasets for wildfire analysis, readers can refer to the paper of Sim2Real-Fire<sup>364</sup>.

## 7.2 Simulation tools (data generators)

In SciML, even with the growing number of public datasets and benchmarks, researchers still need to generate their own datasets using simulation tools, which are essential for customizing domain-specific cases, controlling data quality, and filling the inherent sparsity of public datasets. Table 7 gives a non-exhaustive list of public tools for ODE/PDE solution, fluid simulation, and combustion simulation. There are no clear boundaries between these three types of tools: Fluid simulation often falls under PDE solution, while combustion simulation often falls under either ODE solution or fluid simulation. Some ODE/PDE solution tools can be used for fluid/combustion simulation, while others cannot. For example, The CVODE<sup>366</sup> in SUNDIALS<sup>367,368</sup> has been used in many aforementioned combustion researches<sup>114,115,276,289</sup>. The PyClaw<sup>369</sup>, Python version of Clawpack<sup>370,371</sup>, has been used for simulating supersonic combustion<sup>308</sup>. For fluid simulation, the OpenFOAM<sup>372-375</sup> is a widely-used open-source CFD software and has many solvers for combustion, such as the chemFoam, reactingFoam, fireFoam, flameletFoam<sup>376</sup>, and FGMFoam<sup>377</sup>. Recently, researchers have developed tools that utilize the large language models (LLMs) to automate OpenFOAM programming, including the MetaOpenFOAM<sup>378,379</sup> and OpenFOAMGPT<sup>380,381</sup>. Cantera<sup>382</sup> is an open-source suite of tools for problems involving chemical kinetics, thermodynamics, and transport processes, and has been used in PIML for 1D laminar flames<sup>112</sup>. Some AI-integrated simulators are also provided in Table 7, including (1) the DeepFlame<sup>115</sup>, a deep

## Motivation

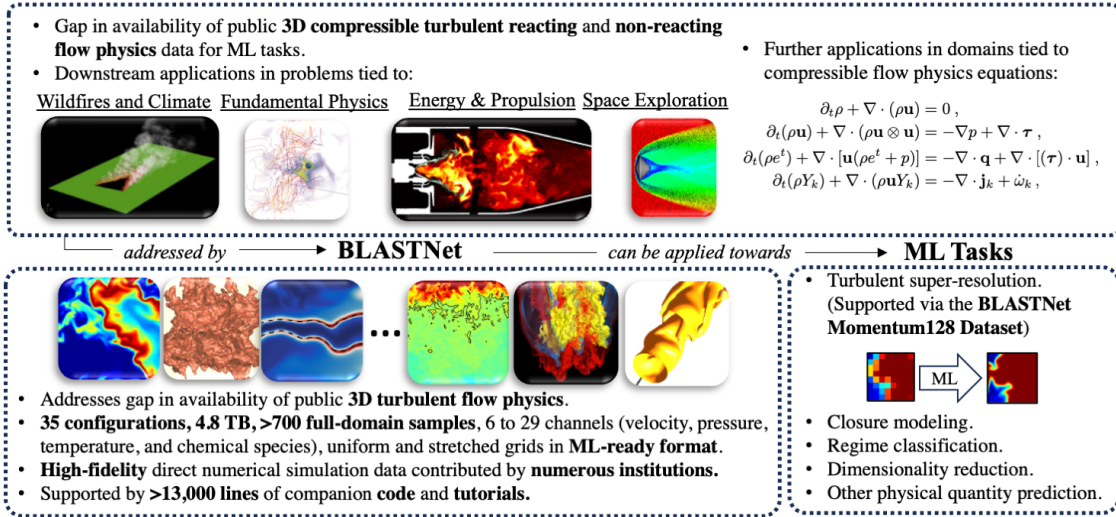


Figure 30: Overview of the BLASTNet<sup>330,361,362</sup>.

learning empowered open-source platform for reacting flow simulations, which coupled the three tools of OpenFOAM, Torch<sup>383</sup>, and Cantera, and (2) differentiable solvers, including the torchdiffeq<sup>384</sup>,  $\Phi_{\text{Flow}}$ <sup>385,386</sup>, JAX-Fluids<sup>387,388</sup>, Arrhenius.jl<sup>389</sup>, and JANC<sup>390</sup>. Table 7 also lists some tools that can be used for or are specifically designed for the DNS of fluid and combustion, including the Dedalus<sup>391</sup>, Nek5000<sup>392</sup>, SENGAs<sup>393</sup>, and AVBP<sup>394</sup>. Note that most DNS tools for combustion are in-house codes, such as the NGA<sup>395</sup>, S3D<sup>396</sup>, and Athena-RFX<sup>397</sup>, which have been used for establishing the BLASTNet<sup>330</sup>. See more examples in this review<sup>398</sup> and the paper of BLASTNet 2.0<sup>330</sup>. However, considering the extremely high cost of DNS for combustion, it is recommended to directly use the public datasets mentioned in Section 7.1 rather than generating them, especially for AI-community researchers.

The tools in Table 7 have been used for generating datasets and benchmarks in Table 6. For example, the Clawpack and  $\Phi_{\text{Flow}}$  were used to establish the PDEBench<sup>138</sup>, while the Clawpack and Dedalus were used to establish the Well<sup>357</sup>. In addition to free tools, researchers can also use some widely-used commercial software for fluid/combustion simulation and dataset generation, such as the ANSYS Fluent<sup>399</sup>, Chemkin<sup>400</sup>, and COMSOL Multiphysics<sup>401</sup>. For example, COMSOL Multiphysics has been used for generating data in PIML for combustion<sup>336</sup> and generating the datasets of PINNacle<sup>349</sup>. An overview of both free and commercial CFD software can be found in Reference<sup>402</sup>.

### 7.3 PIML tools

There are many tools for implementing the classical PIML, i.e., PINNs, some of which are presented in Table 8. Most tools are written in Python, except for the ADCME<sup>414</sup> and NeuralPDE<sup>415</sup>, which are written in Julia. Most tools can serve as solvers in which users only need to define the problem, while other tools, such as the SciANN<sup>416</sup> and ADCME<sup>414</sup>, work as wrappers in which users still need to deal with most of the implementation details. Since AD has been implemented in modern AI frameworks, such as the PyTorch<sup>417,418</sup>, TensorFlow<sup>419</sup>, and Keras<sup>420</sup>, they are usually used as the backend for these PIML tools. Most PIML tools support one or two backends, except for the DeepXDE<sup>167</sup>, which supports the PyTorch, TensorFlow, JAX<sup>421</sup>, and PaddlePaddle<sup>422</sup>. For more details of these PIML tools, readers can refer to these reviews<sup>65,77,89,91</sup>, where Reference<sup>89</sup> also listed the merits and limitations of some tools.

Some PIML tools have been used in PIML for combustion. For example, the NVIDIA PhysicsNeMo<sup>424</sup>, previously known as NVIDIA Modulus and SimNet<sup>431</sup>, was used in Reference<sup>301</sup>. The DeepXDE was used for implementing the FlamePINN-1D<sup>112</sup> and optimizing the extended VDP system<sup>340</sup>. Some studies also implement the PIML for combustion directly using the modern AI frameworks, including the PyTorch<sup>302–304,308</sup> and TensorFlow<sup>306</sup>, which is more flexible but cumbersome than using PIML tools. To show how popular PIML tools can be used for combustion research, a well-commented code demo is provided in Listing A1, which is based on the DeepXDE and adapted from the codes of FlamePINN-1D. Taking the 2D combustion reacting flow as example, the demo shows how to code the Equations (3.38) to (3.42) using a PIML tool, in which the convenience of AD to compute derivatives is clearly demonstrated. To illustrate how to infer unknown parameters in inverse problems, the demo also defines an unknown correction coefficient for viscosity. It is straightforward to modify the demo for 3D combustion. For more details about

Table 7: Some public tools for ODE/PDE solution, fluid simulation, and combustion simulation.

Name	Description	Link
SciPy <sup>403</sup>	An open-source scientific computing library in Python language	<a href="#">URL</a>
SUNDIALS <sup>367,368</sup>	An open-source SUite of Nonlinear and Differential/ALgebraic Equation Solvers	<a href="#">URL</a>
GEKKO <sup>404</sup>	A Python package for ML and optimization of mixed-integer and DAEs	<a href="#">URL</a>
torchdiffeq <sup>384</sup>	Differentiable ODE solvers implemented in PyTorch	<a href="#">URL</a>
FEniCS <sup>405-407</sup>	An open-source computing platform for solving PDEs based on the FEM	<a href="#">URL</a>
FreeFEM++ <sup>408</sup>	A free software for solving PDEs based on the FEM	<a href="#">URL</a>
FiPy <sup>409</sup>	A PDE solver using Python based on the FVM	<a href="#">URL</a>
Clawpack <sup>369-371</sup>	A package that collects FVMs for hyperbolic systems of conservation laws	<a href="#">URL</a>
Dedalus <sup>391</sup>	An open-source framework for solving PDEs using spectral methods	<a href="#">URL</a>
OpenFOAM <sup>372-374</sup>	An open-source CFD software	<a href="#">URL</a>
Nek5000 <sup>392</sup>	A fast and scalable open-source CFD solver using the spectral element method	<a href="#">URL</a>
$\Phi_{\text{Flow}}$ <sup>385,386</sup>	A differentiable PDE solving framework for optimization and ML applications	<a href="#">URL</a>
JAX-Fluids <sup>387,388</sup>	A differentiable CFD solver for 3D compressible single-phase and two-phase flows	<a href="#">URL</a>
CFD Python <sup>410</sup>	An online learning module for CFD with Python	<a href="#">URL</a>
Cantera <sup>382</sup>	An open-source suite of tools for problems involving chemical kinetics, thermodynamics, and transport processes	<a href="#">URL</a>
FlameMaster <sup>411</sup>	An open source C++ package for 0D and 1D laminar combustion calculations	<a href="#">URL</a>
OpenSMOKE++ <sup>412</sup>	A framework for simulating reacting systems with detailed kinetic mechanisms	<a href="#">URL</a>
SENGA+ <sup>393</sup>	A DNS code for 3D compressible turbulent reacting flows	<a href="#">URL</a>
AVBP <sup>394</sup>	A suite of CFD tools for performing LES/DNS of compressible reacting flows	<a href="#">URL</a>
DeepFlame <sup>115</sup>	A deep learning empowered CFD package for reacting flows	<a href="#">URL</a>
Arrhenius.jl <sup>389</sup>	A differentiable combustion simulation package	<a href="#">URL</a>
JANC <sup>390</sup>	A differentiable compressible reacting flow solver	<a href="#">URL</a>
FDS <sup>413</sup>	Fire dynamics simulator, a LES code for fire-driven fluid flows	<a href="#">URL</a>

Table 8: Some public tools of PIML.

Name	Description	Link
DeepXDE <sup>167</sup>	A library for SciML and PIML	<a href="#">URL</a>
PyDEns <sup>423</sup>	A Python framework for solving ODE/PDEs using NNs	<a href="#">URL</a>
NeuroDiffEq <sup>424,425</sup>	A Python package for solving DEs with NNs	<a href="#">URL</a>
NVIDIA PhysicsNeMo <sup>426</sup>	An open-source framework for building, training, and fine-tuning SciML models	<a href="#">URL</a>
Elvet <sup>427</sup>	An NN-based DE and variational problem solver	<a href="#">URL</a>
TensorDiffEq <sup>428</sup>	A Python package on top of Tensorflow for scalable multi-GPU PINN solvers	<a href="#">URL</a>
IDRLnet <sup>429</sup>	A PINN library on top of PyTorch	<a href="#">URL</a>
PINA <sup>430</sup>	A Python library designed to simplify and accelerate the development of SciML	<a href="#">URL</a>
SciANN <sup>416</sup>	A Keras/TensorFlow wrapper for scientific computations and PIML using NNs	<a href="#">URL</a>
ADCME <sup>414</sup>	A Julia framework to solve inverse problems involving physical simulations and NNs	<a href="#">URL</a>
NeuralPDE <sup>415</sup>	A Julia package for solving PDEs using PINNs	<a href="#">URL</a>

the implementation of IC/BC/OCs, network, training, and evaluation, and how to code other equations in Section 3 in a differentiable way, readers can refer to the codes of FlamePINN-1D<sup>112</sup>.

## 8 Discussions and outlooks

After introducing the main existing work, it is necessary to analyze the limitations, provide useful suggestions, and point out potential future directions. This section will first introduce the current challenges and corresponding solutions, then discuss some of the choices that researchers and engineers may face, and finally point out promising opportunities for both combustion and AI.

## 8.1 Challenges and solutions

### 8.1.1 Limitations reinforced by combustion

PIML itself has many limitations in terms of convergence, accuracy, and generalization, while combustion, as an extremely complex multi-physical process, will pose even greater challenges for PIML. As mentioned in Section 2.3, PIML has many failure modes, such as multiscale representation<sup>127</sup>, loss imbalance/conflict<sup>170</sup>, mode differences in multiple subdomains<sup>183</sup>, unreasonable sampling<sup>169</sup>, and ill-conditioned PDEs<sup>193</sup>. The inherent multiscale and multiphysics characteristics of combustion will certainly exacerbate these difficulties. For example, the wide range of scales involved in physical processes such as flow, chemical reaction, and diffusion in combustion reacting flows places higher demands on the multiscale representation of the ML models, while the large number of PDEs and corresponding IC/BCs poses challenges for loss balancing. Moreover, as mentioned in Section 2.3.4, most combustion PDE systems can be considered ill-conditioned. Even reaction problems that do not involve flow and diffusion have the inherent stiffness issue, as detailed in Section 4.1. In fact, the ill-conditioning issue also challenges the traditional numerical methods for combustion.

To deal with these difficulties, the methods introduced in Section 2.3 should be appropriately used and improved. For example, the Fourier multiscale embedding can be used to enhance the multiscale representation<sup>127</sup>, which has already been adopted in PIML for combustion<sup>301</sup>. However, the introduction of hyperparameters is another minor issue, which can be resolved if the scale information is known. Moreover, there is no guarantee that this method will be effective on problems with a wider range of scales. In such cases, it is necessary to combine the domain decomposition methods, which are particularly important for large-domain and long-time problems. Domain decomposition can also facilitate parallel computation, thus accelerating the simulation. It is recommended to use knowledge-based domain decomposition if the approximate distribution characteristics of the solution are known in advance. Examples include combustors with reactant, mixing, reaction, and product regions. Adaptive domain decomposition can also be proposed for more complex problems. Unlike common domain decomposition methods, for combustion problems, each subdomain can use not only different networks but also different physical laws, which is similar to the adaptive combustion models<sup>47</sup>. To deal with the multiphysics issue, imposing hard constraints on certain physical laws can always enhance the physical consistency and generalization ability. As for the ill-conditioning issue, some preconditioning strategies should be adopted, such as the normalization. For a deeper understanding, the ill-conditioning analysis should also be conducted for PIML solving combustion PDEs, which can be enlightened by the papers mentioned in Section 2.3.4. Although the reaction stiffness has been successfully solved in reaction ODE problems (see Section 4.1), it has not been thoroughly solved in reacting flow problems. As summarized in Table 5, when using the direct finite-rate chemistry in PIML, the most detailed reaction mechanism is only a two-step mechanism. Other studies either discard, simplify, tabulate, pre-learn, or online-learn the reaction part. Among these, only tabulating and pre-learning can represent the known detailed mechanism and may serve as feasible ways to tackle the stiffness issue in reacting flows, as long as they are differentiable. In fact, tabulating and pre-learning with NNs can be viewed as preconditioning strategies and can be categorized as building surrogate models of chemical kinetics, as mentioned in Section 4.2, not for CFD, but for PIML.

### 8.1.2 Discrepancies between physics, (physical) model, and data

There are many physical mechanisms involved in combustion that are not yet fully understood, such as the interaction between turbulence and chemical reactions, as well as the reaction mechanisms of specific problems. Therefore, there are no corresponding precise physical models. For PIML, which requires the coupling of physical laws, this presents both a challenge and an opportunity. The challenge lies in the need to carefully determine the physical model, while the opportunity lies in the feasibility to use PIML to model these unknown physical phenomena. Moreover, when real-world data are available, data-physics and data-model discrepancies also pose challenges. In these inverse problems, careful consideration must be given to the relative importance/weights of fitting the data and minimizing the physical model residuals.

As exemplified in Sections 4 and 5, to deal with these discrepancies between physics, model, and data, three strategies can be adopted: (1) Use reduced models, i.e., keep only the certain models and discard the uncertain parts. For example, the mass/continuity equation was adopted in most studies, as shown in Table 5, because it is certain, simple, and do not involve source terms that may need to be modeled for other equations. For the same reason, the energy and species equations are discarded in many studies. (2) Use simplified models. Examples include using RANS or LES models for turbulence and using simplified reaction mechanisms for complex reactions. Filtered PDEs have been proven to be effective for PIML to handle real-world data<sup>204</sup>. (3) Learn the models, especially the turbulence and reaction closures, which have been illustrated in References<sup>106,107,306,307</sup>. These works demonstrate that the potential of PIML in inverse problems is not limited to field reconstruction and parameter inference, but can also assist in physical modeling. In addition to designing strategies to address these discrepancies, it is also necessary to have methods to

measure these discrepancies, i.e., uncertainty quantification (UQ)<sup>213</sup>. The methods for quantifying data and model uncertainties mentioned in Section 2.3.4 can be applied to PIML for combustion.

### 8.1.3 Reproducibility

Reproducibility is the foundation of academic research, ensuring the reliability, transparency, and implementability of the adopted methods in the papers, thereby guaranteeing the credibility of their conclusions. Many fields face reproducibility issues, or the so-called reproducibility crisis<sup>432,433</sup>, and we believe that PIML for combustion is no exception. According to Reference<sup>434</sup>, overoptimism exists in ML for fluid-related PDEs, which is caused by weak baselines and reporting biases. The former does not apply to most studies on PIML for combustion because their goal is not to exceed a baseline model. However, reporting bias is highly likely to exist, which includes selective reporting, outcome switching, and publication bias<sup>434</sup>. In addition to the reporting bias, the reproducibility issues can also be caused by other pitfalls, including the sensitivity to hyperparameters, ambiguity in implementation details, and inaccessibility of data and codes. As demonstrated in Tables 4 and 5, most studies on PIML for combustion do not share codes, which is very different from the open source ecosystem of the AI community.

To deal with the reproducibility issues, McGreivy *et al.*<sup>434</sup> call for bottom-up cultural changes to minimize biased reporting and top-down structural reforms to reduce perverse incentives. We briefly outline some solutions at the researcher level: (1) Provide detailed model configurations, parameter settings, and evaluation metrics. (2) Improve data accessibility by either making data available or using publicly available data, such as those in Table 6. When establishing public datasets, it is preferable to follow the principles of FAIR (Findability, Accessibility, Interoperability, and Reusability)<sup>435</sup>. When establishing public benchmarks, some suggestions can be found in Reference<sup>347</sup>. (3) It is preferable to provide the codes, as we have done in References<sup>112,313</sup> and Listing A1. When developing public software, some suggestions can be found in Reference<sup>436</sup>. (4) Report not only positive results but also negative results. (5) Conduct replicate experiments and report the mean and variance of the results to demonstrate that the impact of randomness is negligible. (6) Conduct hyperparameter sensitivity analysis. For hyperparameters that are highly sensitive, sufficient explanation should be provided. Finally, we emphasize that the reproducibility issues can also be alleviated by the establishment of an open, active, and rigorous community for PIML for combustion, which involves the standardization of processes, tools, and definitions, as well as the open sourcing of data, codes, and tools. There is still a long way to go in this regard.

## 8.2 Discussions on implementation choices

**Forward vs inverse problems.** As shown in Tables 4 and 5, PIML is currently used more for inverse problems than for forward problems, and this is not limited to the field of combustion. There are many reasons for this: (1) Inverse problems are usually simpler than forward problems when both types of problems can be studied because of the involvement of data. When solving forward problems fails, inverse problems are the only option. (2) Inverse problems are more common than forward problems in practice. Forward problems have strict requirements and need complete equations and IC/BCs, while inverse problems have more relaxed requirements. Therefore, it is not that researchers do not study forward problems, but that the specific problems themselves are inverse problems. (3) Inverse problems have richer application significance than forward problems in terms of field reconstruction, parameter inference, physical modeling, and kinetics discovery. Forward problems often only involve simulation, which can also be achieved by traditional numerical methods. (4) Inverse problems are better suited to leveraging the advantages of PIML than forward problems. It is well known that the overall performance of PIML in forward problems is far inferior to that of traditional numerical methods<sup>434</sup>. However, one advantage of PIML is that it can easily couple data and incomplete equations to solve inverse problems, which is not straightforward for traditional numerical methods. In fact, the data-driven characteristic is an inherent advantage of ML, which can be leveraged in PIML. Nevertheless, the forward problems still have two important aspects: (1) In terms of academic research, the forward problem is the basis of the inverse problem. Research on the forward problems helps deepen our understanding of PIML, which in turn helps us understand the inverse problems. Furthermore, many proposed methods on the forward problems in terms of representation models, optimization processes, and PDE systems can be seamlessly transferred to the inverse problems. (2) In terms of practical applications, although PIML is inferior to traditional solvers in solving single PDE, it has demonstrated advantages in parametric/surrogate solving. Examples can be found in Section 2.3.4, Section 2.4, and Reference<sup>301</sup>. Compared with traditional solvers, it is more efficient, provides a continuous representation in the parameter space, and can easily perform parameter sensitivity analysis. Note that parametric/surrogate modeling can also be implemented in the way of inverse problems, where the data can be utilized. To sum up, both types of problems are important. For researchers and engineers, the choice between forward problems and inverse problems should depend on the specific circumstances and objectives.

**Continuous vs discrete PINNs.** As defined in Section 2.3.1, continuous PINNs follow the coordinate-to-variable mapping way, i.e.,  $\hat{\mathbf{u}} = \text{NN}(\mathbf{z})$ , while discrete PINNs follow the field-to-field mapping way, i.e.,  $\hat{\mathbf{U}}_{\text{out}} = \text{NN}(\mathbf{U}_{\text{in}})$ . Both have their own advantages and disadvantages<sup>136</sup>. Continuous PINNs provide a continuous representation of the solution, making them mesh-independent and allowing for easy query of values at any points. However, this greatly increases the difficulty of learning, as it requires learning the entire solution in the spatiotemporal domain. In contrast, discrete PINNs only need to learn the field-to-field mapping. The AD used in continuous PINNs eliminates the error in differentiation, but also increases the computational cost. Additionally, continuity makes it difficult for continuous PINNs to learn large gradients and discontinuous features, which are easier for discrete PINNs. Moreover, discrete PINNs are easier to implement hard constraints on PDEs, which will be elaborated in the part of "soft vs hard constraints" in this section. The choice between continuous PINNs and discrete PINNs should depend on the specific task type. For example, continuous PINNs are more suitable for learning continuous spatiotemporal solutions, reconstructing non-grid-based distributed data, and performing zero-error differentiation. Discrete PINNs are more suitable for tasks such as surrogate modeling of chemical kinetics (Section 4.2), super-resolution (Section 5.5), and AR simulations<sup>116</sup>.

**Complete/detailed vs reduced/simplified physics.** As mentioned in Sections 8.1.1 and 8.1.2, not all studies on PIML for combustion adopt complete/detailed physical models, such as detailed reaction mechanisms, complete PDEs, non-averaged NS equations, and closed turbulence terms. The choice between complete/detailed or reduced/simplified physical models should depend on the specific circumstances. For forward problems, the physical model can be simplified but must be complete, otherwise the problem will be ill-posed. For inverse problems with data, the choice is more flexible, and either a complete/detailed or a reduced/simplified physical model can be used. In fact, sometimes using only a few physical constraints can greatly enhance the overall performance. For example, some studies in Sections 4.2 and 4.3.1 show that using only species and element conservations can achieve a significant improvement. When there are discrepancies between the physics, model, and data, a reduced/simplified physical model can be used. See Section 8.1.2 for details. When both complete models and data are available, comparative studies can be conducted to identify which models have minimal impact on the results and can be omitted, thereby reducing computational costs, as demonstrated in Reference<sup>307</sup>.

**Soft vs hard constraints.** Classical PIML integrates physical laws through loss functions, which is a soft constraint, so there is still a risk of violating the laws. This is why hard constraints are necessary. As mentioned in the Section 2.3.4, there are many ways to implement hard constraints for IC/BCs, PDEs, and other physical laws. For example, IC/BCs for continuous PINNs can be enforced through input and output transformations, while for discrete PINNs, they can be enforced through padding operations. Discrete PINNs can also easily implement hard constraints on PDEs using convolution kernels or traditional numerical methods/solvers. However, it is difficult to implement hard constraints on PDEs for continuous PINNs. Even for the hard constraint projection (HCP)<sup>111</sup>, it is still necessary to minimize the PDE losses after projection. This is one of the advantages of discrete PINNs over continuous PINNs. For physical laws in the form of algebraic equations, i.e., most of the equations in Section 3, hard constraints can be implemented simply by directly specifying them, for both continuous and discrete PINNs. For example, the law of mass action and the Arrhenius law are hard constraints in all the literature that considers them introduced in this paper, because they are explicitly embedded in the intermediate steps of the method rather than constrained by the loss. Hard constraints have both advantages and disadvantages. Imposing hard constraints on certain physical laws will alleviate the burden of loss optimization. For example, enforcing species conservation can reduce one equation of  $Y$  that need to be solved. However, hard constraints can sometimes increase the difficulty of optimization, especially for IC/BCs, as they often involve hyperparameters and "hyperfunctions". In some cases, such as PDEs, complexity is also a disadvantage of hard constraints, which are less straightforward than soft constraints. The choice between soft constraints and hard constraints depends on many factors. By default, hard constraints should be considered first. Soft constraints can be used in the following situations: (1) when the constraint requirements are not strict; (2) when hard constraints are difficult to implement, such as for PDEs in continuous PINNs; (3) when hard constraints are extremely cumbersome to implement; (4) when hard constraints impair or greatly slow down the optimization and convergence, which requires *a posteriori* testing.

### 8.3 Opportunities for combustion and AI

#### Combustion-side opportunities.

- **Academic research.** First, there are still many limitations that need to be further solved, as mentioned in Section 8.1, including large-domain long-time problems, stiffness caused by detailed reaction mechanisms, model-data-physics discrepancies, and reproducibility issues. Second, there are still many combustion scenarios that can be studied using PIML, such as multiphase combustion, pollutant control, combustion diagnostics, microgravity combustion, explosions, and fires. Finally, there are still many tasks that can be achieved using

PIML, such as improving combustion models, gaining insights from experimental data, and developing hybrid solvers.

- **Practical applications.** Combustion has important applications in various fields, including power generation, transportation, fire safety, manufacturing, chemical synthesis, waste disposal, and space exploration. Therefore, the application of PIML for combustion in these fields remains to be explored. One promising application scenario is the construction of digital twins for combustion equipment, with functions of real-time monitoring, detection, prediction, and control. Good digital twins often require both big data and physical knowledge, which is the main advantage of PIML.
- **Integration of advanced AI methods.** As introduced in this paper, various AI methods have been used in PIML for combustion, including the basic MLP, KAN, NO, NODE, GAN, AE, and LSTM. However, there are still many advanced AI methods that have potential for application, such as DM, self-supervised learning, reinforcement learning, transfer learning, foundation models, and PDE discovery. Among these, DM has already been applied to fluid mechanics<sup>166,437,438</sup>. Foundation models are a hot topic due to their notable applications in the NLP field, including LLMs such as GPT<sup>24</sup>, Llama<sup>439</sup>, and DeepSeek<sup>440</sup>. In the SciML field, foundation models are a current key direction<sup>86,441</sup>. Some foundation models for PDEs have been developed, including the PDEformer<sup>442,443</sup>, UPS<sup>444</sup>, Poseidon<sup>445</sup>, PROSE-PDE<sup>446</sup>, and PROSE-FD for fluid PDEs<sup>447</sup>. Therefore, establishing foundation models for combustion is a feasible and promising direction, which also needs to be informed by combustion physics.

### AI-side opportunities.

- **Extension of strengths.** Combustion is a field where AI and PIML can further demonstrate and extend their interdisciplinary capabilities, broad applicability, and powerful versatility. This can be achieved in many of the aforementioned scenarios, such as computation acceleration, data assimilation, combustion diagnostics, fire safety, and digital twins.
- **Mitigation of limitations.** Combustion is a challenging testing ground for AI and PIML, where the shortcomings and limitations of existing model/algorithms may be exposed in terms of multiscale modeling, multiphysics modeling, generalization, and physical consistency. This is an opportunity to improve existing model/algorithms and develop new model/algorithms.
- **Combustion-inspired AI.** Physics-inspired AI paradigms are an important topic, in which AI methods are often proposed or improved by drawing inspiration from physical laws, phenomena, or principles. The inspiration can be achieved in many ways, including embedding physical laws, mimicking physical processes, and borrowing physical principles. Therefore, physics-inspired AI includes physics-informed AI, or it can be considered as physics-informed AI in a broad sense. Jiao *et al.*<sup>448</sup> have reviewed the AI methods that are inspired by classical mechanics, electromagnetism, statistical physics, and quantum mechanics. Additionally, two currently popular generative models are also inspired by physics: DM<sup>160,161</sup> is inspired by nonequilibrium thermodynamics, while the continuity equation in the flow matching<sup>449</sup> originates from fluid mechanics. Therefore, it is natural to ask: can we develop combustion-inspired AI? In fact, CRNN can be regarded as one such effort<sup>75</sup>, with its network architecture designed based on the law of mass action and Arrhenius law. However, given the abundance of combustion laws, phenomena, and principles, there are still many possibilities to explore, which may give rise to some revolutionary AI methods.

## 9 Conclusions

This paper provides a comprehensive review on PIML for combustion, systematically summarizing its fundamental principles, major studies, key advances, and available resources, while also providing constructive discussions and recommendations for researchers and engineers. The main conclusions are as follows: (1) PIML has been widely and successfully applied to combustion chemical kinetics, combustion reacting flows, and other combustion problems, addressing both forward and inverse problems. These applications demonstrate the growing attention, proven effectiveness, and significant potential of PIML in combustion research. (2) Numerous approaches exist for integrating combustion laws into ML. A primary focus of this review is to explain how such laws can be integrated into ML frameworks—either through soft or hard constraints, via loss functions or representation models, within coordinate-to-variable or field-to-field paradigms, and using either complete/detailed or reduced/simplified physics—highlighting the flexibility of PIML. (3) By incorporating combustion knowledge, the physical consistency and accuracy of ML models are always enhanced compared to purely data-driven ML. (4) PIML serves as a unified bridge between physics, models, and data, enabling both model-to-data simulation/reconstruction tasks and data-to-model modeling tasks under the guidance of physics. This integration produces three key outcomes that represent or contain physics: enhanced

data, improved physical models, and more reliable ML models. When discrepancies arise among physics, physical models, and data, PIML can address them through a range of strategies. (5) Challenges remain in terms of the inherent limitations of PIML, physics-model-data discrepancies, and reproducibility. Furthermore, many potential applications and research topics remain unexplored. Both of these points indicate promising directions for the future. In conclusion, PIML for combustion is a rapidly evolving field that calls for increased collaboration between combustion and AI researchers to address significant problems, develop improved strategies, and explore emerging opportunities.

## Acknowledgments

This work is supported by the National Key R&D Program of China (No. 2021YFA0716202), and the National Natural Science Foundation of China (No. 62273149).

## A A code demo of PIML for combustion

```
import torch
import deepxde as dde
import deepxde.grad.jacobian as jacobian
import deepxde.grad.hessian as hessian

def pde(self, xyt, uvpTYS):
    """
    shape of xyt: (n_pnt, 3)
    shape of uvpTYS: (n_pnt, 4 + n_spe)
    n_pnt: the number of sampling points on the domain for the current batch
    n_spe: the number of species
    """
    gas2d = args.gas2d # a class containing gas information and some differentiable functions
    n_spe = gas2d.n_spe
    # scaling/normalizing factors:
    scale_x, scale_y, scale_t = args.scales["x"], args.scales["y"], args.scales["t"]
    scale_u, scale_v, scale_p, scale_T = args.scales["u"], args.scales["v"], args.scales["p"],
    ↪ args.scales["T"]
    scale_Ys = torch.tensor(args.scales["Ys"], dtype=dtype) # shape: (n_spe, )

    u, v, p, T, Ys = uvpTYS[:, 0:1], uvpTYS[:, 1:2], uvpTYS[:, 2:3], uvpTYS[:, 3:4], uvpTYS[:, 4:]

    # compute the derivatives
    u_x = jacobian(uvpTYS, xyt, i=0, j=0)
    u_y = jacobian(uvpTYS, xyt, i=0, j=1)
    u_t = jacobian(uvpTYS, xyt, i=0, j=2)
    # u_xx = hessian(uvpTYS, xyt, component=0, i=0, j=0)
    # u_yy = hessian(uvpTYS, xyt, component=0, i=1, j=1)
    v_x = jacobian(uvpTYS, xyt, i=1, j=0)
    v_y = jacobian(uvpTYS, xyt, i=1, j=1)
    v_t = jacobian(uvpTYS, xyt, i=1, j=2)
    # v_xx = hessian(uvpTYS, xyt, component=1, i=0, j=0)
    # v_yy = hessian(uvpTYS, xyt, component=1, i=1, j=1)
    p_x = jacobian(uvpTYS, xyt, i=2, j=0)
    p_y = jacobian(uvpTYS, xyt, i=2, j=1)
    p_t = jacobian(uvpTYS, xyt, i=2, j=2)
    T_x = jacobian(uvpTYS, xyt, i=3, j=0)
    T_y = jacobian(uvpTYS, xyt, i=3, j=1)
    T_t = jacobian(uvpTYS, xyt, i=3, j=2)
    T_xx = hessian(uvpTYS, xyt, component=3, i=0, j=0)
    T_yy = hessian(uvpTYS, xyt, component=3, i=1, j=1)
    Ys_x = torch.hstack([jacobian(uvpTYS, xyt, i=4+k, j=0) for k in range(n_spe)])
    Ys_y = torch.hstack([jacobian(uvpTYS, xyt, i=4+k, j=1) for k in range(n_spe)])
    Ys_t = torch.hstack([jacobian(uvpTYS, xyt, i=4+k, j=2) for k in range(n_spe)])
    # Ys_xx = torch.hstack([hessian(uvpTYS, xyt, component=4+k, i=0, j=0) for k in range(n_spe)])
    # Ys_yy = torch.hstack([hessian(uvpTYS, xyt, component=4+k, i=1, j=1) for k in range(n_spe)])

    # compute some necessary properties using T and Ys
    rho = gas2d.cal_rho(T, Ys) # density, shape: (n_pnt, 1)
    cps = gas2d.cal_cps(T) # heat capacities, shape: (n_pnt, n_spe)
    cp = gas2d.cal_cp(T, Ys) # mean heat capacity, shape: (n_pnt, 1)
    mu = gas2d.cal_mu(T, Ys) # mean viscosity, shape: (n_pnt, 1)
```

```

lam = gas2d.cal_lam(T, Ys) # mean thermal conductivity, shape: (n_pnt, 1)
Dkm_apo = gas2d.cal_Dkms_apo(T, Ys) # mean diffusion coefficients, shape: (n_pnt, n_spe)
W = gas2d.cal_W(Ys) # mean molecular weight, shape: (n_pnt, 1)
Xs = gas2d.cal_Xs(Ys) # mole fractions, shape: (n_pnt, n_spe)
wdot = gas2d.cal_omega_dot_mass(T, Ys) # species production rates, shape: (n_pnt, n_spe)
wTdot = gas2d.cal_omegaT_dot(T, Ys) # reaction heat, shape: (n_pnt, 1)

# infer the correction coefficient for viscosity (cmu) in inverse problems, if users want
cmu = self.cmu_infe_s / args.scales["cmu"] if "cmu" in args.infer_paras else 1.0
mu = mu * cmu

# compute some terms in the continuity and momentum equations
rho_x = jacobian(rho, xyt, i=0, j=0)
rho_y = jacobian(rho, xyt, i=0, j=1)
rho_t = jacobian(rho, xyt, i=0, j=2)
div_U = u_x + v_y
tau_11 = mu * (4 / 3) * u_x
tau_12 = mu * div_U
tau_21 = mu * div_U
tau_22 = mu * (4 / 3) * v_y
tau_11_x = jacobian(tau_11, xyt, i=0, j=0)
tau_12_y = jacobian(tau_12, xyt, i=0, j=1)
tau_21_x = jacobian(tau_21, xyt, i=0, j=0)
tau_22_y = jacobian(tau_22, xyt, i=0, j=1)

# compute some terms in the species equations
Xs_x = torch.hstack([jacobian(Xs, xyt, i=k, j=0) for k in range(n_spe)]) # (n_pnt, n_spe)
Xs_y = torch.hstack([jacobian(Xs, xyt, i=k, j=1) for k in range(n_spe)]) # (n_pnt, n_spe)
js1 = -rho * (gas2d.Ws / W) * Dkm_apo * Xs_x # species mass flux on x, (n_pnt, n_spe)
js2 = -rho * (gas2d.Ws / W) * Dkm_apo * Xs_y # species mass flux on y, (n_pnt, n_spe)
js1 = js1 - Ys * torch.sum(js1, dim=-1, keepdim=True) # correct the mixture-averaged model
js2 = js2 - Ys * torch.sum(js2, dim=-1, keepdim=True)
js1_x = torch.hstack([jacobian(js1, xyt, i=k, j=0) for k in range(n_spe)]) # (n_pnt, n_spe)
js2_y = torch.hstack([jacobian(js2, xyt, i=k, j=1) for k in range(n_spe)]) # (n_pnt, n_spe)

# compute some terms in the energy equation
lam_x = jacobian(lam, xyt, i=0, j=0)
lam_y = jacobian(lam, xyt, i=0, j=1)
heat_cond = lam * (T_xx + T_yy) + lam_x * T_x + lam_y * T_y
js1_cp_sum = torch.sum(js1 * cps, dim=-1, keepdim=True) # (n_pnt, 1)
js2_cp_sum = torch.sum(js2 * cps, dim=-1, keepdim=True) # (n_pnt, 1)
heat_spediff = -js1_cp_sum * T_x - js2_cp_sum * T_y
heat_pressure = p_t + u * p_x + v * p_y
heat_viscous = tau_11 * u_x + tau_12 * u_y + tau_21 * v_x + tau_22 * v_y

# assemble the equations/residuals
continuity = rho_t + rho * div_U + (u * rho_x + v * rho_y)
momentum_x = rho * (u_t + u * u_x + v * u_y) - (tau_11_x + tau_12_y) + p_x
momentum_y = rho * (v_t + u * v_x + v * v_y) - (tau_21_x + tau_22_y) + p_y
energy = rho * (T_t + u * T_x + v * T_y) - (heat_cond + heat_spediff + wTdot + heat_pressure +
↪ heat_viscous)
species = rho * (Ys_t + u * Ys_x + v * Ys_y) + js1_x + js2_y - wdot # shape: (n_pnt, n_spe)

# scale/normalize the equations
continuity *= scale_u / scale_x
momentum_x *= scale_u * scale_u / scale_x
momentum_y *= scale_v * scale_u / scale_x
energy *= scale_T * scale_u / scale_x / 1000 # 1000 for scaling cp
species *= scale_Ys * scale_u / scale_x

return [continuity, momentum_x, momentum_y, energy] + [species[:, k: k+1] for k in
↪ range(n_spe)]

```

Listing A1: A code demo for the PDEs of 2D unsteady combustion reacting flows using the DeepXDE, with PyTorch as the backend. The Dufour and Soret effects are neglected.

## References

- [1] Rolf D. Reitz and Ganesh Duraisamy. Review of high efficiency and clean reactivity controlled compression ignition (RCCI) combustion in internal combustion engines. *Progress in Energy and Combustion Science*, 46:12–71, 2015. doi:10.1016/j.pecs.2014.05.003.
- [2] Katharina Kohse-Hoinghaus. Combustion, chemistry, and carbon neutrality. *Chemical Reviews*, 123(8):5139–5219, 2023. doi:10.1021/acs.chemrev.2c00828.
- [3] Ekenechukwu C. Okafor, K. D. Kunkuma A. Somarathne, Akihiro Hayakawa, Taku Kudo, Osamu Kurata, Norihiko Iki, and Hideaki Kobayashi. Towards the development of an efficient low-NOx ammonia combustor for a micro gas turbine. *Proceedings of the Combustion Institute*, 37(4):4597–4606, 2019. doi:10.1016/j.proci.2018.07.083.
- [4] Robert J Kee, Michael E Coltrin, and Peter Glarborg. *Chemically reacting flow: Theory and practice*. John Wiley & Sons, 2005. doi:10.1002/0471461296.
- [5] Thierry Poinsoot and Denis Veynante. *Theoretical and numerical combustion*. RT Edwards, Inc., third edition, 2012. URL: <https://elearning.cerfacs.fr/combustion>.
- [6] Chung K Law. *Combustion physics*. Cambridge University Press, 2010. doi:10.1017/CB09780511754517.
- [7] Chemkin theory manual. URL: [https://ansyshelp.ansys.com/public/account/secured?returnurl=/Views/Secured/corp/v242/en/chemkin\\_th/chemkin\\_th.html](https://ansyshelp.ansys.com/public/account/secured?returnurl=/Views/Secured/corp/v242/en/chemkin_th/chemkin_th.html).
- [8] Cantera science reference. URL: <https://www.cantera.org/stable/reference/#science-reference>.
- [9] Guijun Liu, Yuxin Wu, Suhui Li, and Yang Zhang. Instability behaviors and suppression of the unsteady autoignited turbulent jet flame in hot coflow. *Combustion Science and Technology*, 196(17):4923–4941, 2024. doi:10.1080/00102202.2023.2240010.
- [10] Yuxin Wu, Jiansheng Zhang, Philip J. Smith, Hai Zhang, Charles Reid, Junfu Lv, and Guangxi Yue. Three-dimensional simulation for an entrained flow coal slurry gasifier. *Energy & Fuels*, 24(2):1156–1163, 2010. doi:10.1021/ef901085b.
- [11] Nickolay N. Smirnov, Vladimir Borisovich Betelin, Valeriy F. Nikitin, Lyuben I. Stamo, and Dmitrii I. Altoukhov. Accumulation of errors in numerical simulations of chemically reacting gas dynamics. *Acta Astronautica*, 117:338–355, 2015. doi:10.1016/j.actaastro.2015.08.013.
- [12] Javier Urzay. *Supersonic combustion in air-breathing propulsion systems for hypersonic flight*, volume 50 of *Annual Review of Fluid Mechanics*, pages 593–627. 2018. doi:10.1146/annurev-fluid-122316-045217.
- [13] Guihua Zhang, Yuxin Wu, Jiahao Wu, Yang Zhang, and Hai Zhang. State of the art and challenges of flamelet method in gas turbine combustor simulation. *Journal of Tsinghua University (Science and Technology)*, pages 505–20, 2023. URL: <https://www.scopus.com/pages/publications/85153956953>, doi:10.16511/j.cnki.qhdx.2023.25.026.
- [14] Daniel C. Haworth. Progress in probability density function methods for turbulent reacting flows. *Progress in Energy and Combustion Science*, 36(2):168–259, 2010. doi:10.1016/j.pecs.2009.09.003.
- [15] Jeroen A. van Oijen, A. Donini, R. J. M. Bastiaans, J. H. M. ten Hijne Boonkamp, and L. P. H. de Goey. State-of-the-art in premixed combustion modeling using flamelet generated manifolds. *Progress in Energy and Combustion Science*, 57:30–74, 2016. doi:10.1016/j.pecs.2016.07.001.
- [16] Guijun Liu, Suhui Li, and Yuxin Wu. Effects of coflow velocity on the lift-off characteristics of autoignited jet flame in hot air coflow. *Combustion and Flame*, 259, 2024. doi:10.1016/j.combustflame.2023.113124.
- [17] Huina Guo, Lele Feng, Yuxin Wu, and Yang Zhang. Effect of turbulent mixing on combustion behaviours of a single biomass pellet. *Fuel*, 346, 2023. doi:10.1016/j.fuel.2023.128291.
- [18] Huina Guo, Yuxin Wu, Jie Liu, Lele Feng, and Hai Zhang. Effects of turbulent mixing on structural evolution and combustion characteristics of woody biomass particles. *Chemical Engineering Journal*, 503, 2025. doi:10.1016/j.cej.2024.158680.
- [19] Huina Guo, Xinde Zhang, Zhoutao Cen, Xin Li, and Yuxin Wu. Turbulence flow field in a four-fan stirred combustion furnace. *Physics of Fluids*, 37(4), 2025. doi:10.1063/5.0265341.
- [20] Thierry Poinsoot. Prediction and control of combustion instabilities in real engines. *Proceedings of the Combustion Institute*, 36(1):1–28, 2017. doi:10.1016/j.proci.2016.05.007.
- [21] Michael I. Jordan and Tom Mitchell. Machine learning: Trends, perspectives, and prospects. *Science*, 349(6245):255–260, 2015. doi:10.1126/science.aaa8415.
- [22] Yann LeCun, Yoshua Bengio, and Geoffrey Hinton. Deep learning. *Nature*, 521(7553):436–444, 2015. doi:10.1038/nature14539.
- [23] Kaiming He, Xiangyu Zhang, Shaoqing Ren, Jian Sun, and Ieee. Deep residual learning for image recognition. In *2016 IEEE Conference on Computer Vision and Pattern Recognition (CVPR)*, IEEE Conference on Computer Vision and Pattern Recognition, pages 770–778, 2016. doi:10.1109/cvpr.2016.90.
- [24] OpenAI. GPT-4 technical report. *arXiv preprint*, 2023. doi:10.48550/arXiv.2303.08774.
- [25] David Silver, Aja Huang, Chris J. Maddison, Arthur Guez, Laurent Sifre, George van den Driessche, Julian Schrittwieser, Ioannis Antonoglou, Veda Panneershelvam, Marc Lanctot, Sander Dieleman, Dominik Grewe, John Nham, Nal Kalchbrenner, Ilya Sutskever, Timothy Lillicrap, Madeleine Leach, Koray Kavukcuoglu, Thore Graepel, and Demis Hassabis. Mastering the game of Go with deep neural networks and tree search. *Nature*, 529(7587):484–489, 2016. doi:10.1038/nature16961.
- [26] Haixu Wu, Hang Zhou, Mingsheng Long, and Jianmin Wang. Interpretable weather forecasting for worldwide stations with a unified deep model. *Nature Machine Intelligence*, 5(6):602–611, 2023. doi:10.1038/s42256-023-00667-9.
- [27] Yuchen Zhang, Mingsheng Long, Kaiyuan Chen, Lanxiang Xing, Ronghua Jin, Michael I. I. Jordan, and Jianmin Wang. Skilful nowcasting of extreme precipitation with NowcastNet. *Nature*, 619(7970):526–532, 2023. doi:10.1038/s41586-023-06184-4.
- [28] Kaifeng Bi, Lingxi Xie, Hengheng Zhang, Xin Chen, Xiaotao Gu, and Qi Tian. Accurate medium-range global weather forecasting with 3D neural networks. *Nature*, 619(7970):533–538, 2023. doi:10.1038/s41586-023-06185-3.
- [29] Nathan Baker, Frank Alexander, Timo Bremer, Aric Hagberg, Yannis Kevrekidis, Habib Najm, Manish Parashar, Abani Patra, James Sethian, Stefan Wild, et al. Workshop report on basic research needs for scientific machine learning: Core technologies for artificial intelligence. Report, USDOE Office of Science (SC), Washington, D.C. (United States), 2019. URL: <https://www.osti.gov/biblio/1478744>, doi:10.2172/1478744.
- [30] Hanchen Wang, Tianfan Fu, Yuanqi Du, Wenhao Gao, Kexin Huang, Ziming Liu, Payal Chandak, Shengchao Liu, Peter Van Katwyk, Andreea Deac, Anima Anandkumar, Karianne Bergen, Carla P. Gomes, Shirley Ho, Pushmeet Kohli, Joan Lasenby, Jure Leskovec, Tie-Yan Liu, Arjun Manrai, Debora Marks, Bharath Ramsundar, Le Song, Jimeng Sun, Jian Tang, Petar Velickovic, Max Welling, Linfeng Zhang, Connor W. Coley, Yoshua Bengio, and Marinka Zitnik. Scientific discovery in the age of artificial intelligence. *Nature*, 620(7972):47–60, 2023. doi:10.1038/s41586-023-06221-2.
- [31] Tony Hey, Stewart Tansley, Kristin Tolle, and Jim Gray. *The fourth paradigm: Data-intensive scientific discovery*. Microsoft Research, 2009. URL: <http://fourthparadigm.org>.

- [32] Ankit Agrawal and Alok Choudhary. Perspective: Materials informatics and big data: Realization of the "fourth paradigm" of science in materials science. *APL Materials*, 4(5), 2016. doi:10.1063/1.4946894.
- [33] Anuj Karpatne, Gowtham Atluri, James H. Faghmous, Michael Steinbach, Arindam Banerjee, Auroop Ganguly, Shashi Shekhar, Nagiza Samatova, and Vipin Kumar. Theory-guided data science: A new paradigm for scientific discovery from data. *IEEE Transactions on Knowledge and Data Engineering*, 29(10):2318–2331, 2017. doi:10.1109/tkde.2017.2720168.
- [34] John Jumper, Richard Evans, Alexander Pritzel, Tim Green, Michael Figurnov, Olaf Ronneberger, Kathryn Tunyasuvunakool, Russ Bates, Augustin Zidek, Anna Potapenko, Alex Bridgland, Clemens Meyer, Simon A. A. Kohl, Andrew J. Ballard, Andrew Cowie, Bernardino Romera-Paredes, Stanislav Nikolov, Rishub Jain, Jonas Adler, Trevor Back, Stig Petersen, David Reiman, Ellen Clancy, Michal Zielinski, Martin Steinegger, Michalina Pacholska, Tamas Berghammer, Sebastian Bodenstein, David Silver, Oriol Vinyals, Andrew W. Senior, Koray Kavukcuoglu, Pushmeet Kohli, and Demis Hassabis. Highly accurate protein structure prediction with AlphaFold. *Nature*, 596(7873):583–589, 2021. doi:10.1038/s41586-021-03819-2.
- [35] Josh Abramson, Jonas Adler, Jack Dunger, Richard Evans, Tim Green, Alexander Pritzel, Olaf Ronneberger, Lindsay Willmore, Andrew J. Ballard, Joshua Bamber, Sebastian W. Bodenstein, David A. Evans, Chia-Chun Hung, Michael O'Neill, David Reiman, Kathryn Tunyasuvunakool, Zachary Wu, Akvile Zengulyte, Eirini Arvaniti, Charles Beattie, Ottavia Bertolli, Alex Bridgland, Alexey Cherepanov, Miles Congreve, Alexander I. Cowen-Rivers, Andrew Cowie, Michael Figurnov, Fabian B. Fuchs, Hannah Gladman, Rishub Jain, Yousuf A. Khan, Caroline M. R. Low, Kuba Perlin, Anna Potapenko, Pascal Savy, Sukhdeep Singh, Adrian Stecula, Ashok Thillaisundaram, Catherine Tong, Sergei Yakneen, Ellen D. Zhong, Michal Zielinski, Augustin Zidek, Victor Bapst, Pushmeet Kohli, Max Jaderberg, Demis Hassabis, and John M. Jumper. Accurate structure prediction of biomolecular interactions with AlphaFold 3. *Nature*, 630(8016):493–500, 2024. doi:10.1038/s41586-024-07487-w.
- [36] J. Nathan Kutz. Deep learning in fluid dynamics. *Journal of Fluid Mechanics*, 814:1–4, 2017. doi:10.1017/jfm.2016.803.
- [37] Steven L. Brunton, Bernd R. Noack, and Petros Koumoutsakos. *Machine learning for fluid mechanics*, volume 52 of *Annual Review of Fluid Mechanics*, pages 477–508. 2020. doi:10.1146/annurev-fluid-010719-060214.
- [38] Weiwei Zhang, Mingkun Xia, and Jiaqing Kou. A scientometric investigation of artificial intelligence for fluid mechanics: Emerging topics and active groups. *Progress in Aerospace Sciences*, 157:101130, 2025. doi:10.1016/j.paerosci.2025.101130.
- [39] Ricardo Vinuesa, Steven L. Brunton, and Beverley J. McKeon. The transformative potential of machine learning for experiments in fluid mechanics. *Nature Reviews Physics*, 5(9):536–545, 2023. doi:10.1038/s42254-023-00622-y.
- [40] Jonathan Tompson, Kristofer Schlachter, Pablo Sprechmann, and Ken Perlin. Accelerating Eulerian fluid simulation with convolutional networks. In *34th International Conference on Machine Learning (ICML)*, volume 70 of *Proceedings of Machine Learning Research*, pages 3424–3433, 2017. URL: <https://proceedings.mlr.press/v70/tompson17a>.
- [41] Dmitrii Kochkov, Jamie A. Smith, Ayya Alieva, Qing Wang, Michael P. Brenner, and Stephan Hoyer. Machine learning-accelerated computational fluid dynamics. *Proceedings of the National Academy of Sciences of the United States of America*, 118(21), 2021. doi:10.1073/pnas.2101784118.
- [42] Ricardo Vinuesa and Steven L. Brunton. Enhancing computational fluid dynamics with machine learning. *Nature Computational Science*, 2(6):358–366, 2022. doi:10.1038/s43588-022-00264-7.
- [43] Lei Zhou, Yuntong Song, Weiqi Ji, and Haiqiao Wei. Machine learning for combustion. *Energy and AI*, 7:100128, 2022. doi:10.1016/j.egyai.2021.100128.
- [44] Matthias Ihme, Wai Tong Chung, and Aashwin Ananda Mishra. Combustion machine learning: Principles, progress and prospects. *Progress in Energy and Combustion Science*, 91:101010, 2022. doi:10.1016/j.peccs.2022.101010.
- [45] Corentin J. Lapeyre, Antony Misdariis, Nicolas Cazard, Denis Veynante, and Thierry Poinso. Training convolutional neural networks to estimate turbulent sub-grid scale reaction rates. *Combustion and Flame*, 203:255–264, 2019. doi:10.1016/j.combustflame.2019.02.019.
- [46] Andrea Seltz, Pascale Domingo, Luc Vervisch, and Zacharias M. Nikolaou. Direct mapping from LES resolved scales to filtered-flame generated manifolds using convolutional neural networks. *Combustion and Flame*, 210:71–82, 2019. doi:10.1016/j.combustflame.2019.08.014.
- [47] Wai Tong Chung, Aashwin Ananda Mishra, Nikolaos Perakis, and Matthias Ihme. Data-assisted combustion simulations with dynamic submodel assignment using random forests. *Combustion and Flame*, 227:172–185, 2021. doi:10.1016/j.combustflame.2020.12.041.
- [48] Junsu Shin, Yipeng Ge, Arne Lampmann, and Michael Pfitzner. A data-driven subgrid scale model in Large Eddy Simulation of turbulent premixed combustion. *Combustion and Flame*, 231, 2021. doi:10.1016/j.combustflame.2021.111486.
- [49] Jinlong Liu and Haifeng Wang. Machine learning assisted modeling of mixing timescale for LES/PDF of high-Karlovitz turbulent premixed combustion. *Combustion and Flame*, 238, 2022. doi:10.1016/j.combustflame.2021.111895.
- [50] Giuseppe D'Alessio, Alessandro Parente, Alessandro Stagni, and Alberto Cuoci. Adaptive chemistry via pre-partitioning of composition space and mechanism reduction. *Combustion and Flame*, 211:68–82, 2020. doi:10.1016/j.combustflame.2019.09.010.
- [51] Kaidi Wan, Camille Barnaud, Luc Vervisch, and Pascale Domingo. Machine learning for detailed chemistry reduction in DNS of a syngas turbulent oxy-flame with side-wall effects. *Proceedings of the Combustion Institute*, 38(2):2825–2833, 2021. doi:10.1016/j.proci.2020.06.047.
- [52] Kaidi Wan, Camille Barnaud, Luc Vervisch, and Pascale Domingo. Chemistry reduction using machine learning trained from non-premixed micro-mixing modeling: Application to DNS of a syngas turbulent oxy-flame with side-wall effects. *Combustion and Flame*, 220:119–129, 2020. doi:10.1016/j.combustflame.2020.06.008.
- [53] Huu-Tri Nguyen, Pascale Domingo, Luc Vervisch, and Phuc-Danh Nguyen. Machine learning for integrating combustion chemistry in numerical simulations. *Energy and AI*, 5:100082, 2021. doi:10.1016/j.egyai.2021.100082.
- [54] Opeoluwa Owoyele and Pinaki Pal. ChemNODE: A neural ordinary differential equations framework for efficient chemical kinetic solvers. *Energy and AI*, 7:100118, 2022. doi:10.1016/j.egyai.2021.100118.
- [55] Rishikesh Ranade, Genong Li, Shaoping Li, and Tarek Echekki. An efficient machine-learning approach for PDF tabulation in turbulent combustion closure. *Combustion Science and Technology*, 193(7):1258–1277, 2021. doi:10.1080/00102202.2019.1686702.
- [56] Yan Zhang, Shijie Xu, Shenghui Zhong, Xue-Song Bai, Hu Wang, and Mingfa Yao. Large eddy simulation of spray combustion using flamelet generated manifolds combined with artificial neural networks. *Energy and AI*, 2:100021, 2020. doi:10.1016/j.egyai.2020.100021.
- [57] Zeinab Shadram, Tuan M. Nguyen, Athanasios Sideris, and William A. Sirignano. Physics-aware neural network flame closure for combustion instability modeling in a single-injector engine. *Combustion and Flame*, 240, 2022. doi:10.1016/j.combustflame.2021.111973.
- [58] Guihua Zhang, Xin Li, Yuxin Wu, Ruihan Zhang, Huina Guo, and Guangxi Yue. A data driven conditional presumed PDF generation method for FGM with random forest model. *Combustion Science and Technology*, 2025. doi:10.1080/00102202.2025.2481320.
- [59] Guihua Zhang, Jiayue Liu, Yuxin Wu, and Guangxi Yue. Novel data-driven PDF modeling in FGM method based on sparse turbulent flame data. *Energies*, 18(13):3546, 2025. doi:10.3390/en18133546.
- [60] Xingjian Wang, Yu-Hung Chang, Yixing Li, Vigor Yang, and Yu-Hsiang Su. Surrogate-based modeling for emulation of supercritical injector flow and combustion. *Proceedings of the Combustion Institute*, 38(4):6393–6401, 2021. doi:10.1016/j.proci.2020.06.303.

- [61] Zengyi Lyu, Xiaowei Jia, Yao Yang, Keqi Hu, Feifei Zhang, and Gaofeng Wang. A comprehensive investigation of LSTM-CNN deep learning model for fast detection of combustion instability. *Fuel*, 303, 2021. doi:10.1016/j.fuel.2021.121300.
- [62] Min Young Jung, Jae Hun Chang, Min Oh, and Chang Ha Lee. Dynamic model and deep neural network-based surrogate model to predict dynamic behaviors and steady-state performance of solid propellant combustion. *Combustion and Flame*, 250, 2023. doi:10.1016/j.combustflame.2023.112649.
- [63] Lei Deng, Congling Shi, Haoran Li, Mei Wan, Fei Ren, Yanan Hou, and Fei Tang. Prediction of energy mass loss rate for biodiesel fire via machine learning and its physical modeling of flame radiation evolution. *Energy*, 275, 2023. doi:10.1016/j.energy.2023.127388.
- [64] Jiayue Liu, Guijun Liu, Jiahao Wu, Guihua Zhang, and Yuxin Wu. Prediction of flame type and liftoff height of fuel jets in turbulent hot coflow using machine learning methods. *Combustion Science and Technology*, 197(8):1760–1782, 2024. doi:10.1080/00102202.2023.2295323.
- [65] George Em Karniadakis, Ioannis G. Kevrekidis, Lu Lu, Paris Perdikaris, Sifan Wang, and Liu Yang. Physics-informed machine learning. *Nature Reviews Physics*, 3(6):422–440, 2021. doi:10.1038/s42254-021-00314-5.
- [66] Maziar Raissi, Paris Perdikaris, and George Em Karniadakis. Physics-informed neural networks: A deep learning framework for solving forward and inverse problems involving nonlinear partial differential equations. *Journal of Computational Physics*, 378:686–707, 2019. doi:10.1016/j.jcp.2018.10.045.
- [67] Maziar Raissi, Paris Perdikaris, and George Em Karniadakis. Physics informed deep learning (part i): Data-driven solutions of nonlinear partial differential equations. *arXiv preprint*, 2017. doi:10.48550/arXiv.1711.10561.
- [68] Maziar Raissi, Paris Perdikaris, and George Em Karniadakis. Physics informed deep learning (part ii): Data-driven discovery of nonlinear partial differential equations. *arXiv preprint*, 2017. doi:10.48550/arXiv.1711.10566.
- [69] Atılım Gunes Baydin, Barak A. Pearlmutter, Alexey Andreyevich Radul, and Jeffrey Mark Siskind. Automatic differentiation in machine learning: A survey. *Journal of Machine Learning Research*, 18, 2018. URL: <https://jmlr.org/papers/v18/17-468.html>.
- [70] Hyuk Lee and In Seok Kang. Neural algorithm for solving differential-equations. *Journal of Computational Physics*, 91(1):110–131, 1990. doi:10.1016/0021-9991(90)90007-n.
- [71] Mwmg Disisanayake and N. Phanthien. Neural-network-based approximations for solving partial-differential equations. *Communications in Numerical Methods in Engineering*, 10(3):195–201, 1994. doi:10.1002/cnm.1640100303.
- [72] Isaac Elias Lagaris, Aristidis Likas, and Dimitrios I. Fotiadis. Artificial neural networks for solving ordinary and partial differential equations. *IEEE Transactions on Neural Networks*, 9(5):987–1000, 1998. doi:10.1109/72.712178.
- [73] Chengping Rao, Pu Ren, Qi Wang, Oral Buyukozturk, Hao Sun, and Yang Liu. Encoding physics to learn reaction-diffusion processes. *Nature Machine Intelligence*, 5:765–779, 2023. doi:10.1038/s42256-023-00685-7.
- [74] Xin-Yang Liu, Min Zhu, Lu Lu, Hao Sun, and Jian-Xun Wang. Multi-resolution partial differential equations preserved learning framework for spatiotemporal dynamics. *Communications Physics*, 7(1), 2024. doi:10.1038/s42005-024-01521-z.
- [75] Weiqi Ji and Sili Deng. Autonomous discovery of unknown reaction pathways from data by chemical reaction neural network. *Journal of Physical Chemistry A*, 125(4):1082–1092, 2021. doi:10.1021/acs.jpca.0c09316.
- [76] Khemraj Shukla, Mengjia Xu, Nathaniel Trask, and George Em Karniadakis. Scalable algorithms for physics-informed neural and graph networks. *Data-Centric Engineering*, 3, 2022. doi:10.1017/dce.2022.24.
- [77] Salvatore Cuomo, Vincenzo Schiano Di Cola, Fabio Giampaolo, Gianluigi Rozza, Maziar Raissi, and Francesco Piccialli. Scientific machine learning through physics-informed networks: Where we are and what's next. *Journal of Scientific Computing*, 92(3), 2022. doi:10.1007/s10915-022-01939-z.
- [78] Zhongkai Hao, Songming Liu, Yichi Zhang, Chengyang Ying, Yao Feng, Hang Su, and Jun Zhu. Physics-informed machine learning: A survey on problems, methods and applications. *arXiv preprint*, 2022. doi:10.48550/arXiv.2211.08064.
- [79] Sifan Wang, Shyam Sankaran, Hanwen Wang, and Paris Perdikaris. An expert's guide to training physics-informed neural networks. *arXiv preprint*, 2023. doi:10.48550/arXiv.2308.08468.
- [80] Salah A. Faroughi, Nikhil M. Pawar, Celio Fernandes, Maziar Raissi, Subashish Das, Nima K. Kalantari, and Seyed Kourosh Mahjour. Physics-guided, physics-informed, and physics-encoded neural networks and operators in scientific computing: Fluid and solid mechanics. *Journal of Computing and Information Science in Engineering*, 24(4), 2024. doi:10.1115/1.4064449.
- [81] Dongjin Kim and Jaewook Lee. A review of physics informed neural networks for multiscale analysis and inverse problems. *Multiscale Science and Engineering*, 6(1):1–11, 2024. doi:10.1007/s42493-024-00106-w.
- [82] Amer Farea, Olli Yli-Harja, and Frank Emmert-Streib. Understanding physics-informed neural networks: Techniques, applications, trends, and challenges. *AI*, 5(3):1534–1557, 2024. doi:10.3390/ai5030074.
- [83] Weiwei Zhang, Wei Suo, Jiahao Song, and Wenbo Cao. Physics Informed Neural Networks (PINNs) as intelligent computing technique for solving partial differential equations: Limitation and Future prospects. *arXiv preprint*, 2024. doi:10.48550/arXiv.2411.18240.
- [84] Juan Diego Toscano, Vivek Oommen, Alan John Varghese, Zongren Zou, Nazanin Ahmadi Daryakenari, Chenxi Wu, and George Em Karniadakis. From PINNs to PIKANs: Recent advances in physics-informed machine learning. *Machine Learning for Computational Science and Engineering*, 1(1):15, 2025. doi:10.1007/s44379-025-00015-1.
- [85] Jiahao Wu, Yuxin Wu, Guihua Zhang, and Yang Zhang. Variable linear transformation improved physics-informed neural networks to solve thin-layer flow problems. *Journal of Computational Physics*, 500:112761, 2024. doi:10.1016/j.jcp.2024.112761.
- [86] Chuizheng Meng, Sam Griesemer, Defu Cao, Sungyong Seo, and Yan Liu. When physics meets machine learning: A survey of physics-informed machine learning. *Machine Learning for Computational Science and Engineering*, 1(1):20, 2025. doi:10.1007/s44379-025-00016-0.
- [87] Shengze Cai, Zhiping Mao, Zhicheng Wang, Minglang Yin, and George Em Karniadakis. Physics-informed neural networks (PINNs) for fluid mechanics: A review. *Acta Mechanica Sinica*, pages 1–12, 2022. doi:10.1007/s10409-021-01148-1.
- [88] Pushan Sharma, Wai Tong Chung, Bassem Akoush, and Matthias Ihme. A review of physics-informed machine learning in fluid mechanics. *Energies*, 16(5), 2023. doi:10.3390/en16052343.
- [89] Chi Zhao, Feifei Zhang, Wenqiang Lou, Xi Wang, and Jianyong Yang. A comprehensive review of advances in physics-informed neural networks and their applications in complex fluid dynamics. *Physics of Fluids*, 36(10), 2024. doi:10.1063/5.0226562.
- [90] Afila Ajithkumar Sophiya, Sepehr Maleki, Giuseppe Bruni, and Senthil K Krishnababu. Physics-informed neural networks for industrial gas turbines: Recent trends, advancements and challenges. *arXiv preprint*, 2025. doi:10.48550/arXiv.2506.19503.
- [91] Zhiyong Wu, Huan Wang, Chang He, Bingjian Zhang, Tao Xu, and Qinglin Chen. The application of physics-informed machine learning in multiphysics modeling in chemical engineering. *Industrial & Engineering Chemistry Research*, 62(44):18178–18204, 2023. doi:10.1021/acs.iecr.3c02383.
- [92] Derick Nganyu Tanyu, Jianfeng Ning, Tom Freudenberger, Nick Heilenkotter, Andreas Rademacher, Uwe Iben, and Peter Maass. Deep learning methods for partial differential equations and related parameter identification problems. *Inverse Problems*, 39(10):103001, 2023. doi:10.1088/1361-6420/ace9d4.

- [93] Steven L. Brunton and J. Nathan Kutz. Promising directions of machine learning for partial differential equations. *Nature Computational Science*, 4(7):483–494, 2024. doi:10.1038/s43588-024-00643-2.
- [94] Yizheng Wang, Jinshuai Bai, Zhongya Lin, Qimin Wang, Cosmin Anitescu, Jia Sun, Mohammad Sadegh Eshaghi, Yuantong Gu, Xi-Qiao Feng, Xiaoying Zhuang, Timon Rabczuk, and Yinghua Liu. Artificial intelligence for partial differential equations in computational mechanics: A review. *arXiv preprint*, 2024. doi:10.48550/arXiv.2410.19843.
- [95] Lu Lu, Pengzhan Jin, Guofei Pang, Zhongqiang Zhang, and George Em Karniadakis. Learning nonlinear operators via DeepONet based on the universal approximation theorem of operators. *Nature Machine Intelligence*, 3(3):218–229, 2021. doi:10.1038/s42256-021-00302-5.
- [96] Zongyi Li, Nikola Borislavov Kovachki, Kamyar Azizzadenesheli, Kaushik Bhattacharya, Andrew Stuart, and Anima Anandkumar. Fourier neural operator for parametric partial differential equations. In *9th International Conference on Learning Representations (ICLR)*, 2021. URL: <https://iclr.cc/virtual/2021/poster/3281>.
- [97] Sifan Wang, Hanwen Wang, and Paris Perdikaris. Learning the solution operator of parametric partial differential equations with physics-informed DeepONets. *Science Advances*, 7(40):eabi8605, 2021. doi:10.1126/sciadv.abi8605.
- [98] Zongyi Li, Hongkai Zheng, Nikola Kovachki, David Jin, Haoxuan Chen, Burigede Liu, Kamyar Azizzadenesheli, and Anima Anandkumar. Physics-informed neural operator for learning partial differential equations. *ACM/JMS Journal of Data Science*, 1(3):1–27, 2024. doi:10.1145/364850.
- [99] Han Gao, Luning Sun, and Jian-Xun Wang. PhyGeoNet: Physics-informed geometry-adaptive convolutional neural networks for solving parameterized steady-state PDEs on irregular domain. *Journal of Computational Physics*, 428:110079, 2021. doi:10.1016/j.jcp.2020.110079.
- [100] Han Gao, Luning Sun, and Jian-Xun Wang. Super-resolution and denoising of fluid flow using physics-informed convolutional neural networks without high-resolution labels. *Physics of Fluids*, 33(7), 2021. doi:10.1063/5.0054312.
- [101] Zhiyuan Zhao, Xueying Ding, and B Aditya Prakash. PINNsFormer: A Transformer-based framework for physics-informed neural networks. In *12th International Conference on Learning Representations (ICLR)*, 2024. URL: <https://iclr.cc/virtual/2024/poster/19142>.
- [102] Anuj Kumar and Tarek Echekki. Physics-informed machine learning for reduced space chemical kinetics. In *NeurIPS 2023 Workshop: Machine learning and the physical sciences*, 2023. <https://neurips.cc/virtual/2023/76174>. URL: [https://ml4physicalsciences.github.io/2023/files/NeurIPS\\_ML4PS\\_2023\\_132.pdf](https://ml4physicalsciences.github.io/2023/files/NeurIPS_ML4PS_2023_132.pdf).
- [103] Anuj Kumar and Tarek Echekki. Physics-constrained machine learning for reduced composition space chemical kinetics. *Data-Centric Engineering*, 6:e34, 2025. doi:10.1017/dce.2025.10012.
- [104] Ivan Zanardi, Simone Venturi, Marco Panesi, and Aiaa. Towards efficient simulations of non-equilibrium chemistry in hypersonic flows: A physics-informed neural network framework. In *AIAA Science and Technology Forum and Exposition (AIAA SciTech Forum)*, 2022. doi:10.2514/6.2022-1639.
- [105] Ivan Zanardi, Simone Venturi, and Marco Panesi. Adaptive physics-informed neural operator for coarse-grained non-equilibrium flows. *Scientific Reports*, 13(1), 2023. doi:10.1038/s41598-023-41039-y.
- [106] Arsalan Taassob, Anuj Kumar, Kevin M. Gitushi, Rishikesh Ranade, and Tarek Echekki. A PINN-DeepONet framework for extracting turbulent combustion closure from multiscale measurements. *Computer Methods in Applied Mechanics and Engineering*, 429, 2024. doi:10.1016/j.cma.2024.117163.
- [107] Shiyu Liu, Haiou Wang, Zhiwei Sun, Kae Ken Foo, Graham J. Nathan, Xue Dong, Michael J. Evans, Bassam B. Dally, Kun Luo, and Jianren Fan. Reconstructing soot fields in acoustically forced laminar sooting flames using physics-informed machine learning models. *Proceedings of the Combustion Institute*, 40(1-4), 2024. doi:10.1016/j.proci.2024.105314.
- [108] Xiaoyi Lu and Yi Wang. Surrogate modeling for radiative heat transfer using physics-informed deep neural operator networks. *Proceedings of the Combustion Institute*, 40(1-4), 2024. doi:10.1016/j.proci.2024.105282.
- [109] Khemraj Shukla, Juan Diego Toscano, Zhicheng Wang, Zongren Zou, and George Em Karniadakis. A comprehensive and FAIR comparison between MLP and KAN for differential equations and operator networks. *Computer Methods in Applied Mechanics and Engineering*, 431, 2024. doi:10.1016/j.cma.2024.117290.
- [110] Yizheng Wang, Jia Sun, Jinshuai Bai, Cosmin Anitescu, Mohammad Sadegh Eshaghi, Xiaoying Zhuang, Timon Rabczuk, and Yinghua Liu. Kolmogorov-Arnold-Informed neural network: A physics-informed deep learning framework for solving forward and inverse problems based on Kolmogorov-Arnold Networks. *Computer Methods in Applied Mechanics and Engineering*, 433, 2025. doi:10.1016/j.cma.2024.117518.
- [111] Yuntian Chen, Dou Huang, Dongxiao Zhang, Junsheng Zeng, Nanzhe Wang, Haoran Zhang, and Jinyue Yan. Theory-guided hard constraint projection (HCP): A knowledge-based data-driven scientific machine learning method. *Journal of Computational Physics*, 445, 2021. doi:10.1016/j.jcp.2021.110624.
- [112] Jiahao Wu, Su Zhang, Yuxin Wu, Guihua Zhang, Xin Li, and Hai Zhang. FlamePINN-1D: Physics-informed neural networks to solve forward and inverse problems of 1D laminar flames. *Combustion and Flame*, 273:113964, 2025. doi:10.1016/j.combustflame.2025.113964.
- [113] Tinghao Wang, Yuxiao Yi, Junjie Yao, Zhi-Qin John Xu, Tianhan Zhang, and Zheng Chen. Enforcing physical conservation in neural network surrogate models for complex chemical kinetics. *Combustion and Flame*, 275, 2025. doi:10.1016/j.combustflame.2025.114105.
- [114] Tianhan Zhang, Yuxiao Yi, Yifan Xu, Zhi X. Chen, Yaoyu Zhang, Weinan E, and Zhi-Qin John Xu. A multi-scale sampling method for accurate and robust deep neural network to predict combustion chemical kinetics. *Combustion and Flame*, 245, 2022. doi:10.1016/j.combustflame.2022.112319.
- [115] Runze Mao, Minqi Lin, Yan Zhang, Tianhan Zhang, Zhi-Qin John Xu, and Zhi X. Chen. DeepFlame: A deep learning empowered open-source platform for reacting flow simulations. *Computer Physics Communications*, 291, 2023. doi:10.1016/j.cpc.2023.108842.
- [116] Pushan Sharma, Wai Tong Chung, and Matthias Ihme. A physics-informed machine learning approach for predicting dynamic behavior of reacting flows with application to hydrogen jet flames. *Combustion and Flame*, 277, 2025. doi:10.1016/j.combustflame.2025.114190.
- [117] Farshud Sorourifar, You Peng, Ivan Castillo, Linh Bui, Juan Venegas, and Joel A. Paulson. Physics-enhanced neural ordinary differential equations: Application to industrial chemical reaction systems. *Industrial & Engineering Chemistry Research*, 62(38):15563–15577, 2023. doi:10.1021/acs.iecr.3c01471.
- [118] Aleksandr Fedorov, Anna Perechodjuk, and David Linke. Kinetics-constrained neural ordinary differential equations: Artificial neural network models tailored for small data to boost kinetic model development. *Chemical Engineering Journal*, 477, 2023. doi:10.1016/j.cej.2023.146869.
- [119] Tim Kircher, Felix A. Doeppel, and Martin Votsmeier. Global reaction neural networks with embedded stoichiometry and thermodynamics for learning kinetics from reactor data. *Chemical Engineering Journal*, 485, 2024. doi:10.1016/j.cej.2024.149863.
- [120] Tim Kircher, Felix A. Doeppel, and Martin Votsmeier. *Embedding physics into Neural ODEs to learn kinetics from integral reactors*, volume 53, pages 817–822. Elsevier, 2024. doi:10.1016/B978-0-443-28824-1.50137-X.
- [121] Pu Ren, Chengping Rao, Yang Liu, Jian-Xun Wang, and Hao Sun. PhyCRNet: Physics-informed convolutional-recurrent network for solving spatiotemporal PDEs. *Computer Methods in Applied Mechanics and Engineering*, 389, 2022. doi:10.1016/j.cma.2021.114399.
- [122] Nasim Rahaman, Aristide Baratin, Devansh Arpit, Felix Draxler, Min Lin, Fred A. Hamprecht, Yoshua Bengio, and Aaron Courville. On the spectral bias of neural networks. In *36th International Conference on Machine Learning (ICML)*, volume 97 of *Proceedings of Machine Learning Research*, 2019. URL: <https://proceedings.mlr.press/v97/rahaman19a>.

- [123] Zhi-Qin John Xu, Yaoyu Zhang, Tao Luo, Yanyang Xiao, and Zheng Ma. Frequency principle: Fourier analysis sheds light on deep neural networks. *Communications in Computational Physics*, 28(5):1746–1767, 2020. doi:10.4208/cicp.0A-2020-0085.
- [124] Zhi-Qin John Xu, Yaoyu Zhang, and Tao Luo. Overview frequency principle/spectral bias in deep learning. *Communications on Applied Mathematics and Computation*, 7(3):827–864, 2024. doi:10.1007/s42967-024-00398-7.
- [125] Ziqi Liu, Wei Cai, and Zhi-Qin John Xu. Multi-scale deep neural network (MscaleDNN) for solving Poisson-Boltzmann equation in complex domains. *Communications in Computational Physics*, 28(5):1970–2001, 2020. doi:10.4208/cicp.0A-2020-0179.
- [126] Matthew Tancik, Pratul Srinivasan, Ben Mildenhall, Sara Fridovich-Keil, Nithin Raghavan, Utkarsh Singhal, Ravi Ramamoorthi, Jonathan Barron, and Ren Ng. Fourier features let networks learn high frequency functions in low dimensional domains. In *34th Conference on Neural Information Processing Systems (NeurIPS)*, volume 33, pages 7537–7547. Curran Associates, Inc., 2020. URL: [https://papers.nips.cc/paper\\_files/paper/2020/hash/55053683268957697aa39fba6f231c68-Abstract.html](https://papers.nips.cc/paper_files/paper/2020/hash/55053683268957697aa39fba6f231c68-Abstract.html).
- [127] Sifan Wang, Hanwen Wang, and Paris Perdikaris. On the eigenvector bias of Fourier feature networks: From regression to solving multi-scale PDEs with physics-informed neural networks. *Computer Methods in Applied Mechanics and Engineering*, 384, 2021. doi:10.1016/j.cma.2021.113938.
- [128] Yong Wang, Yanzhong Yao, Jiawei Guo, and Zhiming Gao. A practical PINN framework for multi-scale problems with multi-magnitude loss terms. *Journal of Computational Physics*, 510:113112, 2024. doi:10.1016/j.jcp.2024.113112.
- [129] Lu Lu, Raphaël Pestourie, Wenjie Yao, Zhicheng Wang, Francesc Verdugo, and Steven G. Johnson. Physics-informed neural networks with hard constraints for inverse design. *SIAM Journal on Scientific Computing*, 43(6):B1105–B1132, 2021. doi:10.1137/21m1397908.
- [130] Suchuan Dong and Naxian Ni. A method for representing periodic functions and enforcing exactly periodic boundary conditions with deep neural networks. *Journal of Computational Physics*, 435, 2021. doi:10.1016/j.jcp.2021.110242.
- [131] N. Sukumar and Ankit Srivastava. Exact imposition of boundary conditions with distance functions in physics-informed deep neural networks. *Computer Methods in Applied Mechanics and Engineering*, 389, 2022. doi:10.1016/j.cma.2021.114333.
- [132] Carl Leake and Daniele Mortari. Deep theory of functional connections: A new method for estimating the solutions of partial differential equations. *Machine Learning and Knowledge Extraction*, 2(1):37–55, 2020. doi:10.3390/make2010004.
- [133] Enrico Schiassi, Roberto Furfaro, Carl Leake, Mario De Florio, Hunter Johnston, and Daniele Mortari. Extreme theory of functional connections: A fast physics-informed neural network method for solving ordinary and partial differential equations. *Neurocomputing*, 457:334–356, 2021. doi:10.1016/j.neucom.2021.06.015.
- [134] Ameya D. Jagtap, Kenji Kawaguchi, and George Em Karniadakis. Adaptive activation functions accelerate convergence in deep and physics-informed neural networks. *Journal of Computational Physics*, 404, 2020. doi:10.1016/j.jcp.2019.109136.
- [135] Ameya D. Jagtap, Kenji Kawaguchi, and George Em Karniadakis. Locally adaptive activation functions with slope recovery for deep and physics-informed neural networks. *Proceedings of the Royal Society A-Mathematical Physical and Engineering Sciences*, 476(2239), 2020. doi:10.1098/rspa.2020.0334.
- [136] Yining Luo, Yingfa Chen, and Zhen Zhang. CFDBench: A large-scale benchmark for machine learning methods in fluid dynamics. *arXiv preprint*, 2023. doi:10.48550/arXiv.2310.05963.
- [137] Felix Koehler, Simon Niedermayr, Rüdiger Westermann, and Nils Thuerey. APEBench: A benchmark for autoregressive neural emulators of PDEs. In *38th Conference on Neural Information Processing Systems (NeurIPS)*, 2024. URL: <https://nips.cc/virtual/2024/poster/97550>.
- [138] Makoto Takamoto, Timothy Praditia, Raphael Leiteritz, Dan MacKinlay, Francesco Alesiani, Dirk Pflueger, and Mathias Niepert. PDEBench: An extensive benchmark for scientific machine learning. In *36th Conference on Neural Information Processing Systems (NeurIPS)*, Advances in Neural Information Processing Systems, 2022. URL: [https://proceedings.neurips.cc/paper\\_files/paper/2022/hash/0a9747136d411fb83f0cf81820d44afb-Abstract-Datasets\\_and\\_Benchmarks.html](https://proceedings.neurips.cc/paper_files/paper/2022/hash/0a9747136d411fb83f0cf81820d44afb-Abstract-Datasets_and_Benchmarks.html).
- [139] Somdatta Goswami, Ameya D. Jagtap, Hessam Babae, Bryan T. Susi, and George Em Karniadakis. Learning stiff chemical kinetics using extended deep neural operators. *Computer Methods in Applied Mechanics and Engineering*, 419, 2024. doi:10.1016/j.cma.2023.116674.
- [140] Anuj Kumar and Tarek Echehki. Combustion chemistry acceleration with DeepONets. *Fuel*, 365, 2024. doi:10.1016/j.fuel.2024.131212.
- [141] Sonya A. Coleman, Shanmugalingam Suganthan, and Bryan W. Scotney. Gradient operators for feature extraction and characterisation in range images. *Pattern Recognition Letters*, 31(9):1028–1040, 2010. doi:10.1016/j.patrec.2009.12.022.
- [142] Guang-Bin Huang, Qin-Yu Zhu, and Chee-Kheong Siew. Extreme learning machine: Theory and applications. *Neurocomputing*, 70(1-3):489–501, 2006. doi:10.1016/j.neucom.2005.12.126.
- [143] J. Ghosh and A. Nag. *An overview of radial basis function networks*, pages 1–36. Physica-Verlag HD, Heidelberg, 2001. doi:10.1007/978-3-7908-1826-0\_1.
- [144] Charles R. Qi, Hao Su, Kaichun Mo, Leonidas J. Guibas, and Ieee. PointNet: Deep learning on point sets for 3D classification and segmentation. In *2017 IEEE Conference on Computer Vision and Pattern Recognition (CVPR)*, IEEE Conference on Computer Vision and Pattern Recognition, pages 77–85, 2017. doi:10.1109/cvpr.2017.16.
- [145] Ziming Liu, Yixuan Wang, Sachin Vaidya, Fabian Ruehle, James Halverson, Marin Soljačić, Thomas Y Hou, and Max Tegmark. KAN: Kolmogorov-Arnold Networks. *arXiv preprint*, 2024. doi:10.48550/arXiv.2404.19756.
- [146] Ziming Liu, Pingchuan Ma, Yixuan Wang, Wojciech Matusik, and Max Tegmark. KAN 2.0: Kolmogorov-Arnold Networks meet science. *arXiv preprint*, 2024. doi:10.48550/arXiv.2408.10205.
- [147] Vikas Dwivedi and Balaji Srinivasan. Physics Informed Extreme Learning Machine (PIELM)-A rapid method for the numerical solution of partial differential equations. *Neurocomputing*, 391:96–118, 2020. doi:10.1016/j.neucom.2019.12.099.
- [148] Jinshuai Bai, Gui-Rong Liu, Ashish Gupta, Laith Alzubaidi, Xi-Qiao Feng, and YuanTong Gu. Physics-informed radial basis network (PIRBN): A local approximating neural network for solving nonlinear partial differential equations. *Computer Methods in Applied Mechanics and Engineering*, 415, 2023. doi:10.1016/j.cma.2023.116290.
- [149] Ali Kashefi and Tapan Mukerji. Physics-informed PointNet: A deep learning solver for steady-state incompressible flows and thermal fields on multiple sets of irregular geometries. *Journal of Computational Physics*, 468, 2022. doi:10.1016/j.jcp.2022.111510.
- [150] Ehsan Haghighat, Maziar Raissi, Adrian Moure, Hector Gomez, and Ruben Juanes. A physics-informed deep learning framework for inversion and surrogate modeling in solid mechanics. *Computer Methods in Applied Mechanics and Engineering*, 379, 2021. doi:10.1016/j.cma.2021.113741.
- [151] Sifan Wang, Bowen Li, Yuhuan Chen, and Paris Perdikaris. PirateNets: Physics-informed deep learning with residual adaptive networks. *Journal of Machine Learning Research*, 25, 2024. URL: <https://jmlr.org/papers/v25/24-0313.html>.
- [152] Ian J. Goodfellow, Jean Pouget-Abadie, Mehdi Mirza, Bing Xu, David Warde-Farley, Sherjil Ozair, Aaron Courville, and Yoshua Bengio. Generative adversarial nets. In *28th Conference on Neural Information Processing Systems (NIPS)*, volume 27 of *Advances in Neural Information Processing Systems*, pages 2672–2680, 2014. URL: [https://proceedings.neurips.cc/paper\\_files/paper/2014/hash/f033ed80deb0234979a61f95710d0be25-Abstract.html](https://proceedings.neurips.cc/paper_files/paper/2014/hash/f033ed80deb0234979a61f95710d0be25-Abstract.html).

- [153] Diederik P Kingma and Max Welling. Auto-encoding variational Bayes. In *2nd International Conference on Learning Representations (ICLR)*, 2014. URL: <https://openreview.net/forum?id=33X9fd2-9FyZd>.
- [154] Liu Yang, Dongkun Zhang, and George Em Karniadakis. Physics-informed generative adversarial networks for stochastic differential equations. *SIAM Journal on Scientific Computing*, 42(1):A292–A317, 2020. doi:10.1137/18m1225409.
- [155] Weiheng Zhong and Hadi Meidani. PI-VAE: Physics-Informed Variational Auto-Encoder for stochastic differential equations. *Computer Methods in Applied Mechanics and Engineering*, 403:115664, 2023. doi:10.1016/j.cma.2022.115664.
- [156] Sepp Hochreiter and Juergen Schmidhuber. Long short-term memory. *Neural Computation*, 9(8):1735–1780, 1997. doi:10.1162/neco.1997.9.8.1735.
- [157] Yann LeCun, Leon Bottou, Yoshua Bengio, and Patrick Haffner. Gradient-based learning applied to document recognition. *Proceedings of the IEEE*, 86(11):2278–2324, 1998. doi:10.1109/5.726791.
- [158] Jie Zhou, Ganqu Cui, Shengding Hu, Zhengyan Zhang, Cheng Yang, Zhiyuan Liu, Lifeng Wang, Changcheng Li, and Maosong Sun. Graph neural networks: A review of methods and applications. *AI Open*, 1:57–81, 2020. doi:10.1016/j.aiopen.2021.01.001.
- [159] Ashish Vaswani, Noam Shazeer, Niki Parmar, Jakob Uszkoreit, Llion Jones, Aidan N. Gomez, Lukasz Kaiser, and Illia Polosukhin. Attention Is All You Need. In *31st Conference on Neural Information Processing Systems (NIPS)*, volume 30 of *Advances in Neural Information Processing Systems*, 2017. URL: <https://proceedings.neurips.cc/paper/2017/hash/3f5ee243547dee91fbd053c1c4a845aa-Abstract.html>.
- [160] Jascha Sohl-Dickstein, Eric A. Weiss, Niru Maheswaranathan, and Surya Ganguli. Deep unsupervised learning using nonequilibrium thermodynamics. In *32nd International Conference on Machine Learning (ICML)*, volume 37 of *Proceedings of Machine Learning Research*, pages 2256–2265, 2015. URL: <https://proceedings.mlr.press/v37/sohl-dickstein15.html>.
- [161] Jonathan Ho, Ajay Jain, and Pieter Abbeel. Denoising diffusion probabilistic models. In *34th Conference on Neural Information Processing Systems (NeurIPS)*, volume 33, pages 6840–6851, 2020. URL: <https://proceedings.neurips.cc/paper/2020/hash/4c5bfcfec8584af0d967f1ab10179ca4b-Abstract.html>.
- [162] Ling Yang, Zhilong Zhang, Yang Song, Shenda Hong, Runsheng Xu, Yue Zhao, Wentao Zhang, Bin Cui, and Ming-Hsuan Yang. Diffusion models: A comprehensive survey of methods and applications. *ACM Computing Surveys*, 56(4), 2024. doi:10.1145/3626235.
- [163] Ruiyang Zhang, Yang Liu, and Hao Sun. Physics-informed multi-LSTM networks for metamodeling of nonlinear structures. *Computer Methods in Applied Mechanics and Engineering*, 369, 2020. doi:10.1016/j.cma.2020.113226.
- [164] Han Gao, Matthew J. Zahr, and Jian-Xun Wang. Physics-informed graph neural Galerkin networks: A unified framework for solving PDE-governed forward and inverse problems. *Computer Methods in Applied Mechanics and Engineering*, 390, 2022. doi:10.1016/j.cma.2021.114502.
- [165] Cooper Lorscheun, Zijie Li, and Amir Barati Farimani. Physics informed token transformer for solving partial differential equations. *Machine Learning-Science and Technology*, 5(1), 2024. doi:10.1088/2632-2153/ad27e3.
- [166] Dule Shu, Zijie Li, and Amir Barati Farimani. A physics-informed diffusion model for high-fidelity flow field reconstruction. *Journal of Computational Physics*, 478:111972, 2023. doi:10.1016/j.jcp.2023.111972.
- [167] Lu Lu, Xuhui Meng, Zhiping Mao, and George Em Karniadakis. DeepXDE: A deep learning library for solving differential equations. *SIAM Review*, 63(1):208–228, 2021. doi:10.1137/19m1274067.
- [168] Mohammad Amin Nabian, Rini Jasmine Gladstone, and Hadi Meidani. Efficient training of physics-informed neural networks via importance sampling. *Computer-Aided Civil and Infrastructure Engineering*, 36(8):962–977, 2021. doi:10.1111/mice.12685.
- [169] Chenxi Wu, Min Zhu, Qinyang Tan, Yadhu Kartha, and Lu Lu. A comprehensive study of non-adaptive and residual-based adaptive sampling for physics-informed neural networks. *Computer Methods in Applied Mechanics and Engineering*, 403, 2023. doi:10.1016/j.cma.2022.115671.
- [170] Sifan Wang, Yujun Teng, and Paris Perdikaris. Understanding and mitigating gradient flow pathologies in physics-informed neural networks. *SIAM Journal on Scientific Computing*, 43(5):A3055–A3081, 2021. doi:10.1137/20m1318043.
- [171] Sifan Wang, Xinling Yu, and Paris Perdikaris. When and why PINNs fail to train: A neural tangent kernel perspective. *Journal of Computational Physics*, 449, 2022. doi:10.1016/j.jcp.2021.110768.
- [172] Zixue Xiang, Wei Peng, Xu Liu, and Wen Yao. Self-adaptive loss balanced Physics-informed neural networks. *Neurocomputing*, 496:11–34, 2022. doi:10.1016/j.neucom.2022.05.015.
- [173] Levi D. McClenny and Ulisses M. Braga-Neto. Self-adaptive physics-informed neural networks. *Journal of Computational Physics*, 474, 2023. doi:10.1016/j.jcp.2022.111722.
- [174] Sifan Wang, Shyam Sankaran, and Paris Perdikaris. Respecting causality for training physics-informed neural networks. *Computer Methods in Applied Mechanics and Engineering*, 421, 2024. doi:10.1016/j.cma.2024.116813.
- [175] Michael Penwarden, Ameya D. Jagtap, Shandian Zhe, George Em Karniadakis, and Robert M. Kirby. A unified scalable framework for causal sweeping strategies for Physics-Informed Neural Networks (PINNs) and their temporal decompositions. *Journal of Computational Physics*, 493, 2023. doi:10.1016/j.jcp.2023.112464.
- [176] Jeremy Yu, Lu Lu, Xuhui Meng, and George Em Karniadakis. Gradient-enhanced physics-informed neural networks for forward and inverse PDE. *Computer Methods in Applied Mechanics and Engineering*, 393:22, 2022. doi:10.1016/j.cma.2022.114823.
- [177] Haixu Wu, Huakun Luo, Yuezhou Ma, Jianmin Wang, and Mingsheng Long. RoPINN: Region optimized physics-informed neural networks. In *38th Annual Conference on Neural Information Processing Systems (NeurIPS)*, 2024. URL: <https://neurips.cc/virtual/2024/poster/93144>.
- [178] Chuwei Wang, Shanda Li, Di He, and Liwei Wang. Is  $L^2$  physics informed loss always suitable for training physics informed neural network? In *36th Conference on Neural Information Processing Systems (NeurIPS)*, pages 8278–8290, 2022. URL: [https://proceedings.neurips.cc/paper\\_files/paper/2022/hash/374050dc3f211267bd6bf0ea24eae184-Abstract-Conference.html](https://proceedings.neurips.cc/paper_files/paper/2022/hash/374050dc3f211267bd6bf0ea24eae184-Abstract-Conference.html).
- [179] Kart Leong Lim, Rahul Dutta, and Mihai Rotaru. Physics informed neural network using finite difference method. In *2022 IEEE International Conference on Systems, Man, and Cybernetics (SMC)*, pages 1828–1833, 2022. doi:10.1109/smc53654.2022.9945171.
- [180] Pao-Hsiung Chiu, Jian Cheng Wong, Chinchun Ooi, My Ha Dao, and Yew-Soon Ong. CAN-PINN: A fast physics-informed neural network based on coupled-automatic-numerical differentiation method. *Computer Methods in Applied Mechanics and Engineering*, 395, 2022. doi:10.1016/j.cma.2022.114909.
- [181] Vikas Dwivedi, Nishant Parashar, and Balaji Srinivasan. Distributed physics informed neural network for data-efficient solution to partial differential equations. *arXiv preprint*, 2019. doi:10.48550/arXiv.1907.08967.
- [182] Ameya D. Jagtap, Ehsan Kharazmi, and George Em Karniadakis. Conservative physics-informed neural networks on discrete domains for conservation laws: Applications to forward and inverse problems. *Computer Methods in Applied Mechanics and Engineering*, 365, 2020. doi:10.1016/j.cma.2020.113028.
- [183] Ameya D. Jagtap and George Em Karniadakis. Extended physics-informed neural networks (XPINNs): A generalized space-time domain decomposition based deep learning framework for nonlinear partial differential equations. *Communications in Computational Physics*, 28(5):2002–2041, 2020. doi:10.4208/cicp.0A-2020-0164.

- [184] Xuhui Meng, Zhen Li, Dongkun Zhang, and George Em Karniadakis. PPINN: Parareal physics-informed neural network for time-dependent PDEs. *Computer Methods in Applied Mechanics and Engineering*, 370, 2020. doi:10.1016/j.cma.2020.113250.
- [185] Khemraj Shukla, Ameya D. Jagtap, and George Em Karniadakis. Parallel physics-informed neural networks via domain decomposition. *Journal of Computational Physics*, 447, 2021. doi:10.1016/j.jcp.2021.110683.
- [186] Shengfeng Xu, Chang Yan, Guangtao Zhang, Zhenxu Sun, Renfang Huang, Shengjun Ju, Dilong Guo, and Guowei Yang. Spatiotemporal parallel physics-informed neural networks: A framework to solve inverse problems in fluid mechanics. *Physics of Fluids*, 35(6), 2023. doi:10.1063/5.0155087.
- [187] Zheyuan Hu, Ameya D. Jagtap, George Em Karniadakis, and Kenji Kawaguchi. Augmented Physics-Informed Neural Networks (APINNs): A gating network-based soft domain decomposition methodology. *Engineering Applications of Artificial Intelligence*, 126, 2023. doi:10.1016/j.engappai.2023.107183.
- [188] Ben Moseley, Andrew Markham, and Tarje Nissen-Meyer. Finite basis physics-informed neural networks (FBPINNs): a scalable domain decomposition approach for solving differential equations. *Advances in Computational Mathematics*, 49(4), 2023. doi:10.1007/s10444-023-10065-9.
- [189] Victorita Dolean, Alexander Heinlein, Siddhartha Mishra, and Ben Moseley. Multilevel domain decomposition-based architectures for physics-informed neural networks. *Computer Methods in Applied Mechanics and Engineering*, 429, 2024. doi:10.1016/j.cma.2024.117116.
- [190] Diederik P Kingma and Jimmy Ba. Adam: A method for stochastic optimization. In *3rd International Conference on Learning Representations (ICLR)*, 2015. URL: <https://arxiv.org/abs/1412.6980>.
- [191] Dong C. Liu and Jorge Nocedal. On the limited memory BFGS method for large scale optimization. *Mathematical Programming*, 45(3):503–528, 1989. doi:10.1007/bf01589116.
- [192] Jiachen Yao, Chang Su, Zhongkai Hao, Songming Liu, Hang Su, and Jun Zhu. MultiAdam: Parameter-wise scale-invariant optimizer for multiscale training of physics-informed neural networks. In *40th International Conference on Machine Learning (ICML)*, volume 202 of *Proceedings of Machine Learning Research*, pages 39702–39721, 2023. URL: <https://icml.cc/virtual/2023/poster/23480>.
- [193] Pratik Rathore, Weimu Lei, Zachary Frangella, Lu Lu, and Madeleine Udell. Challenges in training PINNs: A loss landscape perspective. In *41st International Conference on Machine Learning (ICML)*, volume 235 of *Proceedings of Machine Learning Research*, pages 42159–42191, 2024. URL: <https://proceedings.mlr.press/v235/rathore24a.html>.
- [194] Shengfeng Xu, Yuanjun Dai, Chang Yan, Zhenxu Sun, Renfang Huang, Dilong Guo, and Guowei Yang. On the preprocessing of physics-informed neural networks: How to better utilize data in fluid mechanics. *Journal of Computational Physics*, 528, 2025. doi:10.1016/j.jcp.2025.113837.
- [195] Seungchan Ko and Sanghyeon Park. VS-PINN: A fast and efficient training of physics-informed neural networks using variable-scaling methods for solving PDEs with stiff behavior. *Journal of Computational Physics*, 529, 2025. doi:10.1016/j.jcp.2025.113860.
- [196] Ehsan Kharazmi, Zhongqiang Zhang, and George Em Karniadakis. Variational physics-informed neural networks for solving partial differential equations. *arXiv preprint*, 2019. doi:10.48550/arXiv.1912.00873.
- [197] Ehsan Kharazmi, Zhongqiang Zhang, and George Em Karniadakis. hp-VPINNs: Variational physics-informed neural networks with domain decomposition. *Computer Methods in Applied Mechanics and Engineering*, 374, 2021. doi:10.1016/j.cma.2020.113547.
- [198] Esteban Samaniego, Cosmin Anitescu, Somdatta Goswami, Vien Minh Nguyen-Thanh, Hongwei Guo, Khader Hamdia, Xiaoying Zhuang, and Timon Rabczuk. An energy approach to the solution of partial differential equations in computational mechanics via machine learning: Concepts, implementation and applications. *Computer Methods in Applied Mechanics and Engineering*, 362, 2020. doi:10.1016/j.cma.2019.112790.
- [199] Hailong Sheng and Chao Yang. PFNN: A penalty-free neural network method for solving a class of second-order boundary-value problems on complex geometries. *Journal of Computational Physics*, 428, 2021. doi:10.1016/j.jcp.2020.110085.
- [200] Yizheng Wang, Jia Sun, Wei Li, Zaiyuan Lu, and Yinghua Liu. CENN: Conservative energy method based on neural networks with subdomains for solving variational problems involving heterogeneous and complex geometries. *Computer Methods in Applied Mechanics and Engineering*, 400, 2022. doi:10.1016/j.cma.2022.115491.
- [201] Yizheng Wang, Jia Sun, Timon Rabczuk, and Yinghua Liu. DCEM: A deep complementary energy method for linear elasticity. *International Journal for Numerical Methods in Engineering*, 125(24), 2024. doi:10.1002/nme.7585.
- [202] Chengping Rao, Hao Sun, and Yang Liu. Physics-informed deep learning for incompressible laminar flows. *Theoretical and Applied Mechanics Letters*, 10(3):207–212, 2020. doi:10.1016/j.taml.2020.01.039.
- [203] Xiaowei Jin, Shengze Cai, Hui Li, and George Em Karniadakis. NSFnets (Navier-Stokes flow nets): Physics-informed neural networks for the incompressible Navier-Stokes equations. *Journal of Computational Physics*, 426:109951, 2021. doi:10.1016/j.jcp.2020.109951.
- [204] Dashan Zhang, Yuntian Chen, and Shiyi Chen. Filtered partial differential equations: a robust surrogate constraint in physics-informed deep learning framework. *Journal of Fluid Mechanics*, 999, 2024. doi:10.1017/jfm.2024.471.
- [205] Guofei Pang, Lu Lu, and George Em Karniadakis. fPINNs: Fractional physics-informed neural networks. *SIAM Journal on Scientific Computing*, 41(4):A2603–A2626, 2019. doi:10.1137/18m1229845.
- [206] Michael Penwarden, Shandian Zhe, Akil Narayan, and Robert M. Kirby. A metalearning approach for Physics-Informed Neural Networks (PINNs): Application to parameterized PDEs. *Journal of Computational Physics*, 477, 2023. doi:10.1016/j.jcp.2023.111912.
- [207] Yanlai Chen and Shawn Koohy. GPT-PINN: Generative Pre-Trained Physics-Informed Neural Networks toward non-intrusive Meta-learning of parametric PDEs. *Finite Elements in Analysis and Design*, 228, 2024. doi:10.1016/j.finel.2023.104047.
- [208] Woojin Cho, Minju Jo, Haksoo Lim, Kookjin Lee, Dongeun Lee, Sanghyun Hong, and Noseong Park. Parameterized physics-informed neural networks for parameterized PDEs. In *41st International Conference on Machine Learning (ICML)*, volume 235 of *Proceedings of Machine Learning Research*, 2024. URL: <https://icml.cc/virtual/2024/poster/33141>.
- [209] Aditi S. Krishnapriyan, Amir Gholami, Shandian Zhe, Robert M. Kirby, and Michael W. Mahoney. Characterizing possible failure modes in physics-informed neural networks. In *35th Conference on Neural Information Processing Systems (NeurIPS)*, volume 34 of *Advances in Neural Information Processing Systems*, 2021. URL: <https://proceedings.neurips.cc/paper/2021/hash/df438e5206f31600e6ae4af72f2725f1-Abstract.html>.
- [210] Tim De Ryck, Florent Bonnet, Siddhartha Mishra, and Emmanuel De Bézénac. An operator preconditioning perspective on training in physics-informed machine learning. In *12th International Conference on Learning Representations (ICLR)*, 2024. URL: <https://iclr.cc/virtual/2024/poster/18473>.
- [211] Songming Liu, Chang Su, Jiachen Yao, Zhongkai Hao, Hang Su, Youjia Wu, and Jun Zhu. Preconditioning for physics-informed neural networks. *arXiv preprint*, 2025. doi:10.48550/arXiv.2402.00531.
- [212] Wenbo Cao and Weiwei Zhang. An analysis and solution of ill-conditioning in physics-informed neural networks. *Journal of Computational Physics*, 520, 2025. doi:10.1016/j.jcp.2024.113494.
- [213] Apostolos F. Psaros, Xuhui Meng, Zongren Zou, Ling Guo, and George Em Karniadakis. Uncertainty quantification in scientific machine learning: Methods, metrics, and comparisons. *Journal of Computational Physics*, 477, 2023. doi:10.1016/j.jcp.2022.111902.

- [214] Yibo Yang and Paris Perdikaris. Adversarial uncertainty quantification in physics-informed neural networks. *Journal of Computational Physics*, 394:136–152, 2019. doi:10.1016/j.jcp.2019.05.027.
- [215] Dongkun Zhang, Lu Lu, Ling Guo, and George Em Karniadakis. Quantifying total uncertainty in physics-informed neural networks for solving forward and inverse stochastic problems. *Journal of Computational Physics*, 397:19, 2019. doi:10.1016/j.jcp.2019.07.048.
- [216] Liu Yang, Xuhui Meng, and George Em Karniadakis. B-PINNs: Bayesian physics-informed neural networks for forward and inverse PDE problems with noisy data. *Journal of Computational Physics*, 425, 2021. doi:10.1016/j.jcp.2020.109913.
- [217] Zongren Zou, Xuhui Meng, and George Em Karniadakis. Correcting model misspecification in physics-informed neural networks (PINNs). *Journal of Computational Physics*, 505, 2024. doi:10.1016/j.jcp.2024.112918.
- [218] Yeonjong Shin, Jerome Darbon, and George Em Karniadakis. On the convergence of physics informed neural networks for linear second-order elliptic and parabolic type PDEs. *Communications in Computational Physics*, 28(5):2042–2074, 2020. doi:10.4208/cicp.0A-2020-0193.
- [219] Siddhartha Mishra and Roberto Molinaro. Estimates on the generalization error of physics-informed neural networks for approximating PDEs. *IMA Journal of Numerical Analysis*, 43(1):1–43, 2023. doi:10.1093/imanum/drab093.
- [220] Siddhartha Mishra and Roberto Molinaro. Estimates on the generalization error of physics-informed neural networks for approximating a class of inverse problems for PDEs. *IMA Journal of Numerical Analysis*, 42(2):981–1022, 2022. doi:10.1093/imanum/drab032.
- [221] Tim De Ryck and Siddhartha Mishra. Error analysis for physics-informed neural networks (PINNs) approximating Kolmogorov PDEs. *Advances in Computational Mathematics*, 48(6), 2022. doi:10.1007/s10444-022-09985-9.
- [222] Tim De Ryck, Ameya D. Jagtap, and Siddhartha Mishra. Error estimates for physics-informed neural networks approximating the Navier-Stokes equations. *IMA Journal of Numerical Analysis*, 44(1):83–119, 2024. doi:10.1093/imanum/drac085.
- [223] Zhiping Mao, Ameya D. Jagtap, and George Em Karniadakis. Physics-informed neural networks for high-speed flows. *Computer Methods in Applied Mechanics and Engineering*, 360, 2020. doi:10.1016/j.cma.2019.112789.
- [224] Ameya D. Jagtap, Zhiping Mao, Nikolaus Adams, and George Em Karniadakis. Physics-informed neural networks for inverse problems in supersonic flows. *Journal of Computational Physics*, 466, 2022. doi:10.1016/j.jcp.2022.111402.
- [225] Simon Wassing, Stefan Langer, and Philipp Bekemeyer. Physics-informed neural networks for parametric compressible Euler equations. *Computers & Fluids*, 270, 2024. doi:10.1016/j.compfluid.2023.106164.
- [226] Jakob G. R. von Saldern, Johann Moritz Reumschuessel, Thomas L. Kaiser, Moritz Sieber, and Kilian Oberleithner. Mean flow data assimilation based on physics-informed neural networks. *Physics of Fluids*, 34(11), 2022. doi:10.1063/5.0116218.
- [227] Hamidreza Eivazi, Mojtaba Tahani, Philipp Schlatter, and Ricardo Vinuesa. Physics-informed neural networks for solving Reynolds-averaged Navier-Stokes equations. *Physics of Fluids*, 34(7), 2022. doi:10.1063/5.0095270.
- [228] Fabian Pioch, Jan Hauke Harmening, Andreas Maximilian Mueller, Franz-Josef Peitzmann, Dieter Schramm, and Ould el Moctar. Turbulence modeling for physics-informed neural networks: Comparison of different RANS models for the backward-facing step flow. *Fluids*, 8(2), 2023. doi:10.3390/fluids8020043.
- [229] Shirui Luo, Madhu Vellakal, Seid Koric, Volodymyr Kindratenko, and Jiahuan Cui. *Parameter identification of RANS turbulence model using physics-embedded neural network*, pages 137–49. 2020. doi:10.1007/978-3-030-59851-8\_9.
- [230] Longfeng Hou, Bing Zhu, and Ying Wang.  $k\varepsilon$ Net: discovering the turbulence model and applying for low Reynolds number turbulent channel flow. *Acta Mechanica Sinica*, 39(5), 2023. doi:10.1007/s10409-022-22326-x.
- [231] Jiahao Wu, Yuxin Wu, Xin Li, and Guihua Zhang. Physics-informed neural networks for Kelvin-Helmholtz instability with spatiotemporal and magnitude multiscale. *Physics of Fluids*, 37(3), 2025. doi:10.1063/5.0251167.
- [232] Aaron B. Buhendwa, Stefan Adami, and Nikolaus A. Adams. Inferring incompressible two-phase flow fields from the interface motion using physics-informed neural networks. *Machine Learning with Applications*, 4, 2021. doi:10.1016/j.mlwa.2021.100029.
- [233] Darioush Jalili, Seohee Jang, Mohammad Jadidi, Giovanni Giustini, Amir Keshmiri, and Yasser Mahmoudi. Physics-informed neural networks for heat transfer prediction in two-phase flows. *International Journal of Heat and Mass Transfer*, 221, 2024. doi:10.1016/j.ijheatmasstransfer.2023.125089.
- [234] Rundi Qiu, Haosen Dong, Jingzhu Wang, Chun Fan, and Yiwei Wang. Modeling two-phase flows with complicated interface evolution using parallel physics-informed neural networks. *Physics of Fluids*, 36(9), 2024. doi:10.1063/5.0216609.
- [235] Hassan Bararnia and Mehdi Esmaeilpour. On the application of physics informed neural networks (PINN) to solve boundary layer thermal-fluid problems. *International Communications in Heat and Mass Transfer*, 132, 2022. doi:10.1016/j.icheatmasstransfer.2022.105890.
- [236] Amirhossein Arzani, Kevin W Cassel, and Roshan M D'Souza. Theory-guided physics-informed neural networks for boundary layer problems with singular perturbation. *Journal of Computational Physics*, 473:111768, 2023.
- [237] Jianlin Huang, Rundi Qiu, Jingzhu Wang, and Yiwei Wang. Multi-scale physics-informed neural networks for solving high Reynolds number boundary layer flows based on matched asymptotic expansions. *Theoretical and Applied Mechanics Letters*, 14(2), 2024. doi:10.1016/j.taml.2024.100496.
- [238] Shengze Cai, Zhicheng Wang, Frederik Fuest, Young Jin Jeon, Callum Gray, and George Em Karniadakis. Flow over an espresso cup: inferring 3-D velocity and pressure fields from tomographic background oriented Schlieren via physics-informed neural networks. *Journal of Fluid Mechanics*, 915, 2021. doi:10.1017/jfm.2021.135.
- [239] Hongping Wang, Yi Liu, and Shizhao Wang. Dense velocity reconstruction from particle image velocimetry/particle tracking velocimetry using a physics-informed neural network. *Physics of Fluids*, 34(1), 2022. doi:10.1063/5.0078143.
- [240] Gazi Hasanuzzaman, Hamidreza Eivazi, Sebastian Merbold, Christoph Egbers, and Ricardo Vinuesa. Enhancement of PIV measurements via physics-informed neural networks. *Measurement Science and Technology*, 34(4), 2023. doi:10.1088/1361-6501/aca9eb.
- [241] Joseph P. Molnar, Lakshmi Venkatakrishnan, Bryan E. Schmidt, Timothy A. Sipkens, and Samuel J. Grauer. Estimating density, velocity, and pressure fields in supersonic flows using physics-informed BOS. *Experiments in Fluids*, 64(1), 2023. doi:10.1007/s00348-022-03554-y.
- [242] Lu Zhu, Xianyang Jiang, Adrien Lefauve, Rich R. Kerswell, and P. F. Linden. New insights into experimental stratified flows obtained through physics-informed neural networks. *Journal of Fluid Mechanics*, 981, 2024. doi:10.1017/jfm.2024.49.
- [243] Shengze Cai, Callum Gray, and George Em Karniadakis. Physics-informed neural networks enhanced particle tracking velocimetry: An example for turbulent jet flow. *IEEE Transactions on Instrumentation and Measurement*, 73, 2024. doi:10.1109/tim.2024.3398068.
- [244] Maziar Raissi, Alireza Yazdani, and George Em Karniadakis. Hidden fluid mechanics: Learning velocity and pressure fields from flow visualizations. *Science*, 367(6481):1026–1030, 2020. doi:10.1126/science.aaw4741.
- [245] Luning Sun, Han Gao, Shaowu Pan, and Jian-Xun Wang. Surrogate modeling for fluid flows based on physics-constrained deep learning without simulation data. *Computer Methods in Applied Mechanics and Engineering*, 361, 2020. doi:10.1016/j.cma.2019.112732.

- [246] Wenbo Cao, Xianglin Shan, Shixiang Tang, Wanli Ouyang, and Weiwei Zhang. Solving parametric high-Reynolds-number wall-bounded turbulence around airfoils governed by Reynolds-averaged Navier-Stokes equations using time-stepping-oriented neural network. *Physics of Fluids*, 37(1), 2025. doi:10.1063/5.0245918.
- [247] Wenbo Cao, Jiahao Song, and Weiwei Zhang. Solving high-dimensional parametric engineering problems for inviscid flow around airfoils based on physics-informed neural networks. *Journal of Computational Physics*, 516, 2024. doi:10.1016/j.jcp.2024.113285.
- [248] Wenbo Cao, Shixiang Tang, Qianhong Ma, Wanli Ouyang, and Weiwei Zhang. Solving all laminar flows around airfoils all-at-once using a parametric neural network solver. *arXiv preprint*, 2025. doi:10.48550/arXiv.2501.01165.
- [249] Shengze Cai, Zhicheng Wang, Sifan Wang, Paris Perdikaris, and George Em Karniadakis. Physics-informed neural networks for heat transfer problems. *Journal of Heat Transfer-Transactions of the ASME*, 143(6), 2021. doi:10.1115/1.4050542.
- [250] Siddhartha Mishra and Roberto Molinaro. Physics informed neural networks for simulating radiative transfer. *Journal of Quantitative Spectroscopy & Radiative Transfer*, 270, 2021. doi:10.1016/j.jqsrt.2021.107705.
- [251] Runlin Zhang, Nuo Xu, Kai Zhang, Lei Wang, and Gui Lu. A parametric physics-Informed deep learning method for probabilistic design of thermal protection systems. *Energies*, 16(9), 2023. doi:10.3390/en16093820.
- [252] R. Laubscher. Simulation of multi-species flow and heat transfer using physics-informed neural networks. *Physics of Fluids*, 33(8), 2021. doi:10.1063/5.0058529.
- [253] Stephen B. Pope. PDF methods for turbulent reactive flows. *Progress in Energy and Combustion Science*, 11(2):119–192, 1985. doi:10.1016/0360-1285(85)90002-4.
- [254] Norbert Peters. Laminar diffusion flamelet models in non-premixed turbulent combustion. *Progress in Energy and Combustion Science*, 10(3):319–339, 1984. doi:10.1016/0360-1285(84)90114-x.
- [255] Jeroen A. van Oijen and L. P. H. de Goey. Modelling of premixed laminar flames using flamelet-generated manifolds. *Combustion Science and Technology*, 161:113–137, 2000. doi:10.1080/00102200008935814.
- [256] Charles David Pierce. *Progress-variable approach for large-eddy simulation of turbulent combustion*. Thesis, 2001. URL: <https://www.proquest.com/dissertations-theses/progress-variable-approach-large-eddy-simulation/docview/304729235/se-2?accountid=14426>.
- [257] Charles David Pierce and Parviz Moin. Progress-variable approach for large-eddy simulation of non-premixed turbulent combustion. *Journal of Fluid Mechanics*, 504:73–97, 2004. doi:10.1017/s0022112004008213.
- [258] Weiqi Ji, Weilun Qiu, Zhiyu Shi, Shaowu Pan, and Sili Deng. Stiff-PINN: Physics-informed neural network for stiff chemical kinetics. *The Journal of Physical Chemistry A*, 125(36):8098–8106, 2021. doi:10.1021/acs.jpca.1c05102.
- [259] Mario De Florio, Enrico Schiassi, and Roberto Furfaro. Physics-informed neural networks and functional interpolation for stiff chemical kinetics. *Chaos*, 32(6), 2022. doi:10.1063/5.0086649.
- [260] Yicun Wang, Jiangkuan Xing, Kun Luo, Haiou Wang, and Jianren Fan. Solving combustion chemical differential equations via physics-informed neural network. *Journal of Zhejiang University (Engineering Science)*, pages 2084–92, 2022. doi:10.3785/j.issn.1008-973X.2022.10.020.
- [261] Evangelos Galaris, Gianluca Fabiani, Francesco Calabro, Daniela di Serafino, and Constantinos Siettos. Numerical solution of stiff ODEs with physics-informed RPNNs. *arXiv preprint*, 2021. doi:10.48550/arXiv.2108.01584.
- [262] Gianluca Fabiani, Evangelos Galaris, Lucia Russo, and Constantinos Siettos. Parsimonious physics-informed random projection neural networks for initial value problems of ODEs and index-1 DAEs. *Chaos*, 33(4), 2023. doi:10.1063/5.0135903.
- [263] Mingjian Li, Zengrong Su, Chuang He, Bingjian Zhang, and Qinglin Chen. Physics-informed neural network for unreacted-core shrinking model of coal gasification. *Chemical Engineering Transactions*, 88:445–450, 2021. doi:10.3303/CET2188074.
- [264] Yuting Weng and Dezhi Zhou. Multiscale physics-informed neural networks for stiff chemical kinetics. *Journal of Physical Chemistry A*, 2022. doi:10.1021/acs.jpca.2c06513.
- [265] Gabriel S. Gusmao, Adhika P. Retnanto, Shashwati C. da Cunha, and Andrew J. Medford. Kinetics-informed neural networks. *Catalysis Today*, 417, 2023. doi:10.1016/j.cattod.2022.04.002.
- [266] Valerie Bibeau, Daria Camilla Boffito, and Bruno Blais. Physics-informed Neural Network to predict kinetics of biodiesel production in microwave reactors. *Chemical Engineering and Processing-Process Intensification*, 196, 2024. doi:10.1016/j.cep.2023.109652.
- [267] Ahmed Almeldein and Noah Van Dam. Accelerating chemical kinetics calculations with physics informed neural networks. *Journal of Engineering for Gas Turbines and Power-Transactions of the Asme*, 145(9), 2023. doi:10.1115/1.4062654.
- [268] Shihong Zhang, Chi Zhang, and Bosen Wang. CRK-PINN: A physics-informed neural network for solving combustion reaction kinetics ordinary differential equations. *Combustion and Flame*, 269, 2024. doi:10.1016/j.combustflame.2024.113647.
- [269] Yuting Weng, Han Li, Hao Zhang, Zhi X. Chen, and Dezhi Zhou. Extended Fourier Neural Operators to learn stiff chemical kinetics under unseen conditions. *Combustion and Flame*, 272, 2025. doi:10.1016/j.combustflame.2024.113847.
- [270] Thomas Readshaw, Tianjie Ding, Stelios Rigopoulos, and W. P. Jones. Modeling of turbulent flames with the large eddy simulation-probability density function (LES-PDF) approach, stochastic fields, and artificial neural networks. *Physics of Fluids*, 33(3), 2021. doi:10.1063/5.0041122.
- [271] Tianjie Ding, Thomas Readshaw, Stelios Rigopoulos, and W. P. Jones. Machine learning tabulation of thermochemistry in turbulent combustion: An approach based on hybrid flamelet/random data and multiple multilayer perceptrons. *Combustion and Flame*, 231, 2021. doi:10.1016/j.combustflame.2021.111493.
- [272] Tianjie Ding, Stelios Rigopoulos, and W. P. Jones. Machine learning tabulation of thermochemistry of fuel blends. *Applications in Energy and Combustion Science*, 12, 2022. doi:10.1016/j.jaecs.2022.100086.
- [273] Thomas Readshaw, W. P. Jones, and Stelios Rigopoulos. On the incorporation of conservation laws in machine learning tabulation of kinetics for reacting flow simulation. *Physics of Fluids*, 35(4), 2023. doi:10.1063/5.0143894.
- [274] Amol Salunkhe, Dwyer Deighan, Paul E. DesJardin, and Varun Chandola. ChemTab: A physics guided chemistry modeling framework. In *22nd Annual International Conference on Computational Science (ICCS)*, Lecture Notes in Computer Science, pages 75–88, 2022. doi:10.1007/978-3-031-08751-6\_6.
- [275] Amol Salunkhe, Dwyer Deighan, Paul E. DesJardin, and Varun Chandola. Physics informed machine learning for chemistry tabulation. *Journal of Computational Science*, 69, 2023. doi:10.1016/j.jocs.2023.102001.
- [276] Vijayamanikandan Vijayarangan, Harshavardhana A. Uranakara, Shivam Barwey, Riccardo Malpica Galassi, Mohammad Rafi Malik, Mauro Valorani, Venkat Raman, and Hong G. Im. A data-driven reduced-order model for stiff chemical kinetics using dynamics-informed training. *Energy and AI*, 15, 2024. doi:10.1016/j.egyai.2023.100325.
- [277] Tadbhagya Kumar, Anuj Kumar, and Pinaki Pal. A physics-constrained NeuralODE approach for robust learning of stiff chemical kinetics. In *NeurIPS 2023 Workshop on Machine Learning and the Physical Sciences*, 2023. <https://nips.cc/virtual/2023/76185>. URL: [https://ml4physicalsciences.github.io/2023/files/NeurIPS\\_ML4PS\\_2023\\_144.pdf](https://ml4physicalsciences.github.io/2023/files/NeurIPS_ML4PS_2023_144.pdf).

- [278] Tadbhagya Kumar, Anuj Kumar, and Pinaki Pal. A physics-constrained neural ordinary differential equations approach for robust learning of stiff chemical kinetics. *Combustion Theory and Modelling*, 2025. doi:10.1080/13647830.2025.2478266.
- [279] Tadbhagya Kumar, Anuj Kumar, and Pinaki Pal. A physics-informed autoencoder-NeuralODE framework (Phy-ChemNODE) for learning complex fuel combustion kinetics. In *NeurIPS 2024 Workshop on Machine Learning and the Physical Sciences*, 2024. URL: <https://neurips.cc/virtual/2024/100084>. URL: [https://ml4physicalsciences.github.io/2024/files/NeurIPS\\_ML4PS\\_2024\\_151.pdf](https://ml4physicalsciences.github.io/2024/files/NeurIPS_ML4PS_2024_151.pdf).
- [280] Benjamin C. Koenig, Suyong Kim, and Sili Deng. ChemKANs for combustion chemistry modeling and acceleration. *Physical Chemistry Chemical Physics*, 2025. doi:10.1039/d5cp02009c.
- [281] Xingyu Su, Weiqi Ji, Jian An, Zhuyin Ren, Sili Deng, and Chung K. Law. Kinetics parameter optimization of hydrocarbon fuels via neural ordinary differential equations. *Combustion and Flame*, 251, 2023. doi:10.1016/j.combustflame.2023.112732.
- [282] Felix A. Doeppel and Martin Votsmeier. Robust mechanism discovery with atom conserving chemical reaction neural networks. *Proceedings of the Combustion Institute*, 40(1-4), 2024. doi:10.1016/j.proci.2024.105507.
- [283] Dingqi Nai, Gabriel S. Gusmao, Zachary A. Kilwein, Fani Boukouvala, and Andrew J. Medford. Micro-kinetic modeling of temporal analysis of products data using kinetics-informed neural networks. *Digital Discovery*, 3(11):2327–2340, 2024. doi:10.1039/d4dd00163j.
- [284] Gabriel S. Gusmao and Andrew J. Medford. Maximum-likelihood estimators in physics-informed neural networks for high-dimensional inverse problems. *Computers & Chemical Engineering*, 181, 2024. doi:10.1016/j.compchemeng.2023.108547.
- [285] Shihong Zhang, Chi Zhang, and Bosen Wang. A physics-informed neural network for solving combustion reaction kinetics. *Journal of Engineering Thermophysics*, 45(06):1872–1881, 2024. URL: [https://www.engineeringvillage.com/app/doc/?docid=cpx\\_6f772beb1906db54414M5b3b10178165134&pageSize=25&index=2&searchId=31daaee5ab1f4773a570554a22d884cd&resultsCount=5&usageZone=resultslist&usageOrigin=searchresults&searchType=Quick](https://www.engineeringvillage.com/app/doc/?docid=cpx_6f772beb1906db54414M5b3b10178165134&pageSize=25&index=2&searchId=31daaee5ab1f4773a570554a22d884cd&resultsCount=5&usageZone=resultslist&usageOrigin=searchresults&searchType=Quick).
- [286] Simone Venturi and Tiernan Casey. SVD perspectives for augmenting DeepONet flexibility and interpretability. *Computer Methods in Applied Mechanics and Engineering*, 403, 2023. doi:10.1016/j.cma.2022.115718.
- [287] Tsung-Yi Lin, Priya Goyal, Ross Girshick, Kaiming He, and Piotr Dollar. Focal loss for dense object detection. In *2017 IEEE International Conference on Computer Vision (ICCV)*, pages 2999–3007. IEEE, 2017. doi:10.1109/iccv.2017.324.
- [288] Ricky T. Q. Chen, Yulia Rubanova, Jesse Bettencourt, and David Duvenaud. Neural ordinary differential equations. In *32nd Conference on Neural Information Processing Systems (NeurIPS)*, pages 6572–6583. Curran Associates Inc., 2018. URL: <https://papers.nips.cc/paper/2018/hash/69386f6bb1dfed68692a24c8686939b9-Abstract.html>.
- [289] Suyong Kim, Weiqi Ji, Sili Deng, Yingbo Ma, and Christopher Rackauckas. Stiff neural ordinary differential equations. *Chaos*, 31(9), 2021. doi:10.1063/5.0060697.
- [290] Aleksei Sholokhov, Yuying Liu, Hassan Mansour, and Saleh Nabi. Physics-informed neural ODE (PINODE): Embedding physics into models using collocation points. *Scientific Reports*, 13(1), 2023. doi:10.1038/s41598-023-36799-6.
- [291] Benjamin C. Koenig, Suyong Kim, and Sili Deng. KAN-ODEs: Kolmogorov-Arnold network ordinary differential equations for learning dynamical systems and hidden physics. *Computer Methods in Applied Mechanics and Engineering*, 432:117397, 2024. doi:10.1016/j.cma.2024.117397.
- [292] Benjamin C. Koenig, Suyong Kim, and Sili Deng. LeanKAN: a parameter-lean Kolmogorov-Arnold network layer with improved memory efficiency and convergence behavior. *Neural Networks*, 192:107883, 2025. doi:10.1016/j.neunet.2025.107883.
- [293] Weiqi Ji, Franz Richter, Michael J. Gollner, and Sili Deng. Autonomous kinetic modeling of biomass pyrolysis using chemical reaction neural networks. *Combustion and Flame*, 240, 2022. doi:10.1016/j.combustflame.2022.111992.
- [294] Gang Tang, He Wang, Chunyan Chen, Yabei Xu, Dongping Chen, Dongli Wang, Yunjun Luo, and Xiaoyu Li. Thermal decomposition of nano Al-based energetic composites with fluorinated energetic polyurethane binders: Experimental and theoretical understandings for enhanced combustion and energetic performance. *Rsc Advances*, 12(37):24163–24171, 2022. doi:10.1039/d2ra03781e.
- [295] He Wang, Yabei Xu, Mingjie Wen, Wei Wang, Qingzhao Chu, Shi Yan, Shengliang Xu, and Dongping Chen. Kinetic modeling of CL-20 decomposition by a chemical reaction neural network. *Journal of Analytical and Applied Pyrolysis*, 169, 2023. doi:10.1016/j.jaap.2023.105860.
- [296] Wei Sun, Yabei Xu, Xinzhe Chen, Qingzhao Chu, and Dongping Chen. Kinetic models of HMX decomposition via chemical reaction neural network. *Journal of Analytical and Applied Pyrolysis*, 179, 2024. doi:10.1016/j.jaap.2024.106519.
- [297] Xinzhe Chen, Yabei Xu, Mingjie Wen, Yongjin Wang, Kehui Pang, Shengkai Wang, Qingzhao Chu, and Dongping Chen. EM-HyChem: Bridging molecular simulations and chemical reaction neural network-enabled approach to modelling energetic material chemistry. *Combustion and Flame*, 275, 2025. doi:10.1016/j.combustflame.2025.114065.
- [298] Qiaofeng Li, Huaibo Chen, Benjamin C. Koenig, and Sili Deng. Bayesian chemical reaction neural network for autonomous kinetic uncertainty quantification. *Physical Chemistry Chemical Physics*, 25(5):3707–3717, 2023. doi:10.1039/d2cp05083h.
- [299] Solji Choi, Ikhwan Jung, Haeun Kim, Jonggeol Na, and Jong Min Lee. Physics-informed deep learning for data-driven solutions of computational fluid dynamics. *Korean Journal of Chemical Engineering*, 39(3):515–528, 2022. doi:10.1007/s11814-021-0979-x.
- [300] Michael Philip Sitte and Nguyen Anh Khoa Doan. Velocity reconstruction in puffing pool fires with physics-informed neural networks. *Physics of Fluids*, 34(8), 2022. doi:10.1063/5.0097496.
- [301] Kai Liu, Kun Luo, Yuzhou Cheng, Anxiong Liu, Haochen Li, Jianren Fan, and S. Balachandar. Surrogate modeling of parameterized multi-dimensional premixed combustion with physics-informed neural networks for rapid exploration of design space. *Combustion and Flame*, 258, 2023. doi:10.1016/j.combustflame.2023.113094.
- [302] Mengze Song, Xinzhou Tang, Jiangkuan Xing, Kai Liu, Kun Luo, and Jianren Fan. Physics-informed neural networks coupled with flamelet/progress variable model for solving combustion physics considering detailed reaction mechanism. *Physics of Fluids*, 36(10), 2024. doi:10.1063/5.0227581.
- [303] Zhen Cao, Kai Liu, Kun Luo, Sifan Wang, Liang Jiang, and Jianren Fan. Surrogate modeling of multi-dimensional premixed and non-premixed combustion using pseudo-time stepping physics-informed neural networks. *Physics of Fluids*, 36(11), 2024. doi:10.1063/5.0235674.
- [304] Shiyu Liu, Haiou Wang, Jacqueline H. Chen, Kun Luo, and Jianren Fan. High-resolution reconstruction of turbulent flames from sparse data with physics-informed neural networks. *Combustion and Flame*, 2024. doi:10.1016/j.combustflame.2023.113275.
- [305] Haoran Peng and Guihua Hu. Reconstruction of Flame D heat flow field based on physical information deep learning algorithm. *Journal of East China University of Science and Technology*, 50(06):878–887, 2024. URL: <https://www.scopus.com/pages/publications/85214972156>, doi:10.14135/j.cnki.1006-3080.20231227002.
- [306] Arsalan Taassob, Rishikesh Ranade, and Tarek Echekki. Physics-informed neural networks for turbulent combustion: Toward extracting more statistics and closure from point multiscalar measurements. *Energy & Fuels*, 37(22):17484–17498, 2023. doi:10.1021/acs.energyfuels.3c02410.

- [307] Vikas Yadav, Mario Casel, and Abdulla Ghani. RF-PINNs: Reactive flow physics-informed neural networks for field reconstruction of laminar and turbulent flames using sparse data. *Journal of Computational Physics*, 524, 2025. doi:10.1016/j.jcp.2024.113698.
- [308] Xutun Wang, Haocheng Wen, Tong Hu, and Bing Wang. Flow-field reconstruction in rotating detonation combustor based on physics-informed neural network. *Physics of Fluids*, 35(7), 2023. doi:10.1063/5.0154979.
- [309] Xue Deng, Mingming Guo, Yi Zhang, Ye Tian, Jingrun Wu, Heng Wang, Hua Zhang, and Jialing Le. Intelligent reconstruction of unsteady combustion flow field of scramjet based on physical information constraints. *Physics of Fluids*, 36(7), 2024. doi:10.1063/5.0217991.
- [310] Mathis Bode, Michael Gauding, Zeyu Lian, Dominik Denker, Marco Davidovic, Konstantin Kleinheinz, Jenia Jitsev, and Heinz Pitsch. Using physics-informed enhanced super-resolution generative adversarial networks for subfilter modeling in turbulent reactive flows. *Proceedings of the Combustion Institute*, 38(2):2617–2625, 2021. doi:10.1016/j.proci.2020.06.022.
- [311] Mathis Bode, Michael Gauding, Dominik Goeb, Tobias Falkenstein, and Heinz Pitsch. Applying physics-informed enhanced super-resolution generative adversarial networks to turbulent premixed combustion and engine-like flame kernel direct numerical simulation data. *Proceedings of the Combustion Institute*, 39(4):5289–5298, 2023. doi:10.1016/j.proci.2022.07.254.
- [312] Xutun Wang, Haocheng Wen, and Bing Wang. Super-resolution flow-field reconstruction in rotating detonation combustors. *Aerospace Science and Technology*, 144, 2024. doi:10.1016/j.ast.2023.108740.
- [313] Xutun Wang, Haocheng Wen, Quan Wen, and Bing Wang. Physics-informed recurrent super-resolution generative reconstruction in rotating detonation combustor. *Proceedings of the Combustion Institute*, 40(1–4), 2024. doi:10.1016/j.proci.2024.105649.
- [314] Sina Amini Niaki, Ehsan Haghighat, Trevor Campbell, Anoush Poursartip, and Reza Vaziri. Physics-informed neural network for modelling the thermochemical curing process of composite-tool systems during manufacture. *Computer Methods in Applied Mechanics and Engineering*, 384, 2021. doi:10.1016/j.cma.2021.113959.
- [315] Son Ich Ngo and Young-II Lim. Solution and parameter identification of a fixed-bed reactor model for catalytic CO<sub>2</sub> methanation using physics-informed neural networks. *Catalysts*, 11(11), 2021. doi:10.3390/catal11111304.
- [316] Qingzhi Hou, Zewei Sun, Li He, and Alireza Karemat. Orthogonal grid physics-informed neural networks: A neural network-based simulation tool for advection-diffusion-reaction problems. *Physics of Fluids*, 34(7), 2022. doi:10.1063/5.0095536.
- [317] Zewei Sun, Honghan Du, Chunfu Miao, and Qingzhi Hou. A physics-informed neural network based simulation tool for reacting flow with multicomponent reactants. *Advances in Engineering Software*, 185, 2023. doi:10.1016/j.advengsoft.2023.103525.
- [318] Qingzhi Hou, Honghan Du, Zewei Sun, Jianping Wang, Xiaojing Wang, and Jianguo Wei. PINN-CDR: A neural network-based simulation tool for convection-diffusion-reaction systems. *International Journal of Intelligent Systems*, 2023, 2023. doi:10.1155/2023/2973249.
- [319] Laura Laghi, Enrico Schiassi, Mario De Florio, Roberto Furfaro, and Domiziano Mostacci. Physics-informed neural networks for 1-D steady-state diffusion-advection-reaction equations. *Nuclear Science and Engineering*, 197(9):2373–2403, 2023. doi:10.1080/00295639.2022.2160604.
- [320] Adrian Corrochano, Rodolfo S. M. Freitas, Manuel Lopez-Martin, Alessandro Parente, and Soledad Le Clairche. A predictive physics-aware hybrid reduced order model for reacting flows. *International Journal for Numerical Methods in Engineering*, 126(11), 2025. doi:10.1002/nme.70058.
- [321] Tarak Nandi, Oliver Hennigh, Mohammad Nabian, Yong Liu, Mino Woo, Terry Jordan, Mehrdad Shahnam, Madhava Syamlal, Chris Guenther, and Dirk VanEssendelft. Progress towards solving high Reynolds number reacting flows in SimNet. National Energy Technology Laboratory (NETL), Pittsburgh, PA, Morgantown, WV, and Albany, OR (United States), 11 2021. URL: <https://www.osti.gov/biblio/1846970>.
- [322] Tarak Nandi, Oliver Hennigh, Mohammad Nabian, Yong Liu, Mino Woo, Terry Jordan, Mehrdad Shahnam, Chris Guenther, and Dirk VanEssendelft. Developing digital twins for energy applications using Modulus. National Energy Technology Laboratory (NETL), Pittsburgh, PA, Morgantown, WV, and Albany, OR (United States), 03 2022. URL: <https://www.osti.gov/biblio/1866819>.
- [323] Robert S. Barlow and Jonathan H. Frank. Effects of turbulence on species mass fractions in methane/air jet flames. *Symposium (International) on Combustion*, 27(1):1087–1095, 1998. doi:10.1016/S0082-0784(98)80510-9.
- [324] Zhiping Mao, Lu Lu, Olaf Marxen, Tamer A. Zaki, and George Em Karniadakis. DeepM&Mnet for hypersonics: Predicting the coupled flow and finite-rate chemistry behind a normal shock using neural-network approximation of operators. *Journal of Computational Physics*, 447:24, 2021. doi:10.1016/j.jcp.2021.110698.
- [325] Shengze Cai, Zhicheng Wang, Lu Lu, Tamer A. Zaki, and George Em Karniadakis. DeepM&Mnet: Inferring the electroconvection multiphysics fields based on operator approximation by neural networks. *Journal of Computational Physics*, 436:17, 2021. doi:10.1016/j.jcp.2021.110296.
- [326] Mingming Guo, Jialing Le, Xue Deng, Ye Tian, Yue Ma, Shuhong Tong, and Hua Zhang. Flow field reconstruction in inlet of scramjet at Mach 10 based on physical information neural network. *Physics of Fluids*, 35(10), 2023. doi:10.1063/5.0170588.
- [327] Mathis Bode. Applying physics-informed enhanced super-resolution generative adversarial networks to large-eddy simulations of ECN Spray C. *SAE International Journal of Advances and Current Practices in Mobility*, 4(6):2211–9, 2022. doi:10.4271/2022-01-0503.
- [328] Mathis Bode. Applying physics-informed enhanced super-resolution generative adversarial networks to finite-rate-chemistry flows and predicting lean premixed gas turbine combustors. *arXiv preprint*, 2022. doi:10.48550/arXiv.2210.16219.
- [329] Mathis Bode. Applying physics-informed enhanced super-resolution generative adversarial networks to turbulent non-premixed combustion on non-uniform meshes and demonstration of an accelerated simulation workflow. *arXiv preprint*, 2022. doi:10.48550/arXiv.2210.16248.
- [330] Wai Tong Chung, Bassem Akoush, Pushan Sharma, Alex Tamkin, Ki Sung Jung, Jacqueline H. Chen, Jack Guo, Davy Brouzet, Mohsen Talei, Bruno Savard, Alexei Y. Poludnenko, and Matthias Ihme. Turbulence in focus: Benchmarking scaling behavior of 3D volumetric super-resolution with BLASTNet 2.0 data. In *37th Conference on Neural Information Processing Systems (NeurIPS)*, 2023. URL: <https://neurips.cc/virtual/2023/poster/73433>.
- [331] Luca Bottero, Francesco Calisto, Giovanni Graziano, Valerio Pagliarino, Martina Scauda, Sara Tiengo, and Simone Azeglio. Physics-informed machine learning simulator for wildfire propagation. *arXiv preprint*, 2020. doi:10.48550/arXiv.2012.06825.
- [332] Joel Janek Dabrowski, Daniel Edward Pagendam, James Hilton, Conrad Sanderson, Daniel MacKinlay, Carolyn Huston, Andrew Bolt, and Petra Kuhnert. Bayesian Physics Informed Neural Networks for data assimilation and spatio-temporal modelling of wildfires. *Spatial Statistics*, 55, 2023. doi:10.1016/j.spasta.2023.100746.
- [333] Konstantinos Vogiatzoglou, Costas Papadimitriou, Vasilis Bontozoglou, and Konstantinos Ampountolas. Physics-informed neural networks for parameter learning of wildfire spreading. *Computer Methods in Applied Mechanics and Engineering*, 434, 2025. doi:10.1016/j.cma.2024.117545.
- [334] Seydi, Seyd Teymoor and Abatzoglou, John T. and Aghakouchak, Amir and Pourmohamad, Yavar and Mishra, Ashok and Sadegh, Mojtaba. Predictive understanding of links between vegetation and soil burn severities using physics-informed machine learning. *Earths Future*, 12(8), 2024. doi:10.1029/2024ef004873.
- [335] Selma Emekci. AI Firefighter: A physics informed decision-making neural network for optimized firefighting on arbitrary landscapes. In *2024 IEEE MIT Undergraduate Research Technology Conference (URTC)*, pages 1–5, 2025. doi:10.1109/urtc65039.2024.10937583.
- [336] Sung Wook Kim, Eunji Kwak, Jun-Hyeong Kim, Ki-Yong Oh, and Seungchul Lee. Modeling and prediction of lithium-ion battery thermal runaway via multiphysics-informed neural network. *Journal of Energy Storage*, 60, 2023. doi:10.1016/j.est.2023.106654.

- [337] Mohamad Mahdi Mozafari Parsa and Amir Mahdi Tahsini. Predicting the transient burning of non-charring materials using physics-informed neural networks. *Fire Safety Journal*, 153, 2025. doi:10.1016/j.firesaf.2025.104379.
- [338] Defne Ege Ozan and Luca Magri. Physics-aware learning of nonlinear limit cycles and adjoint limit cycles. In *INTER-NOISE and NOISE-CON Congress and Conference Proceedings*, volume 265, pages 1191–1199. Institute of Noise Control Engineering, 2023. doi:10.3397/IN\_2022\_0163.
- [339] Sathesh Mariappan, Kamaljiyoti Nath, and George Em Karniadakis. Learning thermoacoustic interactions in combustors using a physics-informed neural network. *Engineering Applications of Artificial Intelligence*, 138, 2024. doi:10.1016/j.engappai.2024.109388.
- [340] Mingke Xie, Xinyu Zhao, Dan Zhao, Jianqin Fu, Cody Shelton, and Bernhard Semmlitsch. Predicting bifurcation and amplitude death characteristics of thermoacoustic instabilities from PINNs-derived van der Pol oscillators. *Journal of Fluid Mechanics*, 998, 2024. doi:10.1017/jfm.2024.800.
- [341] Qianlong Wang and Yingyu Qian. Three-dimensional particulate volume fraction reconstruction in the fluid based on the Lambert-Beer physics information neural network. *Physics of Fluids*, 36(10), 2024. doi:10.1063/5.0233484.
- [342] Qianlong Wang, Mingxue Gong, Alexis Matynia, Linghui Zhang, Yingyu Qian, and Chao Dang. Soot temperature and volume fraction field predictions via line-of-sight soot integrated radiation equation informed neural networks in laminar sooting flames. *Physics of Fluids*, 36(12), 2024. doi:10.1063/5.0245120.
- [343] Cheng Chi, Srijiith Sreekumar, and Dominique Thevenin. Data-driven discovery of heat release rate markers for premixed NH<sub>3</sub>/H<sub>2</sub>/air flames using physics-informed machine learning. *Fuel*, 330, 2022. doi:10.1016/j.fuel.2022.125508.
- [344] Vahid Reza Hosseini, Abbasali Abouei Mehri, Afsin Gungor, and Hamid Hassanzadeh Afrouzi. Application of a physics-informed neural network to solve the steady-state Bratu equation arising from solid biofuel combustion theory. *Fuel*, 332, 2022. doi:10.1016/j.fuel.2022.125908.
- [345] Vikas Yadav, Mario Casel, and Abdulla Ghani. Physics-informed recurrent neural networks for linear and nonlinear flame dynamics. *Proceedings of the Combustion Institute*, 39(2):1597–1606, 2023. doi:10.1016/j.proci.2022.08.036.
- [346] Yeonjoon Kim, Jaeyoung Cho, Nimal Naser, Sabari Kumar, Keunhong Jeong, Robert L. McCormick, Peter C. St John, and Seonah Kim. Physics-informed graph neural networks for predicting cetane number with systematic data quality analysis. *Proceedings of the Combustion Institute*, 39(4):4969–4978, 2023. doi:10.1016/j.proci.2022.09.059.
- [347] Jeyan Thiyaalingam, Mallikarjun Shankar, Geoffrey Fox, and Tony Hey. Scientific machine learning benchmarks. *Nature Reviews Physics*, 4(6):413–420, 2022. doi:10.1038/s42254-022-00441-7.
- [348] Jia Deng, Wei Dong, Richard Socher, Li-Jia Li, Kai Li, Fei-Fei Li, and Ieee. ImageNet: A large-scale hierarchical image database. In *2009 IEEE Conference on Computer Vision and Pattern Recognition (CVPR)*, IEEE Conference on Computer Vision and Pattern Recognition, pages 248–255, 2009. doi:10.1109/cvpr.2009.5206848.
- [349] Zhongkai Hao, Jiachen Yao, Chang Su, Hang Su, Ziao Wang, Fanzhi Lu, Zeyu Xia, Yichi Zhang, Songming Liu, Lu Lu, and Jun Zhu. PINNacle: A comprehensive benchmark of physics-informed neural networks for solving PDEs. In *38th Conference on Neural Information Processing Systems (NeurIPS)*, 2024. URL: <https://neurips.cc/virtual/2024/poster/97621>.
- [350] Ronak Tali, Ali Rabeh, Cheng-Hau Yang, Mehdi Shadkhan, Samundra Karki, Abhisek Upadhyaya, Suriya Dhakshinamoorthy, Marjan Saadati, Soumik Sarkar, Adarsh Krishnamurthy, Chinmay Hegde, Aditya Balu, and Baskar Ganapathysubramanian. FlowBench: A large scale benchmark for flow simulation over complex geometries. *arXiv preprint*, 2024. doi:10.48550/arXiv.2409.18032.
- [351] Yi Li, Eric Perlman, Mingping Wan, Yunke Yang, Charles Meneveau, Randal Burns, Shiyi Chen, Alexander Szalay, and Gregory Eyink. A public turbulence database cluster and applications to study Lagrangian evolution of velocity increments in turbulence. *Journal of Turbulence*, 9(31):1–29, 2008. doi:10.1080/14685240802376389.
- [352] ERCOFTAC Classic Collection Database. URL: <http://cfd.mace.manchester.ac.uk>.
- [353] Links to other online databases and collections. URL: <http://cfd.mace.manchester.ac.uk/ercoftac/doku.php?id=database-links>.
- [354] ERCOFTAC Knowledge Base Wiki. URL: [http://www.kbwiki.ercoftac.org/w/index.php/Main\\_Page](http://www.kbwiki.ercoftac.org/w/index.php/Main_Page).
- [355] Marie-Lena Eckert, Kiwon Um, and Nils Thuerey. ScalarFlow: A large-scale volumetric data set of real-world scalar transport flows for computer animation and machine learning. *ACM Transactions on Graphics*, 38(6), 2019. doi:10.1145/3355089.3356545.
- [356] Florent Bonnet, Jocelyn Ahmed Mazari, Paola Cinnella, and Patrick Gallinari. AirFRANS: High fidelity computational fluid dynamics dataset for approximating Reynolds-averaged Navier-Stokes solutions. In *36th Conference on Neural Information Processing Systems (NeurIPS)*, 2022. URL: <https://neurips.cc/virtual/2022/poster/55720>.
- [357] Ruben Ohana, Michael McCabe, Lucas Meyer, Rudy Morel, Fruzsina J. Agocs, Miguel Beneitez, Marsha Berger, Blakesley Burkhart, Stuart B. Dalziel, Drummond B. Fielding, Daniel Fortunato, Jared A. Goldberg, Keiya Hirashima, Yan-Fei Jiang, Rich R. Kerswell, Suryanarayana Maddu, Jonah Miller, Payel Mukhopadhyay, Stefan S. Nixon, Jeff Shen, Romain Watteaux, Bruno Régalo-Saint Blancard, François Rozet, Liam H. Parker, Miles Cranmer, and Shirley Ho. The Well: A large-scale collection of diverse physics simulations for machine learning. In *38th Conference on Neural Information Processing Systems (NeurIPS)*, 2024. URL: <https://neurips.cc/virtual/2024/poster/97882>.
- [358] NASA Langley Research Center. Turbulence Modeling Resource. URL: <https://turbmodels.larc.nasa.gov>.
- [359] Aaron Towne, Scott T. M. Dawson, Guillaume A. Bres, Adrian Lozano-Duran, Theresa Saxton-Fox, Aadhy Parthasarathy, Anya R. Jones, Hulya Biler, Chi-An Yeh, Het D. Patel, and Kunihiko Taira. A database for reduced-complexity modeling of fluid flows. *AIAA Journal*, 61(7):2867–2892, 2023. doi:10.2514/1.J062203.
- [360] TNF workshop. URL: <https://tnfworkshop.org>.
- [361] Wai Tong Chung, Ki Sung Jung, Jacqueline H. Chen, and Matthias Ihme. The bearable lightness of big data: Towards massive public datasets in scientific machine learning. In *ICML 2022 Workshop on AI for Science*, 2022. URL: <https://icml.cc/virtual/2022/19931>.
- [362] Wai Tong Chung, Ki Sung Jung, Jacqueline H. Chen, and Matthias Ihme. BLASTNet: A call for community-involved big data in combustion machine learning. *Applications in Energy and Combustion Science*, 12, 2022. doi:10.1016/j.jaeacs.2022.100087.
- [363] Tom S. Artes, Duarte Oom, Daniele De Rigo, Tracy Houston Durrant, PIERALBERTO MAIANTI, Giorgio Liberta, and Jesus San-Miguel-Ayanz. A global wildfire dataset for the analysis of fire regimes and fire behaviour. *Scientific Data*, 6, 2019. doi:10.1038/s41597-019-0312-2.
- [364] Yanzhi Li, Keqiu Li, Li. Guohui, Zumin Wang, Changqing Ji, Lubo Wang, Die Zuo, Qing Guo, Feng Zhang, Manyu Wang, and Di Lin. Sim2Real-Fire: A multi-modal simulation dataset for forecast and backtracking of real-world forest fire. In *38th Conference on Neural Information Processing Systems (NeurIPS)*, 2024. URL: <https://neurips.cc/virtual/2024/poster/97800>.
- [365] Qing Wang, Matthias Ihme, Cenk Gazen, Yi-Fan Chen, and John Anderson. A high-fidelity ensemble simulation framework for interrogating wildland-fire behaviour and benchmarking machine learning models. *International Journal of Wildland Fire*, 33(12), 2024. doi:10.1071/wf24097.
- [366] Scott D. Cohen and Alan C. Hindmarsh. CVODE, a stiff/nonstiff ODE solver in C. *Computers in Physics*, 10(2):138–43, 1996. doi:10.1063/1.4822377.
- [367] Alan C. Hindmarsh, Peter N. Brown, Keith E. Grant, Steven L. Lee, Radu Serban, Dan E. Shumaker, and Carol S. Woodward. SUNDIALS: Suite of nonlinear and differential/algebraic equation solvers. *ACM Transactions on Mathematical Software*, 31(3):363–396, 2005. doi:10.1145/1089014.1089020.

- [368] David J. Gardner, Daniel R. Reynolds, Carol S. Woodward, and Cody J. Balos. Enabling new flexibility in the SUNDIALS suite of nonlinear and differential/algebraic equation solvers. *ACM Transactions on Mathematical Software*, 48(3), 2022. doi:10.1145/3539801.
- [369] David I. Ketcheson, Kyle T. Mandli, Aron J. Ahmadi, Amal Alghamdi, Manuel Quezada de Luna, Matteo Parsani, Matthew G. Knepley, and Matthew Emmett. PyClaw: Accessible, extensible, scalable tools for wave propagation problems. *SIAM Journal on Scientific Computing*, 34(4):C210–C231, 2012. doi:10.1137/110856976.
- [370] Clawpack Development Team. Clawpack software, 2024. doi:10.5281/zenodo.13376470.
- [371] Kyle T. Mandli, Aron J. Ahmadi, Marsha Berger, Donna Calhoun, David L. George, Yiannis Hadjimichael, David I. Ketcheson, Grady I. Lemoine, and Randall J. LeVeque. Clawpack: Building an open source ecosystem for solving hyperbolic PDEs. *PeerJ Computer Science*, 2:e68, 2016. doi:10.7717/peerj-cs.68.
- [372] Henry G. Weller, Gavin Tabor, Hrvoje Jasak, and Christer Fureby. A tensorial approach to computational continuum mechanics using object-oriented techniques. *Computers in Physics*, 12(6):620–631, 1998. doi:10.1063/1.168744.
- [373] Hrvoje Jasak, Aleksandar Jemcov, and Zeljko Tukovic. OpenFOAM: A C++ library for complex physics simulations. In *International workshop on coupled methods in numerical dynamics*, volume 1000, pages 1–20. Dubrovnik, Croatia, 2007. URL: <https://csabai.web.elte.hu/http/simulationLab/jasakEtAlOpenFoam.pdf>.
- [374] Hrvoje Jasak. OpenFOAM: Open source CFD in research and industry. *International Journal of Naval Architecture and Ocean Engineering*, 1(2):89–94, 2009. doi:10.3744/jnaoe.2009.1.2.089.
- [375] Fadl Moukalled, Luca Mangani, and Marwan Darwish. *The Finite Volume Method in Computational Fluid Dynamics: An Advanced Introduction with OpenFOAM and Matlab*. Springer Publishing Company, Incorporated, 2015. doi:10.1007/978-3-319-16874-6.
- [376] Hagen Mueller, Federica Ferraro, and Michael Pfitzner. Implementation of a Steady Laminar Flamelet Model for non-premixed combustion in LES and RANS simulations. In *8th International OpenFOAM Workshop*, pages 1–12, 2013. URL: [http://sourceforge.net/projects/openfoam-extend/files/OpenFOAM\\_Workshops/OFW8\\_2013\\_Jeju/Fri/Track3/HagenMueller-OFW8.tar](http://sourceforge.net/projects/openfoam-extend/files/OpenFOAM_Workshops/OFW8_2013_Jeju/Fri/Track3/HagenMueller-OFW8.tar).
- [377] Michael Bertsch. Description of the reacting flow solver FGMFoam. In *Proceedings of CFD with OpenSource Software*, 2019. URL: [https://www.tfd.chalmers.se/~hani/kurser/OS\\_CFD\\_2019/Michael\\_Bertsch/report\\_FGMFoam.pdf](https://www.tfd.chalmers.se/~hani/kurser/OS_CFD_2019/Michael_Bertsch/report_FGMFoam.pdf).
- [378] Yuxuan Chen, Xu Zhu, Hua Zhou, and Zhuyin Ren. MetaOpenFOAM: an LLM-based multi-agent framework for CFD. *arXiv preprint*, 2024. doi:10.48550/arXiv.2407.21320.
- [379] Yuxuan Chen, Xu Zhu, Hua Zhou, and Zhuyin Ren. MetaOpenFOAM 2.0: Large language model driven chain of thought for automating CFD simulation and post-processing. *arXiv preprint*, 2025. doi:10.48550/arXiv.2502.00498.
- [380] Sandeep Pandey, Ran Xu, Wenkang Wang, and Xu Chu. OpenFOAMGPT: A retrieval-augmented large language model (LLM) agent for OpenFOAM-based computational fluid dynamics. *Physics of Fluids*, 37(3), 2025. doi:10.1063/5.0257555.
- [381] Jingsen Feng, Ran Xu, and Xu Chu. OpenFOAMGPT 2.0: end-to-end, trustworthy automation for computational fluid dynamics. *arXiv preprint*, 2025. doi:10.48550/arXiv.2504.19338.
- [382] David G. Goodwin, Harry K. Moffat, Ingmar Schoegl, Raymond L. Speth, and Bryan W. Weber. Cantera: An object-oriented software toolkit for chemical kinetics, thermodynamics, and transport processes, 2022. doi:10.5281/zenodo.8137090.
- [383] Ronan Collobert, Koray Kavukcuoglu, and Clément Farabet. Torch7: A matlab-like environment for machine learning. In *NeurIPS 2011 Workshop on BigLearn*, 2011. URL: [https://publications.idiap.ch/attachments/papers/2011/Collobert\\_NIPSWORKSHOP\\_2011.pdf](https://publications.idiap.ch/attachments/papers/2011/Collobert_NIPSWORKSHOP_2011.pdf).
- [384] Ricky T. Q. Chen. torchdiffeq, 2018. URL: <https://github.com/rtqichen/torchdiffeq>.
- [385] Philipp Holl, Vladlen Koltun, Kiwon Um, and Nils Thuerey. phiflow: A differentiable PDE solving framework for deep learning via physical simulations. In *NeurIPS 2020 Workshop on Differentiable Vision, Graphics, and Physics in Machine Learning*, volume 2, 2020. URL: <https://montrealrobotics.ca/diffcvgp/assets/papers/3.pdf>.
- [386] Philipp Holl and Nils Thuerey.  $\Phi_{\text{Flow}}$ : Differentiable simulations for PyTorch, TensorFlow and Jax. In *41st International Conference on Machine Learning (ICML)*, volume 235, pages 18515–18546, 2024. URL: <https://icml.cc/virtual/2024/poster/35005>.
- [387] Deniz A. Bezin, Aaron B. Buhendwa, and Nikolaus A. Adams. JAX-Fluids: A fully-differentiable high-order computational fluid dynamics solver for compressible two-phase flows. *Computer Physics Communications*, 282, 2023. doi:10.1016/j.cpc.2022.108527.
- [388] Deniz A. Bezin, Aaron B. Buhendwa, and Nikolaus A. Adams. JAX-Fluids 2.0: Towards HPC for differentiable CFD of compressible two-phase flows. *Computer Physics Communications*, 308, 2025. doi:10.1016/j.cpc.2024.109433.
- [389] Weiqi Ji, Xingyu Su, Bin Pang, Sean Joseph Cassady, Alison M. Ferris, Yujuan Li, Zhuyin Ren, Ronald Hanson, and Sili Deng. Arrhenius.jl: A differentiable combustion simulation package. *arXiv preprint*, 2021. doi:10.48550/arXiv.2107.06172.
- [390] Haocheng Wen, Faxuan Luo, Sheng Xu, and Bing Wang. JANC: A cost-effective, differentiable compressible reacting flow solver featured with JAX-based adaptive mesh refinement. *arXiv preprint*, 2025. doi:10.48550/arXiv.2504.13750.
- [391] Keaton J. Burns, Geoffrey M. Vasil, Jeffrey S. Oishi, Daniel Lecoaet, and Benjamin P. Brown. Dedalus: A flexible framework for numerical simulations with spectral methods. *Physical Review Research*, 2(2), 2020. doi:10.1103/PhysRevResearch.2.023068.
- [392] Argonne National Laboratory Illinois. Nek5000. URL: <https://nek5000.mcs.anl.gov>.
- [393] SENGAs+. URL: <https://www.ukctrf.com/index.php/senga>.
- [394] AVBP. URL: <https://avbp-wiki.cerfacs.fr>.
- [395] Olivier Desjardins, Guillaume Blanquart, Guillaume Balarac, and Heinz Pitsch. High order conservative finite difference scheme for variable density low Mach number turbulent flows. *Journal of Computational Physics*, 227(15):7125–7159, 2008. doi:10.1016/j.jcp.2008.03.027.
- [396] Jacqueline H. Chen, A. Choudhary, B. de Supinski, M. DeVries, E. R. Hawkes, S. Klasky, W. K. Liao, Kunling Ma, John M. Mellor-Crummey, Norbert Podhorszki, Ramanan Sankaran, Sameer Shende, and Chu Sang Yoo. Terascale direct numerical simulations of turbulent combustion using S3D. *Computational Science and Discovery*, 2(1):015001, 2009. doi:10.1088/1749-4699/2/1/015001.
- [397] A. Y. Poludnenko and Elaine Oran. The interaction of high-speed turbulence with flames: Global properties and internal flame structure. *Combustion and Flame*, 157(5):995–1011, 2010. doi:10.1016/j.combustflame.2009.11.018.
- [398] Pascale Domingo and Luc Vervisch. Recent developments in DNS of turbulent combustion. *Proceedings of the Combustion Institute*, 39(2):2055–2076, 2023. doi:10.1016/j.proci.2022.06.030.
- [399] ANSYS Fluent. URL: <https://www.ansys.com/products/fluids/ansys-fluent>.
- [400] ANSYS Chemkin. URL: <https://www.ansys.com/products/fluids/ansys-chemkin>.
- [401] COMSOL Multiphysics. URL: <https://www.comsol.com>.

- [402] An overview of both free and commercial CFD software. URL: <https://www.cfd-online.com/Wiki/Codes>.
- [403] Pauli Virtanen, Ralf Gommers, Travis E. Oliphant, Matt Haberland, Tyler Reddy, David Cournapeau, Evgeni Burovski, Pearu Peterson, Warren Weckesser, Jonathan Bright, Stefan J. van der Walt, Matthew Brett, Joshua Wilson, K. Jarrod Millman, Nikolay Mayorov, Andrew R. J. Nelson, Eric Jones, Robert Kern, Eric Larson, C. J. Carey, Ilhan Polat, Yu Feng, Eric W. Moore, Jake VanderPlas, Denis Laxalde, Josef Perktold, Robert Cimrman, Ian Henriksen, E. A. Quintero, Charles R. Harris, Anne M. Archibald, Antonio H. Ribeiro, Fabian Pedregosa, Paul van Mulbregt, and Contributors SciPy. SciPy 1.0: Fundamental algorithms for scientific computing in Python. *Nature Methods*, 17(3):261–272, 2020. doi:10.1038/s41592-019-0686-2.
- [404] Logan D. R. Beal, Daniel C. Hill, R. Abraham Martin, and John D. Hedengren. GEKKO optimization suite. *Processes*, 6(8), 2018. doi:10.3390/pr6080106.
- [405] Anders Logg, Kent-Andre Mardal, and Garth Wells. *Automated solution of differential equations by the finite element method: The FEniCS book*, volume 84. Springer Science & Business Media, 2012.
- [406] Martin Alnæs, Jan Blechta, Johan Hake, August Johansson, Benjamin Kehlet, Anders Logg, Chris Richardson, Johannes Ring, Marie E Rognes, and Garth N Wells. The FEniCS project version 1.5. *Archive of Numerical Software*, 3(100), 2015. doi:10.11588/ans.2015.100.20553.
- [407] Igor A. Baratta, Joseph P. Dean, Jørgen S. Dokken, Michal Habera, Jack S. Hale, Chris N. Richardson, Marie E. Rognes, Matthew W. Scroggs, Nathan Sime, and Garth N. Wells. DOLFINX: The next generation FEniCS problem solving environment, 2023. doi:10.5281/zenodo.10447666.
- [408] Frédéric Hecht. New development in FreeFEM++. *Journal of Numerical Mathematics*, 20(3-4):251–265, 2012. doi:10.1515/jnum-2012-0013.
- [409] Jonathan E. Guyer, Daniel Wheeler, and James A. Warren. FiPy: Partial Differential Equations with Python. *Computing in Science & Engineering*, 11(3):6–15, 2009. doi:10.1109/mcse.2009.52.
- [410] Lorena A Barba and Gilbert F Forsyth. CFD Python: the 12 steps to Navier-Stokes equations. *Journal of Open Source Education*, 2(16):21, 2018. doi:10.21105/jose.00021.
- [411] Heinz Pitsch. FlameMaster. URL: <https://www.itv.rwth-aachen.de/en/downloads/flamemaster>.
- [412] Alberto Cuoci, Alessio Frassoldati, Tiziano Faravelli, and Eliseo Ranzi. OpenSMOKE++: An object-oriented framework for the numerical modeling of reactive systems with detailed kinetic mechanisms. *Computer Physics Communications*, 192:237–264, 2015. doi:10.1016/j.cpc.2015.02.014.
- [413] Kevin McGrattan, Simo Hostikka, Jason Floyd, Randall McDermott, Marcos Vanella, Eric Mueller, and Chandan Paul. *Fire dynamics simulator user's guide*, volume 1019 of *NIST special publication*. 2025. URL: [https://github.com/firemodels/fds/releases/download/FDS-6.10.1/FDS\\_User\\_Guide.pdf](https://github.com/firemodels/fds/releases/download/FDS-6.10.1/FDS_User_Guide.pdf), doi:10.6028/NIST.SP.1019.
- [414] Kailai Xu and Eric Darve. ADCME: Learning spatially-varying physical fields using deep neural networks. In *NeurIPS 2020 Workshop on Machine Learning and the Physical Sciences*, 2020. URL: [https://ml4physicalsciences.github.io/2020/files/NeurIPS\\_ML4PS\\_2020\\_41.pdf](https://ml4physicalsciences.github.io/2020/files/NeurIPS_ML4PS_2020_41.pdf).
- [415] Kirill Zubov, Zoe McCarthy, Yingbo Ma, Francesco Calisto, Valerio Pagliarino, Simone Azeglio, Luca Bottero, Emmanuel Luján, Valentin Sulzer, and Ashutosh Bharambe. NeuralPDE: Automating physics-informed neural networks (PINNs) with error approximations. *arXiv preprint*, 2021. doi:10.48550/arXiv.2107.09443.
- [416] Ehsan Haghighat and Ruben Juanes. SciANN: A Keras/TensorFlow wrapper for scientific computations and physics-informed deep learning using artificial neural networks. *Computer Methods in Applied Mechanics and Engineering*, 373, 2021. doi:10.1016/j.cma.2020.113552.
- [417] Adam Paszke, Sam Gross, Francisco Massa, Adam Lerer, James Bradbury, Gregory Chanan, Trevor Killeen, Zeming Lin, Natalia Gimelshein, Luca Antiga, Alban Desmaison, Andreas Kopf, Edward Yang, Zach DeVito, Martin Raison, Alykhan Tejani, Sasank Chilamkurthy, Benoit Steiner, Lu Fang, Junjie Bai, and Soumith Chintala. PyTorch: An imperative style, high-performance deep learning library. In *33rd Conference on Neural Information Processing Systems (NeurIPS)*, volume 32 of *Advances in Neural Information Processing Systems*, 2019. URL: [https://papers.neurips.cc/paper\\_files/paper/2019/hash/bdbca288fee7f92f2bfa9f7012727740-Abstract.html](https://papers.neurips.cc/paper_files/paper/2019/hash/bdbca288fee7f92f2bfa9f7012727740-Abstract.html).
- [418] Jason Ansel, Edward Yang, Horace He, Natalia Gimelshein, Animesh Jain, Michael Voznesensky, Bin Bao, Peter Bell, David Berard, Evgeni Burovski, Geeta Chauhan, Anjali Chourdia, Will Constable, Alban Desmaison, Zachary DeVito, Elias Ellison, Will Feng, Jiong Gong, Michael Gschwind, Brian Hirsh, Sherlock Huang, Kshiteej Kalambarakar, Laurent Kirsch, Michael Lazos, Mario Lezcano, Yanbo Liang, Jason Liang, Yinghai Lu, C. K. Luk, Bert Maher, Yunjie Pan, Christian Puhresch, Matthias Reso, Mark Saroufim, Marcos Yukio Siraichi, Helen Suk, Michael Suo, Phil Tillet, Eikan Wang, Xiaodong Wang, William Wen, Shunting Zhang, Xu Zhao, Keren Zhou, Richard Zou, Ajit Mathews, Gregory Chanan, Peng Wu, Soumith Chintala, and Machinery Assoc Computing. PyTorch 2: Faster machine learning through dynamic Python bytecode transformation and graph compilation. In *29th ACM International Conference on Architectural Support for Programming Languages and Operating Systems (ASPLOS)*, pages 929–947, 2024. doi:10.1145/3620665.3640366.
- [419] Martin Abadi, Paul Barham, Jianmin Chen, Zhifeng Chen, Andy Davis, Jeffrey Dean, Matthieu Devin, Sanjay Ghemawat, Geoffrey Irving, Michael Isard, Manjunath Kudlur, Josh Levenberg, Rajat Monga, Sherry Moore, Derek G. Murray, Benoit Steiner, Paul Tucker, Vijay Vasudevan, Pete Warden, Martin Wicke, Yuan Yu, Xiaoqiang Zheng, and Usenix Assoc. TensorFlow: A system for large-scale machine learning. In *12th USENIX Symposium on Operating Systems Design and Implementation (OSDI)*, pages 265–283, 2016. URL: <https://www.usenix.org/conference/osdi16/technical-sessions/presentation/abadi>.
- [420] Antonio Gulli and Sujit Pal. *Deep learning with Keras*. Packt Publishing Ltd, 2017.
- [421] James Bradbury, Roy Frostig, Peter Hawkins, Matthew James Johnson, Chris Leary, Dougal Maclaurin, George Neca, Adam Paszke, Jake VanderPlas, Skye Wanderman-Milne, and Qiao Zhang. JAX: composable transformations of Python+NumPy programs, 2018. URL: <http://github.com/google/jax>.
- [422] Yanjun Ma, Dianhai Yu, Tian Wu, and Haifeng Wang. PaddlePaddle: An open-source deep learning platform from industrial practice. *Frontiers of Data and Computing*, 1(05):105–115, 2019. doi:10.11871/jfd.issn.2096.742X.2019.01.011.
- [423] Alexander Koryagin, Roman Khudorozhkov, and Sergey Tsimfer. PyDEns: A Python framework for solving differential equations with neural networks. *arXiv preprint*, 2019. doi:10.48550/arXiv.1909.11544.
- [424] Feiyu Chen, David Sondak, Pavlos Protopapas, Marios Mattheakis, Shuheng Liu, Devansh Agarwal, and Marco Di Giovanni. NeuroDiffEq: A Python package for solving differential equations with neural networks. *The Journal of Open Source Software*, 5(46):1931, 2020. doi:10.21105/joss.01931.
- [425] Shuheng Liu, Pavlos Protopapas, David Sondak, and Feiyu Chen. Recent advances of NeuroDiffEq – An open-source library for physics-informed neural networks. *arXiv preprint*, 2019. doi:10.48550/arXiv.2502.12177.
- [426] PhysicsNeMo Contributors. NVIDIA PhysicsNeMo: An open-source framework for physics-based deep learning in science and engineering, 2023. URL: <https://github.com/NVIDIA/physicsnemo>.
- [427] Jack Y Araz, Juan Carlos Criado, and Michael Spannowsky. Elvet–A neural network-based differential equation and variational problem solver. *arXiv preprint*, 2021. doi:10.48550/arXiv.2103.14575.
- [428] Levi D McClenny, Mulugeta A Haile, and Ulisses M Braga-Neto. TensorDiffEq: Scalable multi-GPU forward and inverse solvers for physics informed neural networks. *arXiv preprint*, 2021. doi:10.48550/arXiv.2103.16034.
- [429] Wei Peng, Jun Zhang, Weien Zhou, Xiaoyu Zhao, Wen Yao, and Xiaoqian Chen. IDRLnet: A physics-informed neural network library. *arXiv preprint*, 2021. doi:10.48550/arXiv.2107.04320.

- [430] Dario Coscia, Nicola Demo, and Gianluigi Rozza. PINA: A PyTorch framework for solving differential equations by deep learning for research and production environments. In *ICLR 2024 Workshop on AI4DifferentialEquations in Science*, 2024. URL: <https://iclr.cc/virtual/2024/21395>.
- [431] Oliver Hennigh, Susheela Narasimhan, Mohammad Amin Nabian, Akshay Subramaniam, Kaustubh Tangali, Zhiwei Fang, Max Rietmann, Wonmin Byeon, and Sanjay Choudhry. NVIDIA SimNet: An AI-accelerated multi-physics simulation framework. In *Computational Science - ICCS 2021*, pages 447–461. Springer International Publishing, 2021. doi:10.1007/978-3-030-77977-1\_36.
- [432] Monya Baker. Is there a reproducibility crisis? *Nature*, 533(7604):452–454, 2016. doi:10.1038/533452a.
- [433] Matthew Hutson. Artificial intelligence faces reproducibility crisis. *Science*, 359(6377):725–726, 2018.
- [434] Nick McGreivy and Ammar Hakim. Weak baselines and reporting biases lead to overoptimism in machine learning for fluid-related partial differential equations. *Nature Machine Intelligence*, 6(10):1256–1269, 2024. doi:10.1038/s42256-024-00897-5.
- [435] Mark D. Wilkinson, Michel Dumontier, IJsbrand Jan Aalbersberg, Gabrielle Appleton, Myles Axton, Arie Baak, Niklas Blomberg, Jan-Willem Boiten, Luiz Bonino da Silva Santos, Philip E. Bourne, Jildau Bouwman, Anthony J. Brookes, Tim Clark, Merce Crosas, Ingrid Dillo, Olivier Dumon, Scott Edmunds, Chris T. Evelo, Richard Finkers, Alejandra Gonzalez-Beltran, Alasdair J. G. Gray, Paul Groth, Carole Goble, Jeffrey S. Grethe, Jaap Heringa, Peter A. C. t Hoen, Rob Hooft, Tobias Kuhn, Ruben Kok, Joost Kok, Scott J. Lusher, Maryann E. Martone, Albert Mons, Abel L. Packer, Bengt Persson, Philippe Rocca-Serra, Marco Roos, Rene van Schaik, Susanna-Assunta Sansone, Erik Schultes, Thierry Sengstag, Ted Slater, George Strawn, Morris A. Swertz, Mark Thompson, Johan van der Lei, Erik van Mulligen, Jan Velterop, Andra Waagmeester, Peter Wittenburg, Katherine Wolstencroft, Jun Zhao, and Barend Mons. Comment: The FAIR Guiding Principles for scientific data management and stewardship. *Scientific Data*, 3, 2016. doi:10.1038/sdata.2016.18.
- [436] Kyle E. Niemeyer, Raymond L. Speth, Bryan W. Weber, and Richard H. West. A review of evidence-based best practices for developing research software in combustion. Report, 2019. doi:10.5281/zenodo.2619549.
- [437] Tianyi Li, Luca Biferale, Fabio Bonaccorso, Martino Andrea Scarpolini, and Michele Buzzicotti. Synthetic Lagrangian turbulence by generative diffusion models. *Nature Machine Intelligence*, 6(4):393–403, 2024. doi:10.1038/s42256-024-00810-0.
- [438] Luca Guastoni and Ricardo Vinuesa. A new perspective on the simulation of stochastic problems in fluid mechanics with diffusion models. *Nature Machine Intelligence*, 2025. doi:10.1038/s42256-025-01060-4.
- [439] Hugo Touvron, Louis Martin, Kevin Stone, Peter Albert, Amjad Almahairi, Yasmine Babaei, Nikolay Bashlykov, Soumya Batra, Prajjwal Bhargava, and Shruti Bhosale. Llama 2: Open foundation and fine-tuned chat models. *arXiv preprint*, 2023. doi:10.48550/arXiv.2307.09288.
- [440] Aixin Liu, Bei Feng, Bing Xue, Bingxuan Wang, Bochao Wu, Chengda Lu, Chenggang Zhao, Chengqi Deng, Chenyu Zhang, and Chong Ruan. DeepSeek-V3 technical report. *arXiv preprint*, 2024. doi:10.48550/arXiv.2412.19437.
- [441] Shashank Subramanian, Peter Harrington, Kurt Keutzer, Wahid Bhimji, Dmitriy Morozov, Michael W Mahoney, and Amir Gholami. Towards foundation models for scientific machine learning: Characterizing scaling and transfer behavior. In *Advances in Neural Information Processing Systems*, volume 36, pages 71242–71262. URL: [https://proceedings.neurips.cc/paper\\_files/paper/2023/hash/e15790966a4a9d85d688635c88ee6d8a-Abstract-Conference.html](https://proceedings.neurips.cc/paper_files/paper/2023/hash/e15790966a4a9d85d688635c88ee6d8a-Abstract-Conference.html).
- [442] Zhanhong Ye, Xiang Huang, Leheng Chen, Hongsheng Liu, Zidong Wang, and Bin Dong. PDEformer: Towards a foundation model for one-dimensional partial differential equations. In *ICLR 2024 Workshop on AI4DifferentialEquations in Science*, 2024. URL: <https://iclr.cc/virtual/2024/21389>.
- [443] Zhanhong Ye, Zining Liu, Bingyang Wu, Hongjie Jiang, Leheng Chen, Minyan Zhang, Xiang Huang, Qinghe Meng Zou, Hongsheng Liu, and Bin Dong. PDEformer-2: A versatile foundation model for two-dimensional partial differential equations. *arXiv preprint*, 2025. doi:10.48550/arXiv.2507.15409.
- [444] Junhong Shen, Tanya Marwah, and Ameet Talwalkar. UPS: Efficiently building foundation models for pde solving via cross-modal adaptation. *Transactions on Machine Learning Research*, 2024. URL: <https://openreview.net/forum?id=Or9mhjRv1E>.
- [445] Maximilian Herde, Bogdan Raonic, Tobias Rohner, Roger Kappeli, Roberto Molinaro, Emmanuel De Bezenac, and Siddhartha Mishra. Poseidon: Efficient foundation models for PDEs. In *38th Conference on Neural Information Processing Systems (NeurIPS)*. URL: <https://neurips.cc/virtual/2024/poster/95731>.
- [446] Jingmin Sun, Yuxuan Liu, Zecheng Zhang, and Hayden Schaeffer. Towards a foundation model for partial differential equations: Multioperator learning and extrapolation. *Physical Review E*, 111(3):035304, 2025. doi:10.1103/PhysRevE.111.035304.
- [447] Yuxuan Liu, Jingmin Sun, Xinjie He, Griffin Pinney, Zecheng Zhang, and Hayden Schaeffer. PROSE-FD: A multimodal PDE foundation model for learning multiple operators for forecasting fluid dynamics. *arXiv preprint*, 2024. doi:10.48550/arXiv.2409.09811.
- [448] Licheng Jiao, Xue Song, Chao You, Xu Liu, Lingling Li, Puhua Chen, Xu Tang, Zhixi Feng, Fang Liu, Yuwei Guo, Shuyuan Yang, Yangyang Li, Xiangrong Zhang, Wenping Ma, Shuang Wang, Jing Bai, and Biao Hou. AI meets physics: a comprehensive survey. *Artificial Intelligence Review*, 57(9), 2024. doi:10.1007/s10462-024-10874-4.
- [449] Yaron Lipman, Ricky TQ Chen, Heli Ben-Hamu, Maximilian Nickel, and Matt Le. Flow matching for generative modeling. In *11th International Conference on Learning Representations (ICLR)*, 2023. URL: <https://iclr.cc/virtual/2023/poster/11309>.